



# ICCRE 2024



**COLLECTION OF ABSTRACTS  
AND EXTENDED ABSTRACTS**



# Preface

---

Included in this collection are a list of conference sponsors, and the abstracts and extended abstracts, including those of all papers in the conference proceedings, presented at the 20th International Conference on Cold Regions Engineering (ICCRE 2024) held from May 13 to May 16, 2024, in Anchorage, Alaska, USA. The abstracts are listed according to alphabetical order of the first author's last name. A detailed program is provided separately in hard copies and is also available in the conference app.

I gratefully acknowledge the technical contributions made to the ICCRE 2024 by the presenters. High-quality presentations are the foundation of any specialty conference like this. Please enjoy the conference.

Zhaohui (Joey) Yang, Ph.D.

Chair, 20th International Conference  
on Cold Regions Engineering

Professor, University of Alaska Anchorage





# Sponsors

The 2024 conference is proudly sponsored by:

## PREMIER

**Stantec**

## PLATINUM

**Alaska Frontier Constructors  
Alaska Native Tribal Health Consortium  
ASRC Energy Services  
CRW Engineering Group**

## GOLD

**Arctic Foundations**

**PND Engineers**

**WSP USA**

## SILVER

**beadedstream  
DOWL  
HDL Engineering Consultants  
Michael Baker International**

**BGC Engineering  
EA Engineering, Science, and Technology  
Kuna Engineering  
Shannon & Wilson**

## BRONZE

**Coffman Engineers  
Northern Geotechnical Engineering  
R&M Consultants**

**Logic Geophysics & Analytics  
PeopleAK  
RESPEC**

# Methodologies for Quantifying Installation-Community Resilience in Cold Regions

Rosa T. Affleck, Ph.D.,<sup>1, a</sup> Kevin Bjella, P.E.,<sup>1, b</sup>  
Matthew Joyner, Ph.D.,<sup>2, c</sup> Margaret Kurth,<sup>2, d</sup>  
James Richards, P.E.,<sup>3, e</sup> John Richards, PhD, P.E.<sup>3, f</sup> and Paige Toebben<sup>1, g</sup>

<sup>1</sup>*U.S. Army Corps of Engineers, Engineer Research and Development Center (ERDC), Cold Regions Research and Engineering Laboratory (CRREL), 72 Lyme Rd, Hanover, NH 03755;*

<sup>a</sup>*email: [rosa.t.affleck@usace.army.mil](mailto:rosa.t.affleck@usace.army.mil); <sup>b</sup>ERDC CRREL-AK, [kevin.bjella@usace.army.mil](mailto:kevin.bjella@usace.army.mil)*

<sup>2</sup>*ERDC, Environmental Laboratory (EL), 3909 Halls Ferry Rd., Vicksburg, MS 39180;*

<sup>c</sup>*[matthew.d.joyner@usace.army.mil](mailto:matthew.d.joyner@usace.army.mil); <sup>d</sup>[margaret.h.kurth@usace.army.mil](mailto:margaret.h.kurth@usace.army.mil)*

<sup>3</sup>*ERDC, Information Technology Laboratory (ITL), 3909 Halls Ferry Rd., Vicksburg, MS 39180; <sup>e</sup>[james.e.richards@erdc.dren.mil](mailto:james.e.richards@erdc.dren.mil); <sup>f</sup>[john.p.richards@erdc.dren.mil](mailto:john.p.richards@erdc.dren.mil);*

<sup>g</sup>*[paige.m.toebben@usace.army.mil](mailto:paige.m.toebben@usace.army.mil)*

## Abstract

The dynamic challenges posed by climate-driven threats indicate an acceleration in complexities surrounding the planning, construction, and maintenance of infrastructure within cold regions installations and their proximate communities. It is imperative for installations, including military posts, bases, and facilities, situated in these regions, to enhance their capacity to address the resilience of critical infrastructure while gaining a comprehensive understanding of the risks entwined with mission-critical functionalities. The proposed approach emphasizes a combined community and installation understanding of threats affecting missions through infrastructure. It seeks to identify prospective interventions geared towards risk reduction and resilience amplification. To develop a systematic assessment, we draw upon existing approaches and data on projected climate-driven hazards, incorporating interdependencies between infrastructure systems, installation capabilities, and nearby communities for our new start resilience project. This assessment focuses on a specific installation and its surrounding community infrastructure exposed to unique and compounding threats in cold regions environments. The purpose of this paper is to highlight existing tools and methodologies applicable to installation resilience assessments such as the Mission Dependency Index (MDI) and Mission Assurance Assessment (MAA), with modifications addressing not only asset management concerns but also other dependencies, including the surrounding communities in cold regions.



# Concrete creep and shrinkage at cold temperatures and their implications to PC girder design

Il-Sang Ahn, Ph.D., P.E.

*Associate Professor, Department of Civil, Geological, and Environmental Engineering,  
University of Alaska Fairbanks*

## **Abstract**

At cold temperatures, concrete creep and shrinkage can be quite different from those at room temperature or warm temperatures. The creep and shrinkage of high strength concrete were measured at temperature-controlled environment and in ambient subarctic weather on the University of Alaska Fairbanks campus. Test results indicated that the concrete creep and shrinkage stayed dormant at the cold temperature (-40°C and -55°C) and resumed once the temperature increased from the cold to room temperature. The creep strain at cold temperatures was about 30% of creep strain from specimens at room temperature. Also, the shrinkage strain was 67% of the shrinkage strain measured at room temperature. A comparison showed that the creep and shrinkage strains in ambient weather were larger than strains at a sustained cold temperature, but they were substantially smaller than strains at room temperature. In design and assessment, concrete creep and shrinkage are important factors for long-term concrete behavior of the structures exposed to subarctic weather. Specifically, the amount of prestress force applied to tendons in pre-stressed concrete (PC) girders should be determined based on appropriate pre-stress loss estimation which heavily depends on concrete creep and shrinkage. The measured concrete creep and shrinkage are compared with those predicted from several practical models including the AASHTO-LRFD model and the ACI model. In addition, effects on PC girder design due to different concrete creep and shrinkage will be identified and discussed.

# Assessing Traffic Safety in Cold Regions For Sustainable and Resilient Infrastructure: A Spatial Analysis and Association Rule Mining Approach

Mulugeta D. Amare, S.M. ASCE,<sup>1</sup> Daba S. Gedafa, Ph.D., P.E., ENV SP, F.ASCE,<sup>2</sup>  
Lemlem A. Asaye, S.M. ASCE,<sup>3</sup>

*1Ph.D. Student, Dept. of Civil Engineering, University of North Dakota, Grand Forks, P.O. Box 8115, Grand Forks, ND 58202-8115, email: mulugeta.amare@und.edu*

*2Department of Civil Engineering, University of North Dakota, Grand Forks, P.O. Box 8115, Grand Forks, ND 58202-8115, email: daba.gedafa@und.edu*

*3Ph.D. Student, Dept. of Civil, Construction and Environmental Engineering, North Dakota State University, P.O. Box 6050, Fargo, ND 58102-6050. email: lemlem.asaye@ndsu.edu*

## **Abstract**

Cold regions present unique challenges for ensuring traffic safety, necessitating sustainable and resilient engineering practices. Significant hotspot crash locations and causes are the key parameters for creating an informed safety measure; however, previous studies on traffic safety have primarily focused on general factors, such as driver behavior and road conditions, without examining the relationships between incident causes and impacts. This study proposes a novel approach that uses Association Rule Mining to analyze significant associations between traffic crash variables and evaluates spatiotemporal clustering using Geographic Information System tools. The findings from the spatiotemporal analysis revealed that more crashes occurred during winter, and the hotspot identification results from the Getis-Ord ( $G_i^*$ ) and Anselin Local Moran's (I) statistics were compelling. The extracted association rules provide a quantitative understanding of the cause-and-effect relationships between various contributing factors. The results will help transportation planners better understand the interrelationships between the factors and their effects, enhancing traffic safety in cold regions.



# Geotechnical Design of Permafrost and Wetland Mitigation for Colorado State Highway 5

James M. Arthurs, M.ASCE, Ph.D., P.E.,<sup>1</sup> Brendan L. McGarity, <sup>2</sup> Jeremy R. Shaw, Ph.D.,<sup>3</sup> and David J. Cooper, Ph.D.<sup>4</sup>

<sup>1</sup>*Federal Highway Administration, Central Federal Lands Highway Division, 12300 W. Dakota Ave., Lakewood, CO 80228; email: james.arthurs@dot.gov*

<sup>2</sup>*Federal Highway Administration, Central Federal Lands Highway Division, 12300 W. Dakota Ave., Lakewood, CO 80228; email: brendan.mcgarity@dot.gov*

<sup>3</sup>*Department of Forest and Rangeland Stewardship, Colorado State University, Fort Collins, CO 80521; email: jeremy.shaw@colostate.edu*

<sup>4</sup>*Department of Forest and Rangeland Stewardship, Colorado State University, Fort Collins, CO 80521; email: david.cooper@colostate.edu*

## Abstract

Colorado State Highway 5 within the Summit Lake Park region has experienced severe roadway damage due to permafrost degradation and freeze-thaw cycling. Passing through a sensitive alpine wetland complex, current roadway configuration has yielded inadequate pavement performance, accelerated permafrost degradation, disrupted surface and subsurface water flow paths, and altered ecological processes. Roadway reconstruction utilizing an air convection embankment (ACE) was selected as the preferred design alternative to meet project priorities of permafrost and wetland restoration and improved roadway performance. A subsurface investigation was conducted, and a two-dimensional finite element model was developed to evaluate the passive cooling capabilities of the ACE and its effects on the soil temperature profile and active zone depth. Model results revealed positive mitigative effects on permafrost degradation, with diminishing cooling capabilities over time due to ongoing global climate warming. Due to the coarse, angular embankment material, and porous nature of the ACE, thaw settlement of the roadway is anticipated to be minimized, and surface water is expected to diffuse through the embankment, contributing to restoration of the downgradient hydrologic regime. All images and illustrations within this paper are attributed to FHWA, unless marked otherwise.

# Shear characteristics and microstructure of cemented soil-concrete interface after artificial freeze-thaw under vibration loading

Jie Zhou<sup>1,2\*</sup>, Chao Ban<sup>1</sup>, Chengjun Liu<sup>1</sup>

<sup>1</sup> *Department of Geotechnical Engineering, College of Civil Engineering, Tongji University, 1239 Siping Road, Shanghai 200092, China*

<sup>2</sup> *Key Laboratory of Geotechnical and Underground Engineering (Tongji University), Ministry of Education, 1239 Siping Road, Shanghai 200092, China*

*\*zhoujie1001@tongji.edu.cn*

## **Abstract**

In Shanghai, artificial ground freezing (AGF) method is widely used in complex engineering projects like the construction adjacent to subway tunnels. And to reduce frost heave and thaw settlement and reinforce the soil, cement will be used together. In this case, the cemented soil-concrete interface will be formed around the underground structures. Because material properties on both sides of the interface are different and the interface is one of the weak parts, it is necessary to study the shear characteristics of the cemented soil-concrete interface after artificial freeze-thaw under the influence of surrounding vibration load in underground construction for the stability of the whole structure. In this paper, large-scale interface shear tests under vibration loading were carried out, and the effect of curing time and artificial freeze-thaw on interface shear characteristics were studied. At the same time, microstructure of the cemented soil was observed by scanning electron microscope (SEM) tests. The results show that the shear strength of the interface increases with the increase of curing time. The artificial freeze-thaw has a reduction on the shear strength of the interface with vibration loading. Microscopically, artificial freeze-thaw will increase pores and produce some tiny cracks. The results in this paper provide help for further research on the shear characteristics of the cemented soil-concrete interface.



# Uncovering the Impact of Freeze-Thaw Cycles on Resilient Modulus of Cement-Stabilized Sulfate-rich Subgrade Soil

Debayan Ghosh, S.M.ASCE<sup>1</sup>; Aritra Banerjee, Ph.D., P.E., M.ASCE<sup>2</sup>

<sup>1</sup>Graduate Research Assistant, Dept. of Civil and Environmental Engineering, South Dakota State Univ., Brookings, SD. Email: [debayan.ghosh@sdstate.edu](mailto:debayan.ghosh@sdstate.edu)

<sup>2</sup>Assistant Professor Dept. of Civil and Environmental Engineering, South Dakota State Univ., Brookings, SD. Email: [aritra.banerjee@sdstate.edu](mailto:aritra.banerjee@sdstate.edu) (Corresponding author)

## Abstract

This experimental study presented the effect of cement stabilization on sulfate-rich soil from South Dakota's Pierre Shale formation. To quantify the effects of the stabilization of sulfate-rich soils and freeze-thaw cycles, control and stabilized soil samples were prepared with cement (Type I) stabilizers (3 and 6 % by weight) for a curing period of 28 days and subjected to freeze-thaw cycles in a closed system. Repeated load triaxial (RLT) tests were conducted to determine the resilient modulus of cement-stabilized sulfate-rich soil for a range of freeze-thaw cycles. Unconfined compressive strength (UCS) tests were conducted to compare the compressive strength of the soil after the 1<sup>st</sup>, 4<sup>th</sup>, 8<sup>th</sup>, and 12<sup>th</sup> freeze-thaw (F-T) cycles. The trend of changes in resilient modulus was illustrated in the study. A significant decrease in compressive strength due to freeze-thaw cycles was observed. Field emission scanning electron microscopy (FESEM) was used to demonstrate the formation of ettringite and calcium-silicate-hydrate (CSH) and determine the changes in microscopic and mineralogy due to freeze-thaw cycles.

# Effective Mitigation Strategies for Tenting of Transverse Cracks in Asphalt Pavement

Manik Chakraborty<sup>1</sup>, Manik Barman<sup>2</sup>

<sup>1</sup> Graduate student, Department of Civil Engineering University of Minnesota, Duluth  
Email: chakr230@d.umn.edu

<sup>2</sup> Associate Professor Department of Civil Engineering University of Minnesota, Duluth  
Email: mbarman@d.umn.edu

## Abstract

In winter, asphalt pavement in the cold climate regions exhibits a localized secondary distress called pavement tenting. It occurs when the ice accumulates around the crack vicinity, which pushes both sides of the transverse crack up, thus the tenting appears on the surface. The conventional theory behind its formation is the frost heave of the base materials. The presence of salt inside the crack acts as a catalyst for its development. Due to its formation, the pavement roughness increases significantly, as does the crack deterioration rate. Although the cause of the problem is well known, the solution is still a concern. The main objective of this study is to find effective mitigative strategies that reduce the pavement roughness of different pavement types. In this study, a number of asphalt road sections were selected for analysis whose most critical distress was transverse crack. Pavement roughness data of the selected road sections were extracted and analyzed from the pavement management database of the Minnesota Department of Transportation (MnDOT). The percentage change in the international roughness index (IRI) before and after the application of treatment was calculated to find out the effectiveness of each different measure. The data analysis led to the prioritization of treatments based on their effectiveness in reducing pavement roughness on different types of pavements. Results showed that micro-surfacing has the highest degree of effectiveness and crack sealing has the lowest compared to the other treatments. However, a significant level of variation was observed in the analyzed data. Finally, the findings of this study will help to select the best mitigative measures to reduce roughness and will generate future research in this topic.



# Erosion Mitigation Design in the Arctic Considering Climate Change Impacts

Kamil Biedka<sup>1</sup>, Fiona Duckett<sup>2</sup>, Lucas Arenson<sup>3</sup>,  
Charles Klengenber<sup>4</sup>, Shawn Stuckey<sup>5</sup>

<sup>1</sup> Baird & Associates, kbiedka@baird.com

<sup>2</sup> Baird & Associates, duckett@baird.com

<sup>3</sup> BGC Engineering, larenson@bgcengineering.ca

<sup>4</sup> Inuvialuit Regional Corporation, CKlengenber@inuvialuit.com

<sup>5</sup> Hamlet of Tuktoyaktuk, sao@tuktoyaktuk.ca

## Background

The Hamlet of Tuktoyaktuk is a low-lying peninsula in the Arctic along the Beaufort Sea that is vulnerable to severe coastal erosion and intermittent flooding. Most residences and buildings located near the coast have been relocated and those remaining are currently at risk of damage or destruction during storm events. In the longer term, cultural sites such as the graveyard are also at risk and the plan is to relocate the community. Nearby Tuktoyaktuk Island, a beach/bluff system which shelters Tuktoyaktuk Harbour from waves, is eroding and if not protected may be gone by 2050. Baird was retained by the Hamlet of Tuktoyaktuk and Inuvialuit Regional Corporation (IRC) to assess erosion mitigation alternatives and select/implement a preferred design to protect the Hamlet (Figure 1) and Island, which comprise a total shoreline length of approximately 2000 m.



Figure 1 – Hamlet of Tuktoyaktuk.

## Climate Change Impacts

Climate change is expected to have a significant impact in the Canadian Arctic and was a critical consideration in the erosion mitigation design process. Impacts for this project include increased water levels, a longer ice-free season, increased wave exposure and permafrost degradation. Relative sea level rise (RSLR) of 0.37 m for the year 2050 was used in the design, which was based on the 95th percentile of the RCP 8.5 emissions scenario (James, 2015).

## Design Conditions

The designs were developed using the 100-year return period wave and water level conditions. The design life for the structure was set as 30 years (to 2050) given the harsh Arctic conditions.

The wave and water level conditions are both dependent on wind driven storms. The wide and

shallow continental shelf at Tuktoyaktuk causes large storm surges (up to 2.5 m) when strong onshore winds are sustained for a significant duration. The MIKE21 HD model was used to determine the design water level, combining the surge, high tide and RSLR. The wave conditions were modelled using MIKE21 SW.

Net longshore sediment transport rates for existing and future climate conditions were estimated through modeling. The projections for future sediment transport rates consider the impact of increased wave action along the project shorelines associated with sea level rise and a longer open water season.

Forces from ice loading were also included in the design. It was determined that the greatest ice loads would occur during the spring break up period when large mobile ice floes may be pushed onshore by strong winds.

Ground ice and permafrost contribute to the challenges of the shore protection design. Ground temperatures were modelled with and without the proposed structures to compare the effect it will have on permafrost degradation and the stability of the structure foundation.

### **Design Alternatives**

Baird developed three design alternatives, including articulated concrete block mattress, concrete slab, and armour stone revetments. Each alternative was tested in a physical model, including tests with wave and water level conditions ranging in severity from the 2 to 500-year return period events. Modifications were made to each design based on the model results and updated quantity/cost estimates were prepared, with the armour stone revetment identified as the most cost-effective solution.

Final design of the armour stone revetment has been completed, with the design including beach nourishment along a section of barrier beach that had previously been breached. The Hamlet and IRC have submitted a funding application, with bidding and construction pending.

### **References**

James, T.S., Henton, J.A., Leonard, L.J., Darlington, A., Forbes, D.L., and Craymer, M. (2015): Tabulated values of relative sea-level projections in Canada and the adjacent mainland United States; Geological Survey of Canada, Open File 7942, 81 p.

# Engineering With Nature® and Progressing Natural and Nature-Based Solutions in Alaska and the Arctic

Lauren Bosche

## Abstract

The use of ecosystems and natural methods to reduce infrastructure and community risk has a long legacy, though the formal civil engineering practice of integrating Natural and Nature-Based Solutions (NNBS) in ‘traditional’ engineered features has only recently been established in the last few decades. The United States Army Corps of Engineers (USACE) Engineering With Nature® (EWN) program has been a leader in this space since 2010, contributing to NNBS projects and demonstrations, policy and research development, and international engagement and partnering with stakeholders to drive NNBS practice forward. Most NNBS and EWN work has taken place at lower latitudes, despite the growing risks and increasing need in the Arctic and sub-Arctic. This disparity is reflected in the guidelines available to support practitioners, such as the International Guidelines on Natural and Nature-Based Features for Flood Risk Management, as there are limited resources that synthesize efforts including NNBS specifically for the Arctic and adjacent regions (Bridges et al., 2021). Many applications of NNBS in warm climates use biologic materials like vegetation, algal mats, and others that may not be viable in cold environments of the Arctic and sub-Arctic. Arctic- specific guidance is critical to NNBS project success in an environment characterized by sea ice cover and thermal dynamics, a distinct cultural and social context, and staggering rates of coastal erosion and permafrost thaw, among other distinct features. This talk will provide a high-level overview of the USACE EWN program and the EWN approach at project sites in Alaska. It will also highlight some of the opportunities to leverage relevant international NNBS guidance documents available in potential applications to Alaska and the Arctic.

## References

Bridges, Todd, Jeffrey King, Jonathan D. Simm, Michael Beck, Georganna Collins, Quirijn Lodder, and Ram Mohan. International guidelines on natural and nature-based features for flood risk management. USACE, 2021.

# Conceptual Design of Quantitative Risk Algorithms for a Geohazard and Geo-asset Management System for Roadway Networks in Permafrost Regions

Heather Brooks, Ph.D., P.E.,<sup>1</sup> Lukas Arenson, Dr.Sc.Techn.ETH., P.Eng.,<sup>2</sup> Khatereh Roghangar, M.Sc.<sup>3</sup>, Jan Stirling, P.Eng.,<sup>4</sup> Frank Hung, M.Eng., E.I.T.<sup>5</sup>

<sup>1</sup> BGC Engineering Inc., Suite 2600, 425 – 1<sup>st</sup> Street SW, Calgary, AB T2P 3L8; email: hbrooks@bgcengineering.ca

<sup>2</sup> BGC Engineering Inc., Suite 500 – 980 Howe Street, Vancouver, BC, V6Z 0C8; email: larenson@bgcengineering.ca

<sup>3</sup> Ph.D. Candidate, Department of Civil Engineering, University of Calgary, Suite 2600, 425 – 1<sup>st</sup> Street SW, Calgary, AB T2P 3L8; email: khatereh.roghangar@ucalgary.ca

<sup>4</sup> BGC Engineering Inc., Level 3, 31 Merivale Street, South Brisbane, QLD 4101, Australia; email: jstirling@bgcengineering.ca

<sup>5</sup> BGC Engineering Inc., Suite 200 – 318 Richmond Road, Ottawa, ON, K1Z 6X6; email: fhung@bgcengineering.ca

## Abstract

Within the Northwest Territories, Canada, permafrost is ubiquitous with communities and industrial development requiring transportation infrastructures (e.g., roadways, airports, and railways) or other linear infrastructure (e.g., pipelines and transmission lines) to accommodate potentially unstable subgrades. In these regions, transportation is of vital social, economic, and political importance. However, warming climate conditions are and will impact the integrity of existing and future transportation infrastructure constructed in permafrost regions. Existing analytical frameworks and tools for geohazard and geo-asset management have not included hazards derived from permafrost; where the ubiquity of permafrost results in the hazard being nearly ever-present underlying the infrastructure and ever changing as climate warming continues through time. This paper presents the conceptual design of quantitative risk algorithms for a geohazard assessment system using dynamic segmentation techniques to discretize the infrastructure spatially based on credibility factors for individual dangers specific to permafrost and changing thermal conditions. The hazard (probability of occurrence) will be calculated based on current conditions and projected using IPCC climate projects for the infrastructure region. This discretized approach will allow infrastructure owners to determine current high-risk areas as well as projections for high-risk areas in the future allowing for more efficient infrastructure improvement planning and an overall increase in roadway network safety.



# Evaluation of the Impact of Thermal Shock on Roofing Materials Properties Maha

Dabas, PhD.<sup>1</sup>, P.Eng., Flonja Shyti, M.A.Sc.<sup>1</sup>, James Saragosa, M.A. Sc<sup>1</sup>

<sup>1</sup>National Research Council of Canada (NRC), 1200 Montreal Road, [maha.dabas@nrc-cnrc.gc.ca](mailto:maha.dabas@nrc-cnrc.gc.ca)

## Abstract

The intensity and frequency of extreme weather events are expected to increase, leading to temperature and humidity shock due to climate change. Shock can accelerate material deterioration and significantly decrease their service life. However, little research is available on its effect on roof materials' properties and performance. Thus, experimental tests were carried out at the National Research Council of Canada (NRC) to evaluate the hygrothermal and mechanical performance of materials commonly used in the roofing industry, such as wood sheathing. Exposed materials are evaluated in terms of the rate of mass loss, dimensional stability, and modulus of rupture (Flexural strength) as damage indicators, according to ASTM standards. Results indicate a general trend in the increase of material instability as the number of thermal cycles/shocks increases. There is more than a 10% reduction in wood sheathing flexural strength.

Keywords: Thermal shock, thermal cycles, OSB, plywood wood sheathing

## Introduction

In North America, components of roof systems are expected to experience more rapid temperature fluctuations (shocks) and warming and cooling shifts within a day each season (Government of Canada 2019). In the roofing industry, thermal shock is defined as the impact of rapid temperature fluctuations on a vulnerable roof system and components (Smyth. M. 2022; Bulger. B. 2020; Smyth. M. 2022; Shyti et al. 2023). This adversely affects aged roofing, ranging from buckling, cracking, and leaking (Bulger. B. 2020 and Smyth. M. 2022). This cyclic trend of temperature fluctuations can accelerate roof material deterioration as materials expand and contract. Subsequently, material service life is reduced, leading to premature failure. Materials' resistance to thermal shock depends primarily on materials' inherent properties and restraining effects (attachment within a roof assembly). Free/unrestrained components expand and contract when subjected to temperature fluctuations, irrespective of their cross-sectional size. However, thermal stresses are generated when the components are restrained from shortening or expanding. If the thermal stresses exceed the ultimate strength of a material, failure (rupture/cracks) will occur. Repeated cycles of expansion and contraction of materials (dimensional instability) lead to wear and tear (fatigue) and widen/narrow existing gaps (Mcknight. M 2019). A stress differential may develop for restrained material within roof assembly materials, leading to material cracking in the case of a membrane or material buckling for wood sheathing. OSB wood sheathing over time retains more moisture than plywood materials as it dries relatively slowly. OSB wood swells around the edges and remains swollen after the material dries. Plywood tends to swell and dry out quickly leading to dimensional instability. Signs of damage potentially related to thermal stresses include excessive roof sheathing warping due to dimensional instability. Little research is available on their material performance under such extreme conditions. The National Building Code of Canada (NBCC) (NBC 2020) provides climatic design loads that do not account for future temperature projections or shock, while the National Energy Code of Canada for Buildings (NECB) (NECB 2020) provides general specifications at standard hygrothermal conditions. ASTM D2126 (ASTM 2020) briefly notes that where a thermal shock (rapid heating or cooling) is expected, further investigation should be undertaken to evaluate its impact on the insulation's dimensional stability. Existing research focuses on the wood sheathing response under extreme scenarios of elevated temperature and humidity conditions (Barnes et al. 2009). Standard tests attempt to replicate field

conditions by creating accelerated tests under extreme temperature and humidity conditions. However, these tests often involve steady-state exposure due to the constraints of laboratory testing and time limitations (ASTM 2018). However, the actual response of wood should reflect the in-service conditions adopted from data collected in the field for each climatic zone. Correlate thermal degradation and serviceability deteriorations of the wood sheathing to the field hygrothermal fluctuations. This work aims to propose a testing procedure considering different test protocols simulating followed by experimental tests to determine material properties. Thus, an experimental program was conducted at the National Research Council of Canada (NRC) to develop an experimental testing procedure to evaluate the dimensional stability and mechanical performance of different materials (engineered wood sheathing) commonly used in the roofing industry. Roof material samples were exposed to a thermal shock. Another set of material samples was exposed to thermal cycling and a steady state of cold and hot exposure to better understand the impact of each test protocol on material performance.

### Experimental Evaluation of Roofing Materials Thermal Shock Protocol

A general framework was developed by (Shyti et al. 2023) to quantify the impact of thermal shock on roofing materials' durability. The framework utilized future climatic data and industry feedback in its development to allow practical application. This was combined with the individual materials' surface temperature, as it was found that the impact of weather shocks and thermal stresses will vary among the different materials comprising roofing systems. As a result, exposed roof components will have different responses than those located within the roof assembly. Hence, this research aims to assess the effects of shock on various roofing materials within the roofing assembly. This will be achieved by creating customized sub-testing protocols for each material under examination, specifically engineered wood sheathing. These protocols are developed based on field data obtained from the literature and field monitoring to assess the properties of these materials. Details of the test protocols for each are summarized below.

#### Test Protocol for Thermal Shock (TS)

This procedure was developed to simulate climatic conditions in the field. In the development of this protocol, climatic data were retrieved from existing literature or field monitoring. The test protocol consists of a cyclic exposure of hot-to-warm (70°C to 23°C) exposure at 60% RH, which was repeated in four cycles. This was followed by four cycles of cold-to-cool (-40°C to 23°C) exposure. The hot cycles (4) and cold cycles (4) were completed in one day (24 hours) for a total of eight (8) cycles in one day and 112 cycles in 14 days. The test protocol was conducted in an automated environmental chamber at the NRC facility to simulate in-service climate exposure (Figure 1). Materials tested were engineered wood sheathing such as OSB sheet of 11.1mm (7/16"), an OSB sheet of 15.9mm (5/8") thick, and a plywood sheet of 15.9mm (5/8") thick.



Figure 1: Test protocol details (left) and diagram (right) of OSB and plywood

#### Test Protocol for Thermal Cycling (TC)

Samples of engineered wood such as OSB sheet of 11.1mm (7/16") thick, OSB sheet of 15.9mm (5/8") thick, and plywood sheet of 15.9mm (5/8") thick were exposed to thermal cycling. This test protocol comprised of 8 hours of hot (55°C) exposure at 60% RH followed by 16 hours of 10°C warm exposure at

60% RH for seven days for a total cycle period of 24 hours. In the next seven days, the samples were exposed to 16 hours of cold (-40°C) exposure and 8 hours of cool (10°C) exposure in one day. The total duration of the thermal cycling was 14 days in a combination of hot-warm exposure (7 days) followed by cold-cool exposure (7 days). Measurements were collected on days 0, 7, and 14 days of thermal cycling testing.

## Discussion of Results

### Dimensional Changes

Results indicate that the OSB is prone to absorb and gain moisture when exposed to humid or wet conditions compared to plywood. However, the extent to which OSB can gain moisture depends on various factors, including thickness, the specific resin and adhesive used in its construction, and the duration and severity of exposure to moisture. Wood (OSB) sheet absorbs moisture through its exposed edges, surface, and any imperfections in the protective coatings or finishes. Considering wood is a natural material that expands and contracts with changes in temperature and humidity. The extent of dimensional changes (length, width and thickness) of OSB sheet of 11.1mm (7/16") thick, OSB sheet of 15.9mm (5/8") thick, and the plywood sheet of 15.9mm (5/8") thick are assessed following thermal cycling, and thermal shock compared to steady-state exposure. Moisture content measurements were conducted after each exposure test for OSB sheet of 11.1mm (7/16") thick, OSB sheet of 15.9mm (5/8") thick, and a plywood sheet of 15.9mm (5/8") thick (Figure 2). The findings reveal that, in comparison to steady-state exposure to hot and cold conditions, OSB sheets of 11.1mm (7/16") thick had higher moisture gain following thermal shock and cycling (Figure 2). Moisture gain was reduced as the thickness of the OSB increased from 11.1mm (7/16") to 15.9mm (5/8").

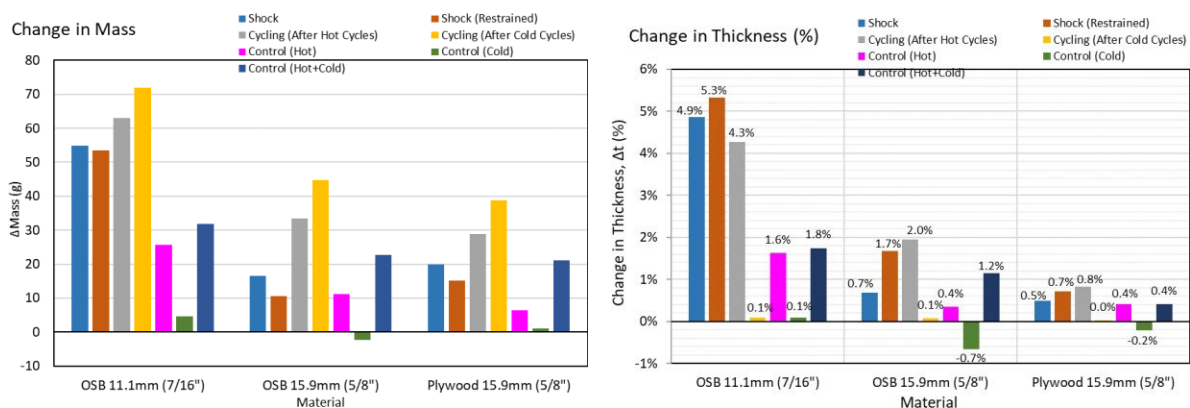
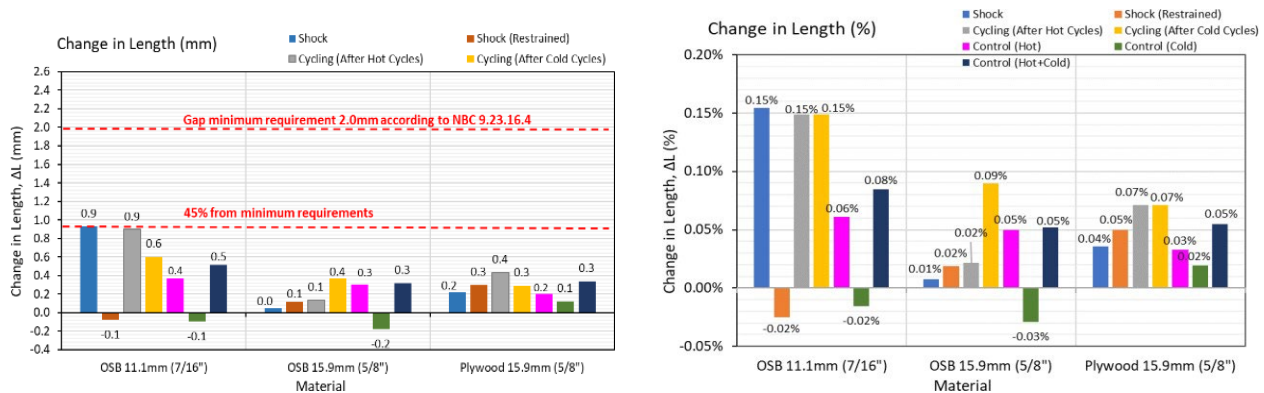


Figure 2: Percent change in MC (right) thickness (left) for OSB and Plywood after TS and TC

Excessive or prolonged exposure to moisture can lead to swelling, warping, and deterioration of OSB. This can weaken its structural integrity and affect its performance in construction applications. The National Building Code of Canada (NBCC) NBC 9.23.16.4 (NBC 2020) sets a minimum requirement of 2mm between sheets of plywood and OSB when installing it on a roofing structure to allow for natural



movement without causing damage. Selecting the appropriate type and grade of OSB for a specific application and ensuring proper installation and maintenance can help manage moisture-related concerns. Figure 3 illustrates that thinner 11.1mm (7/16") OSB sheathing reached 45% of NBC limitations, corresponding to a 0.15% change in board length after thermal shock and thermal cycling exposure. The percentage change will generally increase as the number of cycles increases. Moreover, Figure 3 illustrates that thicker 15.9mm (5/8") OSB sheets generally have a higher moisture penetration resistance than thinner ones. Thicker sheathing can provide a more effective barrier against moisture infiltration, essential for roofing applications where exposure to rain or humidity is a concern. Thicker OSB may be less susceptible to moisture-related issues because it has a greater volume of material that can absorb and distribute moisture, reducing the likelihood of localized problems such as delamination. The local climate and environmental conditions should also be considered when selecting OSB thickness.

Figure 3: Change in length in mm (left) and percent change (%) in length for OSB, plywood Modulus of Rupture (Flexural Strength) of Engineered Wood

Modulus of Rupture (MOR) measures peak flexural (bending) strength. The flexural properties of wood materials were determined according to ASTM D3043 (ASTM 2017) (Figure 4). The MOR of OSB can vary depending on factors such as the wood species used in its production process and the specific grade or quality of the OSB panel. Generally, plywood has a higher MOR than OSB, making it suitable for various structural and load-bearing applications in construction. Results show that thermal cycling and thermal shock exposure reduced the wood's peak strength (MOR), as shown in Figure 4. For plywood, reduction in MOR was most significant for specimens exposed to thermal cycling. Compared to the hot control and cold control conditioning protocol results, it is noticeable that plywood sheathing was more susceptible to thermal cycling and shock than OSB material. This may be attributed to plywood being porous, which absorbs water faster. However, the extended steady state of hot and humid exposure allowed adequate moisture to enter the sheet, which reduced the MOR of the 11.1mm (7/16") thick OSB sheet by 34%. Increasing the thickness of OSB of 15.9mm (5/8") slightly improved the sheet resistance to hot and humid exposure at a steady state.

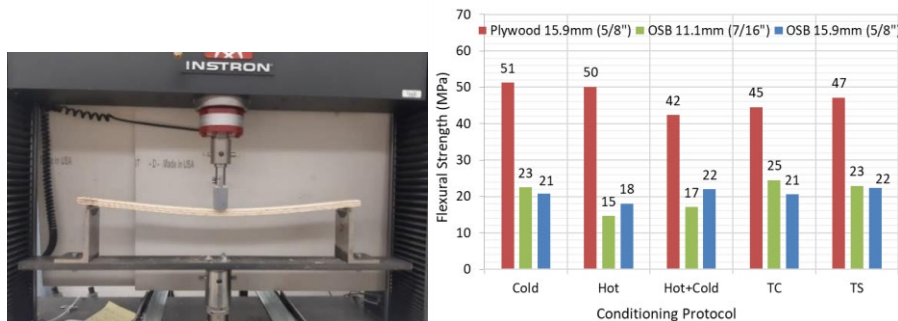


Figure 4: MOR test (ASTM 2017) (left), MOR results (right) for OSB, plywood after TS and TC

## Conclusions

In the evaluation of the impact of different environmental exposures on the deterioration of roof materials, several outcomes were achieved, as follows:

The extent of damage (material deterioration) depends on exposure time (duration and number of cycles), which varies from material to material. Different types of wood sheathing absorb water to various degrees. Wood sheathing expands or shrinks with changes in moisture content. The increase in moisture content is influenced by time and the capillary effect inherent to each wood type.

Below 80%RH, only minor liquid water is transported through the material, whereas as the humidity level increases, the amount of liquid transport begins to increase. Below 80%, RH plywood absorbs less water



compared to OSB sheets.

An OSB sheet of 11.1mm (7/16") thick experienced the most increase in thickness for all exposure conditions, followed by an OSB sheet of 15.9mm (5/8") thick. The water absorption rate is reduced as the OSB thickness is increased.

Plywood sheets of 15.9mm (5/8") thick had the slightest change (increase) in thickness compared to an OSB sheet performance result for 60% RH exposures.

OSB after thermal shock and thermal cycling had the most effect on thickness increase compared to steady-state conditioning. On the other hand, cold conditioning had the most negligible effect.

Thermal cycling is the predominant factor causing the increase in the thickness of materials having a thickness equal to or higher than 5/8".

Selecting the appropriate thickness and grade of OSB for a specific application considering local climate and ensuring proper installation can help manage moisture-related concerns.

Reduction in plywood MOR was most significant for specimens exposed to thermal cycling. Hot temperature allows for more water accumulation, followed by a cold exposure, which reduces material strength.

## References

ASTM D2126. 2020. "Standard Test Method for Response of Rigid Cellular Plastics to Thermal and Humid Aging." West Conshohocken, PA, USA, [www.astm.org](http://www.astm.org).

ASTM D3043 (2017). "Standard test methods for structural panels in flexure." West Conshohocken, PA, USA. ASTM D5516 (2018). "Standard Test Method for Evaluating the Flexural Properties of Fire-Retardant Treated Softwood Plywood Exposed to Elevated Temperatures." West Conshohocken, PA, USA.

Barnes. A, Winandy. J, McIntyre. C. Jones. P. (2009). "Laboratory and Field Exposures of FRT Plywood: Part 2— Mechanical Properties Parameters: Simulate field conditions, hygrothermal exposure and duration, and experimental design considerations." *Wood and fibre science: Journal of the Society of Wood Science and Technology* 42(1)

Bulger. B 2020. "Thermal Shock & Commercial Roofs – Signs And Remedies." [Thermal Shock & Commercial Roofs- Signs and Remedies - Weathercoat](#) accessed Aug 2023.

Canadian Commission on Building and Fire Codes. The National Building Code of Canada (NBCC) (2020). National Research Council of Canada (NRC)

Canadian Commission on Building and Fire Codes. The National Energy Code of Canada for Buildings (NECB) (2020). National Research Council of Canada (NRC)

Government of Canada. 2019. *Canada's Changing Climate Report*. (D. S. Bush, E. and Lemmen, ed.). Ottawa: Environment and Climate Change. CANADA.

Mcknight. M (2019). "How to prepare for thermal expansion." <https://www.phpsd.com/blog/>. Accessed May 2023.

Shyti. F., A. Gaur. A., Baskaran. B., (2023) "A Weather Shocks Protocol to Investigate Building Envelope Components for Changing Climate." Ontario Building Envelope Council. <https://obec.on.ca/sites/>

Smyth. M (2022). "HOT & GETTING HOTTER: Impact of Heat on Residential Roofs." <[HOT & GETTING HOTTER: Impact of Heat on Residential Roofs - Roofing Elements \(roofingelements.com\)](https://roofingelements.com)> Accessed June 2023.

# Can't Stop This: Documenting the Collision of Frozen Debris Lobe-A with the Dalton Highway, Alaska

Margaret M. Darrow, Ph.D., P.E., M.ASCE<sup>1</sup> and Ronald P. Daanen, Ph.D. (Posthumously)

<sup>1</sup>*Department of Civil, Geological, and Environmental Engineering, University of Alaska Fairbanks, P.O. Box 755900, Fairbanks, AK 99775-5900; email: [mmdarrow@alaska.edu](mailto:mmdarrow@alaska.edu)*

<sup>2</sup>*Alaska Division of Geological & Geophysical Surveys, 3354 College Road; Fairbanks, AK 99709*

## Abstract

The Dalton Highway, given its location and length, has experienced its share of geohazards and issues related to frozen ground since its construction. In the South-Central Brooks Range, the highway is currently being impacted by a slow-moving landslide in permafrost – otherwise known as Frozen Debris Lobe-A. We have mapped more than 40 frozen debris lobes (FDLs) within the Dalton Highway corridor; FDL-A is the largest and closest to the road. This forested landslide consists of frozen granular soil and woody debris that it incorporates on its way downslope. Over the past decade, FDL-A's rate of motion increased as it steadily moved towards the infrastructure. Recognizing the imminent threat, in 2018 the Alaska Department of Transportation and Public Facilities (ADOT&PF) realigned a portion of the Dalton Highway approximately 120 m downslope, leaving the abandoned section of highway embankment in place. In 2020, as part of an ADOT&PF-sponsored project, we installed inclinometers, piezometers, temperature sensors, pressure plates, and tilt meters within the abandoned highway embankment, and field cameras along the alignment, to monitor and record FDL-A's impact. As soon as the subsurface instrumentation was in place, it recorded horizontal displacement – FDL-A was already impacting the engineered structure at depth despite the fact that it was still 10 m away on the ground surface. FDL-A continued its steady pace downslope, officially touching the embankment in 2022. Here we present some of the initial results from the collision of FDL-A with the abandoned Dalton Highway embankment.

**Keywords:** Frozen Debris Lobe, Landslide, Dalton Highway Introduction

Like most highways in Alaska, the Dalton Highway has it rough; it endures frost heaving, thaw settlement, slush flows, avalanches, and unstable slopes. Here, we focus on one kind of unstable slope within the Brooks Range: Frozen Debris Lobes (FDLs). FDLs are slow-moving landslides in permafrost, typically consisting of silty sand with gravel and woody debris / organic material that is entrained within the lobe as it moves downslope (Darrow et al. 2016; Simpson et al. 2016). We began our observations of four FDLs in 2008 (Daanen et al. 2012), and have increased our scope to monitor nine FDLs. FDL-A (located at Dalton Highway Milepost 219) has received the most attention due to its proximity to infrastructure and steadily increasing rate of movement (Figure 1). Based on our initial research results (e.g., Darrow et al. 2013), engineers from the Alaska Department of Transportation and Public Facilities (ADOT&PF) decided to realign a portion of the Dalton Highway approximately 120 m downslope away from FDL-A; this realignment was completed in 2018. A portion of the original highway embankment was left in place in front of FDL-A, providing a unique opportunity to document the collision of a landslide with an engineered embankment. In 2020, our research team worked with personnel from the ADOT&PF Northern Region Materials Section to conduct a subsurface investigation and install geotechnical instrumentation. Here we summarize this full-scale field experiment, and present some of the initial results from the collision of FDL-A with the abandoned Dalton Highway embankment.

## Methodology

In August 2020, the research team drilled four 12.19-m deep boreholes through the abandoned embankment (see locations in Figure 1), in which we installed a MEMS-based in-place inclinometer (M-IPI), a vibrating wire piezometer (VWP), and a temperature sensor cable. On the uphill side slope (i.e., towards FDL-A) immediately adjacent to each borehole, we installed a 2 MPa pressure plate and tilt meter. We mounted each pressure plate and tilt meter to a steel plate, which we installed vertically into a slot dug into the embankment material. We installed a second pressure plate with a 5 MPa range adjacent to TH20-02. We routed all cables through a shallow trench to automated data acquisition systems (ADAS) located on the embankment surface and currently out of danger from FDL-A. At the ADAS location, we installed a time-lapse camera system programmed to take a daily photograph of FDL-A. We supplemented this with two additional field cameras, which served as backup and collected images of FDL-A from different viewpoints.

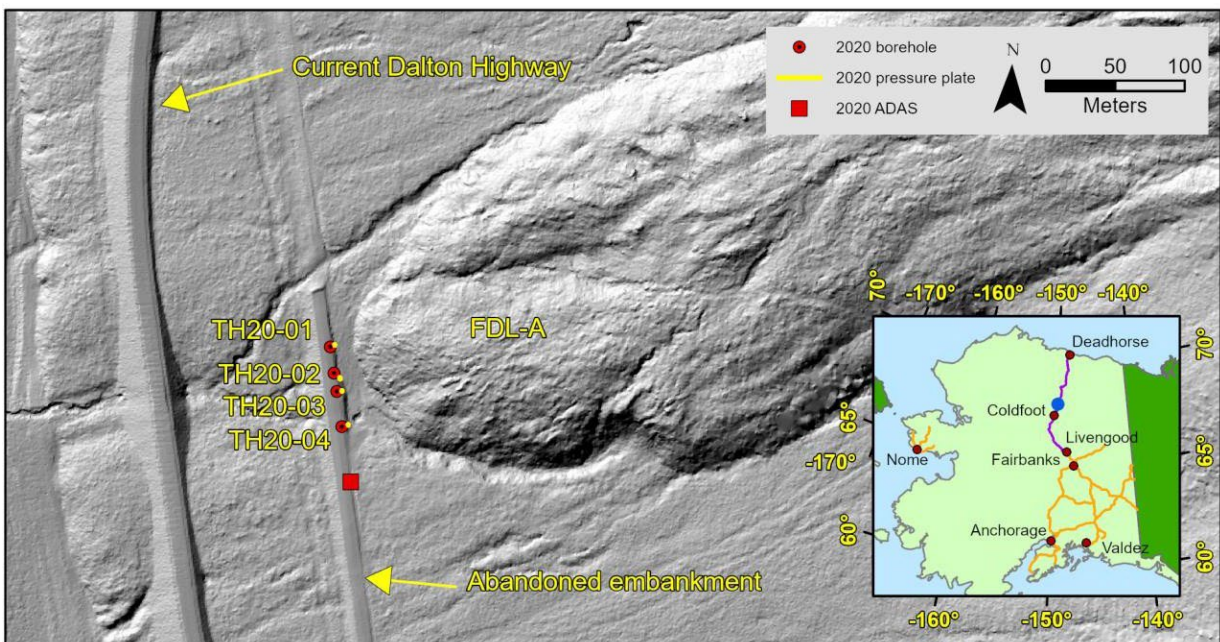


Figure 1. Location of FDL-A, 2020 boreholes, and instrumentation. Project location indicated by blue dot in the Alaska map inset.



### Preliminary Findings

Drilling indicated the embankment ranged from 3.05- to 3.66-m thick, and overlaid brown silty sand over highly weathered white mica schist bedrock, which we intercepted 4.27 to 9.75 m below the embankment surface. We intercepted the permafrost table in the three boreholes (TH20-01 through TH20-03), and a water table in TH20-01, TH20-02, and TH20-04.

The most significant finding comes from the M-IPI installations, some of which immediately recorded displacement in September 2020 while FDL-A was still approximately 10 m away from the abandoned embankment. By November 1, 2023 (i.e., date of last data download), the M-IPI in TH20-01 recorded 0.32 m of horizontal displacement (Figure 2), with shearing occurring approximately 7.6 m below the embankment surface at this location. This M-IPI also recorded about three times the displacement as in TH20-02 and TH20-03, indicating the close proximity of FDL-A to the northernmost borehole. The M-IPI in TH20-04, which was the farthest from the toe of FDL-A, demonstrated minor movement. As of November 1, 2023, we could not discern the 0.32 m of horizontal displacement in the daily photographs of the site; however, deformation of the western / downhill side slope became apparent in photographs from mid-December 2023.

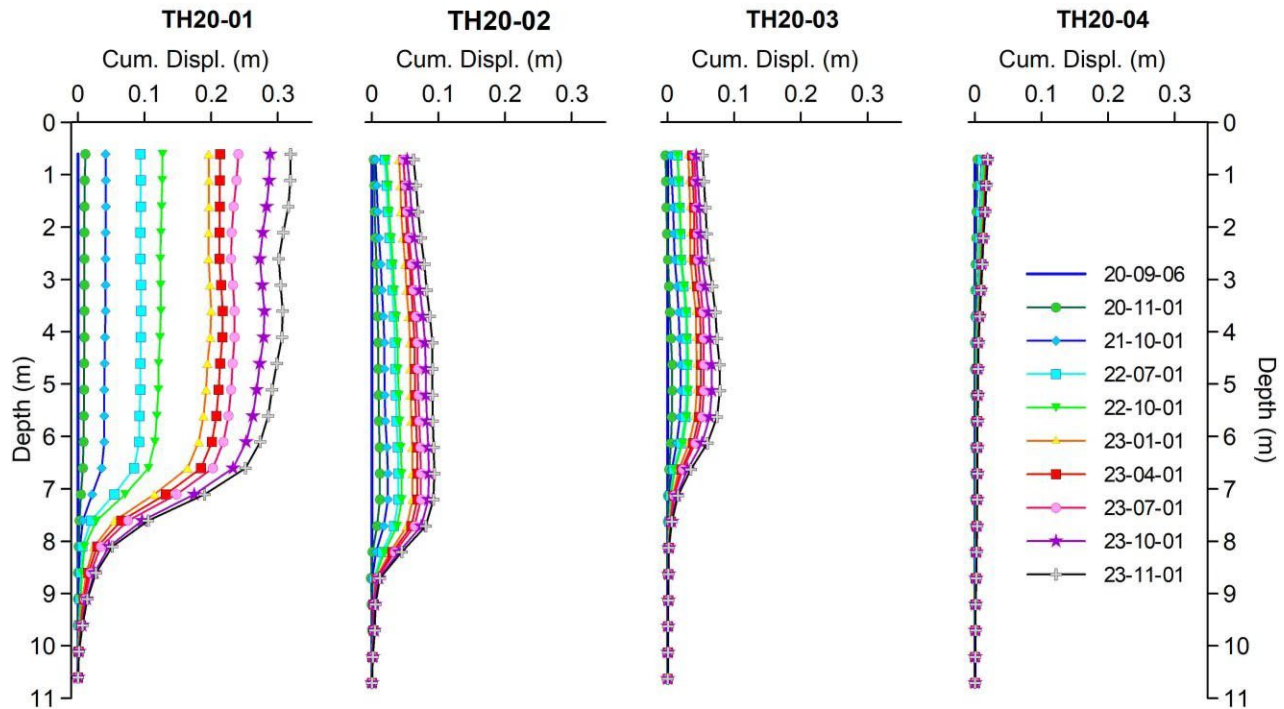


Figure 2. Cumulative displacement measurements in the A0 direction (i.e., west) for the 2020 M-IPI installations. Boreholes are from north (left) to south (right).

## Conclusions

The time-lapse photography and field observations indicated that FDL-A “officially” impacted the abandoned highway embankment in the summer of 2022, when it overlapped the uphill embankment side slope. The geomechanical instrumentation revealed, however, that FDL-A was already impacting the embankment years earlier, manifested as shearing at approximately 4 m below the bottom of the embankment at one borehole location. Based on analysis of the geology in the area, we hypothesize that FDL-A is shearing along the bedrock surface, and thus the presence of the highway embankment will do little to stop its downslope progression. More information about this research, including time-lapse videos of FDL-A’s movement, can be found at [fdlalaska.org](http://fdlalaska.org).

## Dedication

The lead author dedicates this publication to her co-author, long-time colleague in FDL research, and dear friend – Dr. Ronald (“Ronnie”) Daanen – who died in a helicopter crash while conducting field work on the North Slope of Alaska on July 20, 2023.

## Acknowledgments

This research was supported by a Pacific Northwest Transportation Consortium (PacTrans) grant (UWSC10217), an ADOT&PF grant (ADN 45-2-1065), and by ongoing support from the Alyeska Pipeline Service Company (APSC). The authors thank all of the University of Alaska Fairbanks students and ADOT&PF personnel for their expertise and enthusiasm during field work.

## References

- Daanen, R. P., Grosse, G., Darrow, M. M., Hamilton, T. D., Jones, B. M. (2012). “Rapid movement of frozen debris-lobes: implications for permafrost degradation and slope instability in the south-central Brooks Range, Alaska.” *Nat. Hazards Earth Syst. Sci.*: 12, 1521-1537, [doi:10.5194/nhess-12-1521-2012](https://doi.org/10.5194/nhess-12-1521-2012)
- Darrow, M. M., Daanen, R. P., Simpson, J. M. (2013). “Analysis of a frozen debris lobe: a first look inside an impending geohazard.” *ISCORD 2013: Planning for Sustainable Cold Regions*: <https://doi.org/10.1061/9780784412978.014>
- Darrow, M. M., Gyswyd, N. L., Simpson, J. M., Daanen, R. P., Hubbard, T. D. (2016). “Frozen debris lobe morphology and movement: an overview of eight dynamic features, southern Brooks Range, Alaska.” *The Cryosphere*: 10, 977-993, [doi:10.5194/tc-10-977-2016](https://doi.org/10.5194/tc-10-977-2016)
- Simpson, J. M., Darrow, M. M., Huang, S. L., Daanen, R. P., Hubbard, T. D. (2016). “Investigating movement and characteristics of a frozen debris lobe, South-Central Brooks Range, Alaska.” *Environmental and Engineering Geoscience*: 22, 259-277.

# History and update of the Cold Regions Utilities Monograph: a time-honored reference manual

Bridget Eckhardt

## **Abstract**

The American Society of Civil Engineers (ASCE) Cold Regions Engineering Division (CRED) was established in 1979 under the name Technical Council on Cold Regions Engineering (TCCRE) to assess and report the unique conditions that cold region environments have on infrastructure. The “Cold Regions Utility Monograph” (CRUM), originally published in 1979 under the name “Cold Climate Utilities Delivery Manual,” has been the staple reference manual for cold regions sanitation engineers for over three decades. The 3rd and most recent edition was published in 1996. While much of the information is still relevant, advances in technology and climate change suggest it is time to update the manual. The ASCE CRED Environmental & Public Health Engineering (EPHE) committee is updating the CRUM through a series of booklets. Each booklet will focus on an aspect of utilities engineering that is encountered when working in the arctic and subarctic regions. Design and construction considerations as well as case studies will be discussed. The initial proposed chapters include “Climate Change Resiliency”, “Water Source Development”, “Water Treatment,” “Geotechnical Considerations,” “Water Storage and Distribution,” and “Wastewater Collection and Treatment.” The booklets will be stand-alone, peer-reviewed publications. This presentation will review the history of the CRUM and the progress-to-date in the development of its successors.

# Evaluating the Impact of Microencapsulated Phase Change Material on Low Temperature Cracking Resistance of Asphalt Binder

Ayyaz Fareed, Anil Kumar Baditha, Ayman Ali, Ph.D., Yusuf Mehta, Ph.D., P.E., Wade Lein, Ph.D., P.E.

<sup>1</sup>*Center for Research and Education in Advanced Transportation Engineering Systems (CREATES), Rowan University, New Jersey 08028, USA. Email: fareed27@students.rowan.edu*

<sup>2</sup>*Center for Research and Education in Advanced Transportation Engineering Systems (CREATES), Rowan University, New Jersey 08028, USA. Email: baditha@rowan.edu*

<sup>3</sup>*Center for Research and Education in Advanced Transportation Engineering Systems (CREATES), Rowan University, New Jersey 08028, USA. Email : alia@rowan.edu*

<sup>4</sup>*Department of Civil and Environmental Engineering, Rowan University, Director, CREATES. Email: mehta@rowan.edu*

<sup>5</sup>*US Army Corps of Engineers, Engineering Research and Development Center, Cold Regions Research and Engineering laboratory. 72 Lyme Road, Hanover, NH 03755-1290, USA. Email: Wade.A.Lein@usace.army.mil*

## Abstract

This study aims to assess the impact of microencapsulated phase change material (MPCM) on the low-temperature cracking of asphalt binders. To achieve this objective, MPCM6D with melting point of 6°C was selected. This MPCM was introduced into PG 64-22 binder at varying dosages (0%, 5%, 10%, and 20% by binder weight) using a low-shear mixer. Subsequently, the laboratory tests were conducted on prepared binders to evaluate the influence of MPCM on thermoregulation, encompassing parameters like enthalpy change, low temperature properties (creep stiffness and stress relaxation) and complex shear modulus change rate of binders. The results of the study revealed a direct correlation between the dosage of MPCM and the observed enthalpy changes. Moreover, matching of measured enthalpies with the expected values confirmed effective thermoregulation achieved during blending process, demonstrating survivability of capsules. Additionally, analysis using bending beam rheometer results indicated increase in creep stiffness and slight reduction in creep rate, depicting decrease in low-temperature cracking resistance, for MPCM modified binders. Further, it was observed from temperature sweep results that the MPCM6D exhibited the ability to enhance low-temperature cracking within the thermoregulation range. In conclusion, this study recommends exploring MPCMs with broader thermoregulation ranges or combinations of MPCM to extend their performance across wider spectrum of temperatures.



# Designing a Lower Salt Future

Connie Fortin <sup>1</sup>

<sup>1</sup> *Low Salt Strategist. Bolton and Menk. Email: connie.fortin@bolton-menk.com*

## **Abstract**

Chloride, found in road salt to combat icy conditions, is a growing pollutant of concern across the snowbelt. This permanent pollutant contaminates drinking water, is toxic to aquatic life, ruins our infrastructure, and harms vegetation.

The amount of salt used on roads, parking lots and sidewalks is driven by many factors, including public pressure for high levels of service, changes to climate, winter maintenance strategies, infrastructure design, and planning.

Through Connie Fortin's passion for chloride reduction, over 20,000 winter maintenance professionals have been trained to integrate science into winter operations, with a focus on driving down salt use while still maintaining winter safety. In 2022, Connie launched a low salt design initiative to train Bolton & Menk's civil engineers, landscape architects, and stormwater experts for how to design for better winter performance. She tackled the problem areas described by plow drivers and brought new ideas to the desks of the designers.

Most of the already-existing sustainable initiatives are "green" and summer-focused: rain barrels, rain gardens, green roofs, cover crops, etc. It is time to increase our diversity by giving winter a prime seat at the table. As we look ahead to the next generation of low salt infrastructure planning and design, there is no extra cost, only extra benefit, to making safer winter surfaces with less salt required.

# Temperature Effects on CT in Un-Baffled Water Storage Tanks

William Fraser<sup>1</sup>

<sup>1</sup> *Lead Mechanical Engineer. Alaska Native Tribal Health Consortium. Email: william.fraser@anthc.org*

## Abstract

Water storage tanks have commonly been used as chlorine contact chambers to achieve regulatory disinfection requirements throughout the US and Alaska. The Alaska Department of Environmental Conservation (ADEC) and other regulators have accepted this strategy provided the engineer accounts for the incomplete mixing of chlorinated water within the tank. Baffle factor is defined as the quantity of water pumped into the tank from time = 0 to time when concentration at the outlet reaches 10% of the inlet concentration, divided by the volume of water in the tank. ADEC allows use of water storage tanks as contact tanks provided the engineer uses an assumed Baffling Factor of 0.1 and the tank inlet and tank outlet are located on opposite sides of the tank.

The regulations do not specify the orientation or configuration of the tank inlet and outlet other than requiring they are on opposite sides of the tank. In 2003 the US Environmental Protection Agency (EPA) published baffling factors for various tank configurations, with a baffling factor of 0.1 allowance in unbaffled mixed flow tanks. In 2014 The Colorado Department of Public Health and Environment published contact time guidance, recommending between 0.1 and 0.2 baffle factor for tanks without an inlet manifold, and between 0.1 and 0.5 with an inlet manifold. Colorado's recommendations were based on computational fluid dynamics (CFD) models of uniform temperature (isothermic) water flow through a tank and were conducted by Jordan M Wilson for his Master's thesis in 2011.

ANTHC has conducted tracer studies in the past of water storage tanks and found that an assumed baffling factor of 0.1 does not reliably provide the expected contact time, even with an inlet manifold. The effective baffling factor can vary from less than ½ to more than two times the regulatory allowance depending on the conditions under which the tracer study is performed and the effect is strongly dependent on the difference in temperature between water entering the tank and water in the tank.

To better understand observed performance, the Division of Environmental Health and Engineering (ANTHC- DEHE) developed a CFD model of the Igiugig, AK water storage tank that includes temperature effects under non-isothermic conditions. The Igiugig tank was chosen because two tracer studies were performed in 2016 which could be used to validate the model.

# Forensic Engineering in Snow Avalanche Science

Barbara Frigo<sup>1</sup>

<sup>1</sup>*Department of Structural, Buildings and Geotechnical Engineering, Politecnico di Torino, Corso Duca degli Abruzzi, 24 – Torino, Italy, email: barbara.frigo@polito.it*

## Abstract

The charm of the mountains in winter shows its tragic side when, due to natural causes or otherwise, it interferes with human leisure, work or daily activities. Snow engineering is characterized by considerable complexity, mainly due to the physical-mechanical properties of snow. If one adds to this basic complexity the complex and often-unknown dynamics of the initiation and propagation of the avalanche phenomenon, strongly influenced by human behavior, it is certain that the forensic engineer in this field faces a not simple task. Unlike civil engineering problems, avalanche accidents (avalanches affecting buildings, roads, cableways, infrastructures or accidents in the mountains or on snowy slopes) are rarely repetitive. So far, the case history (although not limited in the number of cases studied) does not help to establish a single investigation protocol. The paper proposes an overview of the critical issues addressed by the author in this field, together with some examples that may help (Frigo et al., 2015).

**Keywords:** Exceptionality, Predictability, Unrepeatable investigation, Acceptable risk, Rigopiano avalanche.

## Introduction

This increase in the "exposure" or "value" factor in the definition of risk has a major impact on avalanche damage to structures or infrastructure and/or avalanche accidents. Until the 1960s, the memory of avalanche accidents in the alpine environment was marked by catastrophic events in which numerous villages were swept away or destroyed. The causes of these extreme events were sought and identified in the lack of knowledge of the snowy terrain or the unpredictability of avalanches. The economic boom of the 1980s led to a greater use of the mountains, with a strong development of both urbanisation and winter sports, which now include activities outside the controlled areas (ski resorts). This increase in the "exposure" or "value" factor in the definition of natural hazards has a strong impact on avalanche damage to structures or infrastructure and/or avalanche accidents (Pivot, 2023).

While from a technical/engineering point of view, avalanches are classified according to, for example, their release (e.g. slab avalanches, spontaneous or artificial) or their dynamics (dense, powder or mixed avalanches), from a legal point of view, an avalanche can be 'unpredictable', 'intentional' or 'culpable', according to the possible offences and consequent penalties. In journalistic terms, they are always 'homicidal'.

Like Geotechnical Engineering, but in a more articulated way, Snow Engineering deals with the study of snow material, the design of defense infrastructures, the stability of snow-covered slopes and the dynamics of snow avalanches. In addition to the typical skills of snow science and meteorology, snow engineering also includes skills in structural, environmental, geotechnical and materials engineering.

The branch of forensic engineering that deals with this field is quite distinctive because of the technical problems (e.g. the well-known "non-replicability" of the state of the snow material), the innumerable casualties that can occur, and the strong influence of human behavior. As we know, any human behavior can give rise to criminal and/or civil liability if it involves the violation of rules established by law or is characterized by negligence, carelessness, incompetence or imprudence. For this reason, the avalanche offence - with consequential damage to persons or property - is expressly included in the offence of "public danger", within the framework of the rules governing "offences against public safety".

There are two basic questions on which the experts are called upon to provide a technical (i.e., objective) explanation to support judicial investigation: 1) whether the avalanche was foreseeable, despite its exceptional and extraordinary nature; 2) the cause of the triggering and subsequent release of the event that subsequently caused damage, injuries or victims (Frigo et al., 2015). Reflections on these two aspects are proposed here, based on the author's experience.

#### *The exceptional, but predictable snow avalanche*

These few lines show how complex the analysis of snow accidents is. The first difficulty lies in the large number of avalanche accidents and interferences: from the most frequent releases caused by ski mountaineers, to accidents on ski slopes or at their edge; from the interference on buildings, even in a "safe" area, to the inefficiency of defense structures, etc. ....

Hence, the first analysis is checking the predictability of the event. However, when analysing the occurrence of a natural (artificial or spontaneous) phenomenon, it is necessary to take into account the exceptionality of the event, a label that is immediately - and sometimes superficially - applied to these unrepeatable avalanche (Augenti and Chiaia, 2011). About snow avalanches, the exceptional nature of snow avalanche is often mistakenly assessed in terms of the (catastrophic) effects of the natural event and, therefore its dynamics; whereas the predictability must usually take into account the mechanisms of avalanche release. This technical predictability is variable depending on the scale of observation. The Avalanche Bulletin - or avalanche forecast - is valid for more or less extensive sectors on a regional or larger scale. The great variability of snow and weather conditions, which are strongly influenced by local orography and solar radiation, prevents the Avalanche Warning Service from providing an exact forecast. For this reason, the assessment of the local avalanche danger, i.e. the analysis of the local stability of the snowpack, is left to the individual user. Although it is difficult for the Avalanche Bulletin to assess the likelihood of a local avalanche, especially if it is caused by an accidental overload (e.g. the passage of a skier or snowmobiler), it is extremely negligent not to consult the Avalanche Bulletin before undertaking any activity on a snow-covered slope.

An example is the event occurred in the Cheneil basin in Valtournenche (AO, Italy) in February 2014, when an extreme avalanche surprised three forecasters of the regional Aosta Valley Avalanche Warning Service and a Heli-ski group, killing one of their guides (Chiambretti et al., 2016). Although the consultation of the regional Avalanche Bulletin by the Heli-ski guides was not part of the preventive measures for organising the excursion, it was documented for the forecasters: one of them had written it the day before. An example of the contextual validity of the regional Avalanche Bulletin was an exceptional spontaneous event that destroyed chalets in a supposedly safe area in the Gran Paradiso National Park, Valle d'Aosta - IT, in December 2008 (De Biagi et al., 2015). The avalanche, caused by an exceptional snowfall (more than 2 m of new snow in three days), was correctly forecast with the highest danger level, 5-VERY HIGH, so that, apart from the damage to buildings, there were no injuries or casualties. The same snow-meteorological criticality had a different outcome on the Piedmont side of the Gran Paradiso National Park, where a known large avalanche basin produced a spontaneous avalanche that destroyed houses (Maggioni et al., 2009). Two critical issues emerged in this case. The first was the presence of an improperly constructed avalanche defence structure in the upper part of the basin. The second highlighted a problem with the avalanche hazard map in the area, which defined the area as "safe" from avalanche interference, whereas it should have been in at least a medium hazard zone, according to historical data.



Figure 1. The Rigopiano avalanche of 18 January 2017 in Farindola, Abruzzo, IT with 29 victims. The destroyed hotel (a) before and (b) after the avalanche. (Frigo et al., 2020; Braun et al., 2020; Chiambretti et al., 2018).

### *The triggering causes*

Identifying the triggering causes of a snow avalanche is the most difficult task for the expert. There are many, but the most common are three: (1) snowpack stability (directly descending from the snow material and its layered structure, as well as the boundary and meteorological conditions); (2) local induced overload; (3) skier(s) behavior and unloading distances.

Among them, there is certainly the trigger, while the others will remain among the predisposing causes of the release. The most common problem encountered is the snowpack stability. It is precisely because of the strong temporal and spatial variability of the snowpack that it is difficult to study its structure and subsequent stability ex-post without the information provided by a stratigraphic survey and stability tests carried out immediately after the accident. The induced overload is also not easy to determine: a skier's load varies according to his or her weight, the



skiing mode (e.g. uphill or downhill, narrow or wide turns, speed, skiing with jumps or falls, etc.) and the distances maintained to other skiers (safe or lighter distances). Therefore, the analysis of the problem starts with an examination of the possible triggering scenarios, to arrive at the identification of the most probable triggering causes, thanks to the modelling of the possible structure of the snowpack and the induced point loads.

An example is an accident involving two skiers in the winter of 2013/14 (Frigo et al., 2015). They ventured down a well-known off-piste slope adjacent to controlled ski resort in Piedmont, IT. The second skier, who is less experienced, is in difficulty and on his way down, trying to follow the tracks of the first skier (who is waiting for him, but at a safety distance), falls several times. An avalanche breaks out and sweeps them both away. The less experienced skier was fatally buried. The subsequent investigation showed that the avalanche was triggered by this skier's fall, which generated a strong dynamic and impulsive overload.

#### *The unrepeatable investigation ad promptness*

On the analysis of snowpack stability, it is important to stress that it must be assessed locally, precisely because of the characteristics of the snow material. In fact, the snow material has mechanical characteristics that are variable in space and time, they cannot be defined ex-post, they cannot be reproduced, and they are strongly influenced by weather conditions, location and deformation, including artificial deformation (i.e. the phenomenon of fatigue to which the snowpack is subjected when skiers pass by). This prevents the technical expert from replicating the conditions and associated laboratory tests for the analysis of snow material properties. This raises another issue: the promptness of the investigation. Ideally, the expert should have immediate access to the accident location, along with the rescue crew. As this is usually not possible, it is necessary that post-event investigations are carried out by trained personnel who, in addition to the classic geometric measurements (e.g. avalanche perimeter, height of deposit, etc...), immediately document any skier tracks, the presence of signs, etc. with photographic material, snow surveys and snowpack stability tests. Quite rightly, rescue operations are given priority and any survey is postponed until days after the event, risking that the location may have been even only by wind action alone or by fresh snowfall.

#### **Conclusions**

As can be seen from these few lines, the forensic engineer in the "snow" sector needs to have an interdisciplinary technical and cultural background, ranging from structural, environmental, geotechnical and materials engineering skills to snow and meteorological expertise, as well as in-depth knowledge of technical and administrative operations, etc... The subject matter is so specific, so vast, and so lacking in regulatory and behavioural recommendations that it is almost impossible to draw up a single investigation protocol to guide the professional entrusted with the task of expert witness. It also touches on a sector at the interface between the ski industry (ski resorts, technical equipment, etc.), mountain culture and passion (ski mountaineering, snowmobile routes, etc...) and social behavior. In this way, 'technically acceptable risk' takes a back seat to 'socially acceptable risk'. The latter is often conflated with the concept of 'freedom'.

#### **References**

Frigo B., Chiaia B. (2015). L'ingegneria Forense e la neve. III Convegno di Ingegneria Forense VI Convegno su CRolli, Affidabilità Strutturale, Consolidamento - IF CRASC'15, Sapienza Università di Roma, 14-16 maggio 2015, pp. 795 -806. ISBN 978-88-579-0447-4.

Pivot, S. (2023). “Incidenti da valanga in Italia: stagione 2021-2022”. *Neve e Valanghe*, n. 96, pagg. 4 - 11.

Augenti N., Chiaia B. (2011): *Ingegneria Forense – metodologie, protocolli, casi studio*. Dario Flaccovio Ed., ISBN 9788857901015, pagg. 504.

Chiambretti I, Chiaia B. and Frigo B. (2016). Triggered avalanches – A case study in Italian Alps. *Proceeding of I International Snow Science Workshop, Breckenridge- Colorado, October 3-7.*

De Biagi V., Chiaia B., Frigo B. (2015): Impact of snow avalanches on buildings: Forces estimation from structural back-analyses. *Engineering Structures* 06/2015; 92. DOI: 10.1016/j.engstruct.2015.03.004

Maggioni, M., Caimi, A., Godone, D., Freppaz, M., Bertea, A., Cordola, M., Prola, M.C., Bertoglio, V., and Frigo, B. (2009). The avalanche events of December 2008 in Ceresole Reale (Piedmont Western Italian Alps), *Proceedings of ISSW 2009, September 28 – October 2nd, 2009, Davos (CH)*, pagg. 25-29.

Frigo, B., Bartelt, P., Chiaia, B., Chiambretti, I., Maggioni, M., 2020. Reverse Dynamical Investigation of the Catastrophic Wood-Snow Avalanche of 18 January 2017 at Rigopiano, Gran Sasso National Park, Italy. *Int J Disaster Risk Sci.* <https://doi.org/10.1007/s13753-020-00306-6>.

Braun, T., Frigo, B., Chiaia, B., Bartelt, P., Famiani, D., Joachim Wassermann, J., 2020. Seismic signature of the deadly snow avalanche of January 18, 2017, at Rigopiano (Italy). *Sci Rep* 10, 18563. <https://doi.org/10.1038/s41598-020-75368-z>.

Chiambretti, I; Chiaia, B; Frigo, B; Marelli, S; Maggioni, M; Fantucci, R; Bernabei, M. 2018. The 18th January 2017 Rigopiano avalanche disaster in Italy - Analysis of the applied forensic field investigation techniques, In: *Proceedings of International Snow Science Workshop, Innsbruck (A) 2018*, pag. 1208- 1212

Frigo B., Prola M. C., Faletto M. (2012): Valutazione della stabilità del manto nevoso: linee guida per la raccolta e l'interpretazione dei dati. *Regione Autonoma Valle d'Aosta*. pagg. 111

# Temperature effect on the Relationship between flexural strength and compressive strength of ice

Alessandro P. Fantilli<sup>1</sup>, Barbara Frigo<sup>2</sup>, Farmehr M. Dehkordi<sup>3</sup>

<sup>1</sup>*Corso Duca degli Abruzzi 24 – Torino (Italy), alessandro.fantilli@polito.it, Politecnico di Torino.*

<sup>2</sup>*Corso Duca degli Abruzzi 24 – Torino (Italy), barbara.frigo@polito.it, Politecnico di Torino.*

<sup>3</sup>*Corso Duca degli Abruzzi 24 – Torino (Italy), farmehr.mohammadpourdehkordi@studenti.polito.it, Politecnico di Torino.*

## **Abstract**

The practical usage of ice has increased significantly in recent times, as it is a readily available material utilized in various applications, such as temporary constructions and permanent hydraulic structures. Consequently, there is a growing practical interest in developing models that can accurately compute the flexural strength of ice based on its compressive strength. Following the testing procedure recommended by UNI EN 196 for cement-based mortars, three-point bending, and compression tests were conducted on 40mm × 40mm × 160mm ice prisms, specifically prepared under different temperature conditions. Through these tests, the ratio between flexural and compressive strengths of ice were determined. As the effect of temperature on ice is comparable with that of water/binder ratio on cement-based mortars, the flexural/compressive strength ratio of ice also depends on the frozen temperature.

# Climate Change Impacts to Arctic Airfields

James J. Frye, M.S.<sup>1</sup>

<sup>1</sup>*The Civil Engineer School, Air Force Institute of Technology, 2950 Hobson Way, Wright-Patterson AFB, OH 45433; email: james.frye.6@us.af.mil*

## **Abstract**

This open-ended research investigates the correlation between climate history, climate change, and pavement infrastructure performance for specific airfields in Arctic and Subarctic Alaska. Parameters such as temperature, air indices, and permafrost extent are compared to PAVER pavement management system data and construction costs for four locations. Site criteria are developed and implemented to select airfields for analysis that provide representative conditions. Climate data is analyzed to show the range of variability and temporal trends. Geotechnical borehole data is consolidated to portray nominal local permafrost extent. Data trends show that the depth of upper extent of permafrost at locations is increasing with time. PAVER family curves compare degradation rates and airfield pavements in areas with permafrost were shown to degrade two-three times faster compared to locations absent of permafrost. Regression of Pavement Condition Index (PCI) degradation rate and permafrost upper extent showed correlation. Construction cost histories from the Federal Aviation Administration Airport Improvement Program are included in trend analyses. Cost estimates for typical maintenance treatments are generated and applied to pavement inspections to model maintenance requirements and predict changes in airfield rehabilitation frequency.

# Sliplining a Failing 54-inch Stormwater with 42-inch FRP in Anchorage

Brian Gastrock<sup>1</sup>, Jonathan Hartford<sup>1</sup>

<sup>1</sup> *Coffman Company*

## Abstract

In Anchorage, Alaska, an existing 54-inch corrugated metal pipe (CMP), approximately 1,600 feet in length, is nearing the end of its useful life. The pipe experienced a sinkhole and the alignment is difficult to access private residential back yards. The sinkhole prompted a closed-circuit television (CCTV) inspection in 2019/2020. To prevent further development of the existing sinkhole, as well as allow time to complete the design and bidding, an emergency repair pipe-patch was installed in 2021 at the sinkhole location. The new slipline product design was a 42-inch fiber reinforced polymer (FRP) to accommodate the design flows. Design included evaluation of multiple trenchless technologies, including cured in place pipe (CIPP) and sliplining. Limited site access along the alignment, property easements, limited soils information, and bypassing flows impacted the design.

The project challenges included:

- Restricted access to back yards for access to manholes and excavations, with long-term surface improvements including sheds, fences, and landscaping.
- Gravity sewer main installed through existing stormwater pipe alignment, requiring a detailed bypass design.
- Reduced cross-sectional area due to ovality required smaller slipline pipe.
- Temporary construction easements required to minimize surface disturbance.
- Reroute and abandonment of parallel smaller stormwater pipe required additional survey, inspection, and design.

Initial evaluation of the project anticipated cured in place pipe (CIPP) installation, but the evaluation of the process concluded the need for excavations at each manhole, requiring significant surface upgrades and access improvements. Sliplining was determined as a viable alternative requiring two excavations which ultimately was selected for the rehabilitation design. The project was constructed in the summer of 2023.



# Role of Aggregate Types on De-Icing Salt Resistance of Ultra-High-Performance Concrete

Nader Ghafoori<sup>1</sup>, Andrew Pappas<sup>2</sup>, Ariful Hasnat<sup>3</sup>, Aderemi Gbadamosi<sup>3</sup>

<sup>1</sup>Professor Department of Civil and Environmental and Construction, University of Nevada, Las Vegas, USA. Phone: (702) 8952531, Email: [nader.ghafoori@unlv.edu](mailto:nader.ghafoori@unlv.edu).

<sup>2</sup>MSE student, Department of Civil and Environmental Engineering and Construction, University of Nevada, Las Vegas, USA. Email: [pappaa3@unlv.nevada.edu](mailto:pappaa3@unlv.nevada.edu).

<sup>3</sup>PhD candidate, Department of Civil and Environmental Engineering and Construction, University of Nevada, Las Vegas, USA. Email: [hasnat@unlv.nevada.edu](mailto:hasnat@unlv.nevada.edu).

<sup>3</sup>PhD student, Department of Civil and Environmental Engineering and Construction, University of Nevada, Las Vegas, USA. Email: [aderemi.gbadamosi@unlv.edu](mailto:aderemi.gbadamosi@unlv.edu).

## Abstract

In recent years, ultra-high-performance concrete (UHPC) has attracted interest from the research community because of its excellent physical, mechanical, and durability properties. However, due to its very high production cost, utilization of UHPC is very limited. In this context, a detailed experimental investigation was conducted to utilize locally-available fine aggregates in producing UHPCs that will help in reducing their production cost. This study reports on freeze-thaw resistance with deicing salt of the non-propriety UHPCs containing different fine aggregate and cementitious materials. Two distinct fine aggregate types, plaster sand and masonry sand, were each combined with coarser concrete sand to create a unique aggregate blend for the studied UHPCs. A total of 12 plain and fiber - reinforced UHPCs were batched using a uniform water-to-cementitious materials ratio of 0.21. The aggregate-to-cementitious materials ratio of 1.2 was kept uniform for all studied UHPCs. Due to the dense microstructure of the studied UHPCs, both masonry and plaster fine aggregates displayed similar resistance to freezing and thawing with deicing salt with mass losses ranging from +0.05 to -0.15% after 60 F-T cycles. The studied tertiary UHPCs exhibited reduced mass loss in comparison to that of the equivalent reference UHPC.

# Mapping coastal bluff erosion. Case study at Pt. Woronzof, Alaska

Gennady Gienko, Ph.D.

*Department of Geomatics, University of Alaska Anchorage, 3211 Providence Drive  
Anchorage, AK 99508; email: ggienko@alaska.edu*

## **Abstract**

The paper illustrates the use of historical survey data and aerial photographs to calculate the rate of erosion at Pt. Woronzof from 1909 until the present. The high-resolution 3D spatiotemporal models of the bluff since 2016 were created using methods of terrestrial photogrammetry and SFM and used to evaluate the impact of wave actions on the erosion.

**Keywords:** Coastal erosion, 3D modeling, photogrammetry, SFM

## **Introduction**

Erosion of coastal bluffs can be characterized by several parameters, including bluff retreat rates representing long-term averages useful over the lifespan of economic development in the area, and slope stability analysis which is used to evaluate the likelihood of sudden (catastrophic) failures based on a quantitative model of stability of a slope. The retreat rates can be evaluated in planimetric view (2D), but the assessment of bluff stability requires extensive datasets to evaluate material strength (cohesion, friction angle) and weight, as well as a detailed 3D spatio-temporal model of slope geometry (Johnsson, 2003).

Classical methods for 2D mapping of coastal shorelines employ topographic maps, historical surveying observations, and aerial photographs. These data provide a very good chronological perspective of coastal erosion, including the estimation of long-term averages of coastal retreat rates, but they do not allow for a comprehensive assessment of the dynamics coastal bluffs. In topographic maps, the surface relief is shown by contour lines, but due to abrupt elevation changes, bluffs in topographic maps are often represented by symbols indicating the presence of a bluff rather than quantitative details of elevation. In classical aerial surveying, the nadir-viewing cameras take nearly horizontal photographs to be parallel to the average ground surface; these camera settings were optimized for topographic mapping. Such horizontal photographs have been available since the 1950s until the present. They are a great source of 2D mapping of the coastline, but not suitable for precision mapping of inclined surfaces such as faces of steep slopes.

A typical approach in 3D coastal mapping is to create a series of profiles using surveying methods such as profile leveling or topographic surveys with a total station or RTK GPS. Those methods have certain limitations in mapping the topography at a high resolution; besides, if the bluff face is steep and not accessible on foot, surveys are often limited to the beach area (terrace). Very detailed and precise 3D models of bluffs can be created using terrestrial laser scanning. Apart from high cost, substantial weight, and bulky equipment, challenges of transportation to remote areas and data collection in inclement Arctic weather conditions are among the prohibitive factors.

The recent developments in two areas, low-cost aerial platforms (drones) and semi-automatic photogrammetry (Structure From Motion, SFM), open some new avenues for creating 3D models of coastal bluffs. Drones can take oblique images, solving the limitations of classical aerial

photography. Drone mapping is a promising technique but it comes with its limitations, including flight stability in winds. While some studies illustrate the stability of fixed-wing drones in wind speed up to 25mph (ATMOS, 2021), the most cost-effective and widely used multi-rotor drones have more challenges. For example, if the wind is strong enough, one or more motors can momentarily be driven in reverse, potentially causing the propeller to unscrew and spin off (McCord, 2018). At the same time, terrestrial photography with a consumer-grade digital camera is a proven and reliable method for high-precision 3D modeling of slant and vertically oriented surfaces. Low cost and compact equipment, no need for extensive training, user-friendly software, and accuracy comparable with terrestrial laser scanning are clear advantages for using terrestrial photogrammetry for precise 3D mapping of coastal bluffs.

The goal of this paper is two-fold. First, to evaluate the bluff retreat rate at Pt. Woronzof using all available 2D data from the 1900s until the present. Second, to use terrestrial photography and SFM to create a high-resolution spatial-temporal 3D model of the bluff face for analysis of the stability of the slope.

### **Literature review**

Many publications relate coastal erosion to climate change, sea rise, and economic development, highlighting the importance of this topic (USGS, 2016, USGS, 2022, Warren, et.al., 2006, Horen, et. al., 2023). The use of classical surveying instruments (cross-section leveling and electronic theodolites) for monitoring coastal erosion in Alaska is presented in (Monitoring, 2009). (Cunningham, et. al., 2015) used terrestrial laser scanning to understand changes in slope characteristics along Alaskan highways. There is an extensive range of literature related to the use of Structure from Motion for mapping coastal erosion (Letortu, 2017, Pikelj, 2018, Westoby, 2018). For example, (Kelly & Belmont, 2018) used a combination of SFM and time-lapse photogrammetry to document rapid river bluff erosion in south-central Minnesota. (Coveney et. al., 2010) used RTK GPS and very high-resolution terrestrial laser scanning to quantify the elevation accuracy of a 10 km coastal section of DEM compiled from conventional aerial photography. One of the most extensive studies using terrestrial laser scanning for coastal 3D mapping was done in 2003-2006 in California (Collins & Sitar, 2008). Over 5 years, they used a terrestrial laser scanner up to four times over each winter season. The point cloud with an average point spacing of 10 cm is then post-processed to provide high-resolution (0.5 m maximum point-to-point spacing) surfaces and cross-sections for analysis including volumetric change, overall crest retreat, and failure morphology.

They also collected terrestrial photographs, but used them for visual interpretation only.

### **Methodology**

Coastal bluff at Pt. Woronzof is in direct proximity to Ted Stevens International Airport in Anchorage. It is also a popular place for recreation along the Tony Knowles coastal trail. Its steep shoreline slope is formed in sediment (loose material such as clay, sand, and gravel) that has about 120 ft vertical elevation above the high tide line. The bluff spans over 2700 ft and its steep face is exposed to the combined impact of the weathering and waves at high tides. The tide range at Pt. Woronzof is 32 ft, which is the highest in the United States. According to the classification, provided by (Maine Geological Survey, 2011), Pt. Woronzof is a highly unstable bluff with an unvegetated bluff face and a beach/gravel flat shoreline. The bluff face is too unstable to support vegetation. The bluff is eroded by waves to create a mixed sand and gravel beach in front of the bluff.

Evaluation of the bluff retreat rate. The earliest documented surveying observations (single point measurements) at Pt. Woronzof are dated 1909 and then scattered between 1920-1960s (NGS, 2023). The survey points provide valuable historical insight into the erosion, but to calculate the retreat rate, the observations should be made at the edge of the bluff. Overlaid with the bluff edge locations from 1909 to 1954 published by USGS (Miller & Dobrovlny, 1959), the data were used to calculate the average retreat rate of 1.9 feet per year. The rate of erosion between 1950 and 2018 was calculated using aerial photographs. Fig. 1 represents the digitized bluff edge. The average retreat rates at different sections of the bluff range from 0.9 ft/yr to 1.8 ft/yr. The cross-section shown in yellow is placed at the same location used to evaluate the erosion rate from 1909-1954.

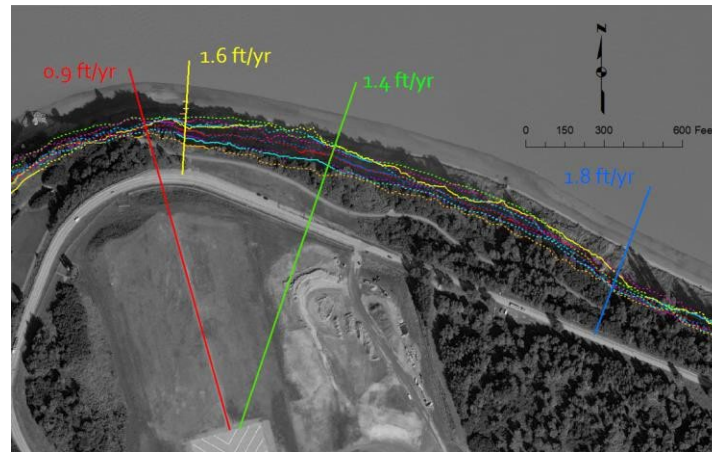


Fig. 1. Coastal line reconstructed from aerial photographs from 1950-2018, with the average erosion rate along different cross-sections.

*High-resolution 3D surface modeling.* Several sets of terrestrial photographs of the bluff were collected twice a year in 2016-2018, and 2022-2023, and comprise over 9,500 photographs. A typical one-day data set contains 250-300 photographs, processed using Structure from Motion (SFM). Each SFM model has a very high uniform spatial resolution (1-2 inches on the ground) over the entire span of the bluff (2700 ft), resulting in a dense point cloud up to 275M points. To evaluate the impact of the waves on the erosion some data sets were captured daily, 4-5 days before and after the highest tide, covering 8-10 consecutive days. These high-spatial and high-temporal resolution “snap-shot” models can be used to analyze the short-term dynamics of the bluff, including time lapsing the hot spots and documenting episodic failures. Coupled with the observations of wind, temperature, and precipitation, such time-stamped models can be used to build comprehensive prediction models of erosion during the high tides (erosion peaks).

The periodic nature of the bluff erosion process can be described in terms of the frequency of harmonic signals: low frequency (seasonal weathering) and high frequency (wave actions during high tides). Figure 2 (left) illustrates the harmonic nature of the weathering and wave actions.

During the high tides, the sea level rises to 4 feet above the base of the bluff, and, if the winds are strong, the waves excavate the bottom of the bluff at a high, sometimes, dramatic rate. Figure 2 (right) illustrates the recess of the bluff as a combined result of two consecutive high-tide actions and weathering that occurred in 35 days in Fall 2016.

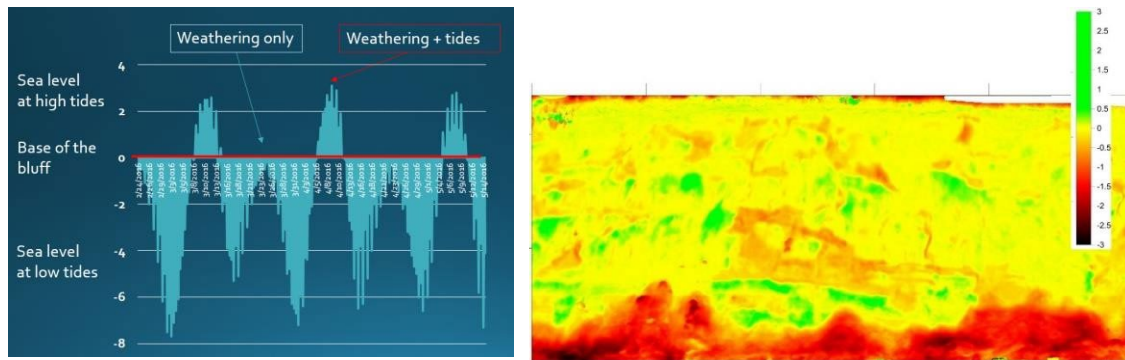


Fig. 2. Tide heights relative to the bluff base level (left, tides are in feet), and retreat of the bluff between October 13 - November 18, 2016 (right, displacements are in meters)

## Findings

The first part of the study focuses on the assessment of the long-term dynamics of coastal bluff erosion at Pt. Woronzof. The average retreat rate, calculated over the history of all observations at Pt. Woronzof from 1909 until present, is 1.9 ft/yr. Another focus was to create a time series of 3D models for precision modeling of bluff erosion. The time-lapsed models indicate that erosion at the hot spots, triggered by wave actions, can reach up to 1-1.5 m (3-5 ft) in a single day.

Compared to seasonal variations, deviations in the high-frequency component are more noticeable, and often can be linked to episodic bluff failures and the appearance of the local “hot spots”. The detected hot spots of erosion can be used to guide the detailed geological mapping of the bluff to evaluate the softness of the bluff material, as well as the identification of prevailing winds (and seasonal atmospheric conditions) defining the intensity of waves during the high tides. The aggressiveness of waves during high tides depends on the wind, so the slope analysis model should include weather observations such as air temperature, wind speed and direction, and rain, as well as the slope aspect and exposure to the sun to evaluate the impact of seasonal weathering.

## Conclusions

This study illustrates the effectiveness of terrestrial photography and SFM for the 3D modeling of coastal bluffs in Arctic and sub-Arctic regions. The collected data and models can be used for the assessment of potential risks, planning for measures for shoreline stabilization at the Pt. Woronzof, and serve as a framework for studying sandy bluff erosion in Dillingham, Utqiagvik, and other coastal communities in Alaska.

## Acknowledgments

Aleksey Voloshin, Evan Venechuk, and Brandon Hoxie were instrumental in collecting several data sets and building 2D and 3D models of the bluff as part of their capstone projects at UAA.

## References

ATMOS. (2021) Drone surveying in high-wind conditions <https://geo-matching.com/articles/drone-surveying-in-high-wind-conditions>

Collins, B.D., Sitar, N. (2008). Processes of coastal bluff erosion in weakly lithified sands, Pacifica, California, USA. *Geomorphology* 97 (2008) 483–501, doi:10.1016/j.geomorph.2007.09.004



- Coveney, S., Fotheringham, A.S., Charlton, M., and McCarthy, T. (2010) Dual-scale validation of a medium-resolution coastal DEM with terrestrial LiDAR DSM and GPS. *Computers & Geosciences*, Volume 36, Issue 4, 2010, Pages 489-499, ISSN 0098-3004, <https://doi.org/10.1016/j.cageo.2009.10.003>.
- Cunningham, K.W., Olsen, M., Wartman, J., Dunham, L. (2015). A Platform for Proactive Risk- Based Slope Asset Management – Phase II. Final Project Report. (2015). Alaska University Transportation Center.
- Horen, K., Nieminski, N., Poisson, A., Christian, J. (2023). Monitoring Event-driven Erosion in Wainwright, Alaska. The importance of high-resolution data for capturing change on the Arctic Coast. (2023) Alaska Division of Geological & Geophysical Surveys (DGGS). <https://storymaps.arcgis.com/stories/f79f67a5f92b4110b09ebef0b5e2f466/print>
- Johnsson, M.J. (2003). A primer on coastal bluff erosion. California Coastal Commission. <https://www.coastal.ca.gov/publiced/waves/coastal-erosion.pdf>
- Kelly, S.A., Belmont, P. (2018) High-Resolution Monitoring of River Bluff Erosion Reveals Failure Mechanisms and Geomorphically Effective Flows. (2018) *Water* 2018, 10, 394; doi:10.3390/w10040394
- Letortu, P., Jaud, M., Grandjean, P., Ammann, J., Costa, S., Maquaire, O., Delacourt, C. (2017). Examining high-resolution survey methods for monitoring cliff erosion at an operational scale. *GIScience & Remote Sensing*, 55(4), 457-476. doi:10.1080/15481603.2017.1408931
- Maine Geological Survey (2011). Types of bluffs along Maine's coast. <https://www.maine.gov/dacf/mgs/explore/marine/facts/bluff.htm>
- McCord, M. (2018). Flying in High Winds – What Could Possibly Go Wrong? <https://www.fad-photo.com/2018/10/25/flying-your-drone-in-high-winds>
- Miller, R.D., and Dobrovolsky, E., (1959). Surficial geology of Anchorage and vicinity, Alaska. U.S. Geological Survey Bulletin 1093, 128 p.
- Monitoring Beach Erosion at Hooper Bay, Alaska (2009). [https://engineering.purdue.edu/CE/AboutUs/News/Geomatics\\_Features/files/Hooper\\_Bay.pdf](https://engineering.purdue.edu/CE/AboutUs/News/Geomatics_Features/files/Hooper_Bay.pdf)
- NGS (2023). Survey marks and datasheets. NOAA, National Geodetic Survey. <https://geodesy.noaa.gov/datasheets/>
- Pikelj, K., Ružić, I., Ilić, S., James, M. R., & Kordić, B. (2018). Implementing an efficient beach erosion monitoring system for coastal management in Croatia. *Ocean & Coastal Management*, 156, 223-238. doi:10.1016/j.ocecoaman.2017.11.019
- USGS (2016). An Inside Look at Eroding Coastal Bluffs on Alaska's North Slope (U.S. Geological Survey, 2016) <https://www.usgs.gov/centers/pcmssc/news/inside-look-eroding-coastal-bluffs-alaskas-north-slope>
- USGS (2022). Coastal Climate Impacts. USGS Pacific Coastal and Marine Science Center. June 27, 2022 <https://www.usgs.gov/centers/pcmssc/science/coastal-climate-impacts>
- Warren, J.A., Berner, J.E., Tine Curtis, T. (2006) *Climate Change and Human Health: Infrastructure*

Impacts to Small Remote Communities in the North. *International Journal of Circumpolar Health* 64(5):487-97 DOI: 10.3402/ijch.v64i5.18030

Westoby, M. J., Lim, M., Hogg, M., Pound, M. J., Dunlop, L., & Woodward, J. (2018). Cost-effective erosion monitoring of coastal cliffs. *Coastal Engineering*, 138, 152-164.  
doi:10.1016/j.coastaleng.2018.04.008

# Vibration Characteristics of Degrading Warm Permafrost from the Analysis of Ambient Noise Data: A Case Study from Bethel, Alaska

Annika Goozen<sup>1</sup>, Yue Zhao<sup>2</sup>, Utpal Dutta, Ph.D.<sup>3</sup>, Zhaohui (Joey) Yang, Ph.D., M. ASCE<sup>4</sup>

<sup>1</sup>Department of Civil Engineering, University of Alaska Anchorage, Anchorage, 3211 Providence Drive, Anchorage, AK 99508 USA; email: [aggoozen@alaska.edu](mailto:aggoozen@alaska.edu)

<sup>2</sup>College of Engineering and Mines, University of Alaska Fairbanks, PO BOX 755960, Fairbanks, AK 99775-5960, AK, USA; email: [yzhao8@alaska.edu](mailto:yzhao8@alaska.edu)

<sup>3</sup>Department of Civil Engineering, University of Alaska Anchorage, Anchorage, 3211 Providence Drive, Anchorage, AK 99508 USA; email: [udutta2@alaska.edu](mailto:udutta2@alaska.edu)

<sup>4</sup>Department of Civil Engineering, University of Alaska Anchorage, Anchorage, 3211 Providence Drive, Anchorage, AK 99508 USA; email: [zyang2@alaska.edu](mailto:zyang2@alaska.edu)

## Abstract

Climate-induced permafrost warming poses a threat to seismic hazards in regions like western Alaska, adding the need for a deeper understanding of this intricate relationship. Despite the potential risks, a significant research gap persists, and this study fills that void by analyzing twelve months' worth of ambient noise time series data from accelerometers strategically installed in Southwest Alaska, where permafrost degradation has caused severe threats to the built-in infrastructure. By delving into the seismic intricacies of areas characterized by both permafrost and heightened seismic activity, the research aims to fortify preparedness strategies against seismic hazards exacerbated by permafrost degradation.

**Keywords:** Seismic Hazard, Ambient Noise, Permafrost, Accelerometers

## Introduction

Examining data from two seismic sensors reveals a compelling correlation between soil conditions and ground motion amplification. Notably, ground motion amplification peaks during months with unfrozen soil, underlining the profound impact of permafrost degradation on seismic vulnerability. These findings underscore the critical necessity of comprehending the dynamics in predicting and mitigating seismic risks in permafrost-laden regions.

Permafrost degradation, exacerbated by the anthropogenic activities and relentless forces of climate change, imposes multifaceted challenges on Alaskan communities. Its adverse effects span infrastructure deterioration, soil instability, and heightened seismic vulnerability. Understanding the intricate interplay between permafrost degradation and seismic attributes becomes imperative in regions like Alaska, characterized by a susceptibility to powerful seismic events and an underlying permafrost foundation. The potential amplification of seismic waves due to permafrost degradation amplifies seismic hazards and ground shaking, further underscoring the pressing need for comprehensive research in this domain.

## Methodology

University of Alaska Anchorage (UAA), in collaboration with the Alaska Earthquake Center (AEC), installed two accelerometers (i.e., BE01 and BE02 stations) in Bethel, Alaska, in 2022. BE01 is located on the ground underneath a one-storied pile-supported school building, while BE02 is located on the floor of the school building itself. These stations are equipped with three components (north-south, east-west, and vertical) accelerometers (EpiSensors) connected with a 24-bit Delta-Sigma converter with a dynamic range of approximately 136 dB per channel and a bandwidth of DC to 200 Hz (Etna-2 of Kinemetrics). To capture the ambient noise data and to minimize the cultural noise, the

time series data from both sensors are downloaded via the web portal of the IRIS Data Services Center in mini-Standard for the Exchange of Earthquake Data (miniSEED or .mseed) files during quiet night hours (3:00:00.000 to 4:00:00.000 AKST or 11:00:00.000 to 12:00:00.000 UTC) at 250 samples per second. The Horizontal-to-Vertical Spectral Ratio (HVSr) technique (Nakamura, 1989), implemented through an open-source web-based Python package application tool called HVSrweb (Vantassel, 2020), is applied to the collected noise data to facilitate the analysis of spectral characteristics of the noise on frozen and unfrozen soil conditions.

After the initial data filtering, three-component noise records (.mseed data format) of one-hour duration were divided into sixty small one-minute time windows. The HVSrweb tool computes the HVSr curves in the frequency range from 0.05 to 70.0 Hz by taking the Fourier amplitude spectra (FAS) ratio of the horizontal and vertical components from each time window. The geometric mean of the NS and EW components (Bard & SESAME Team, 2004) was used to compute the resultant horizontal component. For each window, the computed HVSr amplitude at each frequency was assumed to be lognormally distributed (Figure 1), and the median HVSr curve was determined from the median amplitudes at each frequency from the different windows (Cox et al., 2020). Similarly, the peak frequency ( $f_0$ ) of the individual HVSr curves was also estimated for each window, and then by

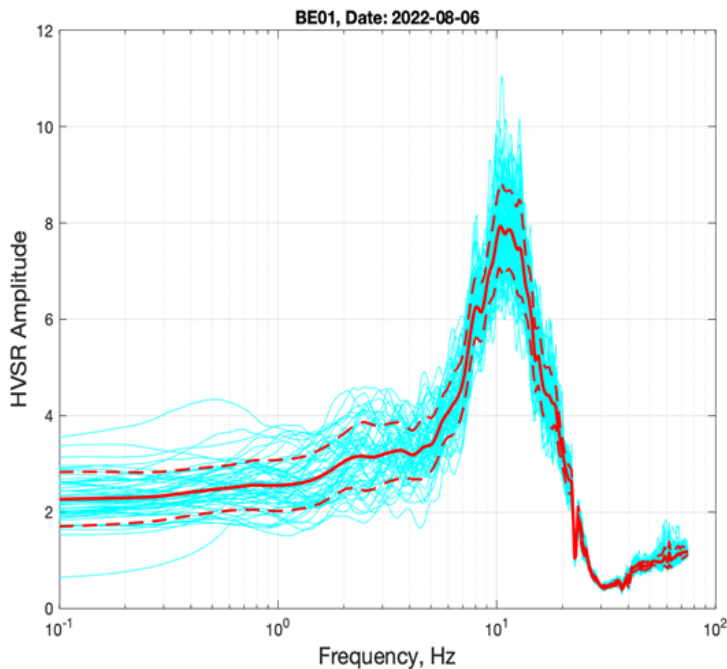


**Figure 1:** The observed HVSr at the BE01 site for different time windows (cyan color) and the lognormal average (solid red) with  $\pm 1\sigma$  variation (dashed red lines) for 6th August 2022.

using probabilistic sampling of a set of  $f_0$  values for each time window, the median peak frequency ( $f_0, mc$ ) corresponding to the resonance frequency of the HVSr was computed. Thus, the noise data for one year, from August 2022 to July 2023, were analyzed using the same approach with identical filter settings, and monthly averaged HVSr curves based on fifteen or more days of data records per month were generated. The seasonal variations of the amplitude and frequency ( $f_0$ ) of these monthly averaged HVSr curves are discussed below. The study meticulously processed one year of data, from August 2022 to July 2023, providing a comprehensive understanding of seasonal variations in HVSr amplitude and frequency.

#### Findings or Results

The analysis of HVSr amplitude versus frequency data reveals a significant correlation between soil state and ground motion amplification. Months with unfrozen soils exhibit higher amplitudes and lower resonant frequencies (Figure 2), indicative of a higher potential for seismic damage. Conversely, frozen soils exhibit smaller amplitudes and higher resonant frequencies. Ground motion amplification is notably higher during months with unfrozen soil, solidifying the direct link between permafrost degradation and seismic hazards.

The study's findings highlight the importance of understanding the dynamics between frozen and unfrozen soils for predicting and preparing for amplified ground motion in seismically active permafrost regions. Resonant frequencies, representing the vibrational frequencies of subsurface soil

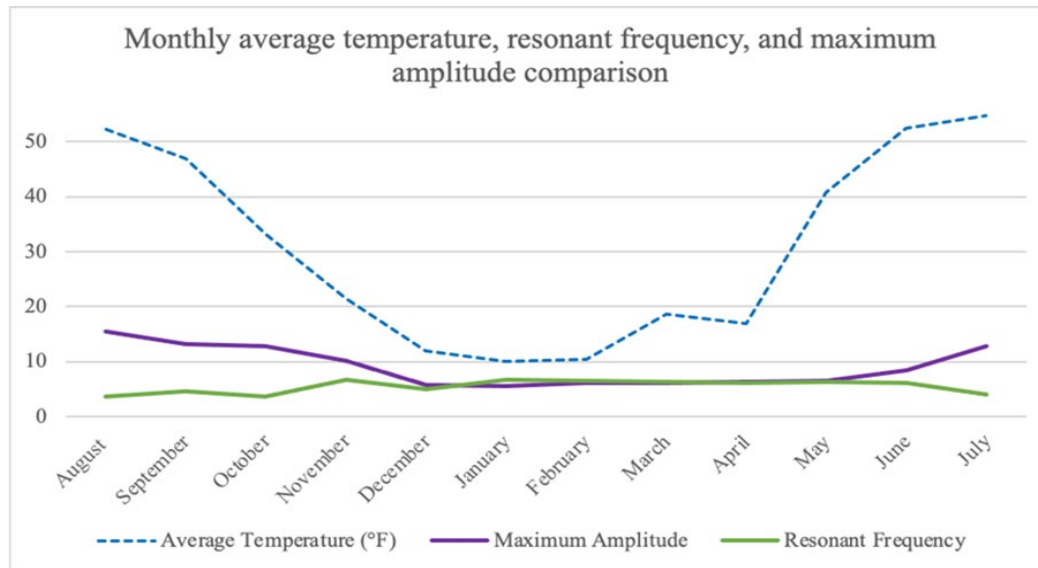


**Figure 2:** Monthly variation of maximum HVSR amplitude, resonating frequency, and the temperature

layers, provide crucial insights into potential ground motion amplification and, consequently, the risk of seismic damage. In conclusion, this research bridges a critical research gap, unraveling the relationship between permafrost degradation and seismic

attributes. Beyond the scientific implications, these findings hold profound implications for public health and safety, emphasizing the urgent need to comprehend and mitigate the impact of permafrost degradation on seismic events. As a foundational step, this study contributes valuable data. It lays the groundwork for further research endeavors to refine predictions and bolster our collective resilience against the escalating challenges posed by climate-induced permafrost degradation and its seismic repercussions.

### Conclusions

The study shows the ambient vibration of the frozen and unfrozen soil has different characteristics which are essential to understand for the assessment of seismic hazard over the area which are located in a degraded permafrost area on a seismically prone zone.

### Acknowledgments

We thankfully acknowledge the ConocoPhillips Arctic Science and Engineering research grant received by two of us (Z. Yang and U. Dutta) from the University of Alaska Anchorage to carry out the current work in Bethel, AK. We also extend our gratitude for the assistance that we received from Alaska Earthquake Center, in Fairbanks, Alaska for installation of seismic sensors. We are also thankful to the Lower Kuskokwim School District, in Bethel, Alaska, the Principal, and other staff members of Gladys Jung Elementary School for allowing us to install sensors in the school building and use the data communication facilities.

### References

Bard, P.-Y., & SESAME-team (2004). Guidelines for the implementation of the H/V spectral ratio technique on ambient vibrations measurements, processing and interpretation, SESAME European research project EVG1-CT-2000-00026.

Cox, B. R., T. Cheng, J. P. Vantassel and L. Manuel (2020). A statistical representation and frequency-domain window-rejection algorithm for single-station HVSR measurements, *Geophys. J. Int.* (2020)



221, 2170–2183.

Nakamura, Y. (1989). A method for dynamic characteristics estimation of surface using microtremor on the ground surface, Q. Rep. Railw. Tech. Res. Inst., 30(1, 25–33).

Vantassel, J.P. (2020) jpvantassel/hvsrpy: v0.2.1 (Version v0.2.1). Zenodo.  
<http://doi.org/10.5281/zenodo.3668353>

# Navigating the New Arctic: Insights into Ship Activities, Ice Modeling, and Stakeholder Engagement in the U.S. Arctic Waters

Grant Peel<sup>1</sup>, Virginia Groeschel<sup>2,3</sup>, Jonas Behnen<sup>1</sup>, Ozgur Demir<sup>1,4</sup>, Hayo Hendrikse<sup>5</sup>, Oceana Francis<sup>2</sup>, Ersegun Deniz Gedikli<sup>1</sup>

<sup>1</sup>*Department of Ocean and Resources Engineering, University of Hawaii at Manoa, 2540 Dole Street, Honolulu, HI 96822*

<sup>2</sup>*Department of Civil, Environmental and Construction Engineering, University of Hawaii at Manoa, 2540 Dole Street, Honolulu, HI 96822*

<sup>3</sup>*U.S. Army Corps of Engineers (USACE), Alaska District, Anchorage, AK 99506*

<sup>4</sup>*Department of Naval Architecture and Marine Engineering, Yildiz Technical University, Istanbul, 34349, Turkey*

<sup>5</sup>*Department of Hydraulic Engineering, Delft University of Technology, Stevinweg 1, 2628 CN Delft, the Netherlands*

## Abstract

In this paper, we focus on investigating ship activities in the United States' Arctic waters and developing new viscoelastic materials that can mimic specific ice behavior. This is a significant challenge, and we discuss potential positive outcomes and how the acquired knowledge can contribute to understanding ice behavior in Arctic and Sub-Arctic regions. We first define ice and ship statistics, providing a foundational understanding of potential ice-ship interactions. We then describe the development of thought experiments for wave-ice interactions and the creation of a numerical environment for modeling purposes. This step is crucial for simulating various scenarios related to ice and wave dynamics, ultimately contributing to the design of ships capable of navigating safely in diverse Arctic conditions. Finally, stakeholder and community engagement is addressed, recognizing the importance of involving local perspectives and insights to ensure practical, socially responsible, and effective solutions.

# Alaskan Pavement Resilience: Navigating Climate Change in Cold Regions

Robert P. Halcomb, P.E,<sup>1</sup> and Osama Abaza, Ph.D. C. Eng.<sup>2</sup>

<sup>1</sup> *Kinney Engineering, LLC. Email: robert.halcomb@kinneyeng.com*

<sup>2</sup> *Professor, Civil Engineering Dept, University of Alaska Anchorage. Email: oabaza@alaska.edu*

## **Abstract**

The global phenomenon of climate change has led to significant environmental transformations, particularly affecting cold regions due to their extreme temperature dynamics. Among the critical elements facing the consequences of climate change in these regions are pavement structures, essential components of roadway and airport infrastructure. This study explores the repercussions of climate change on pavement structures within cold regions, focusing specifically on shifts in temperature patterns and, subsequently, frost depth.

Through the analysis of temperature records, this research investigates the annual average temperatures, emphasizing trends spanning multiple decades. Complementary to this, freezing degree day data is utilized to compute frost penetration depths and establish average trends over the same extended timeframe. By comparing three prominent Alaskan regions in terms of both temperature variations and frost penetration, the study aims to discern the direct implications of climate change.

The regression analysis reveals noteworthy statistical changes in frost penetration depths across all studied locations. Projecting from current trends, future estimates for frost penetration indicate potential variations of around 15 centimeters over a 40-year period, contingent on the region. This study not only investigates if tangible effects of climate change on pavement structures exists but also offers valuable insights into potential long-term consequences for infrastructure in cold regions.

# Creep Performance of High R-value Structural Insulated Panels (SIPs)

Scott Hamel, PE, SE, Ph.D.

## Abstract

Structural Insulated Panels (SIPs) are a manufactured “sandwich” panel used for walls, floors, and roofs in residential and light commercial construction. SIPs are made of two exterior “skin” faces that encase a foam core. The panel have few solid wood members to “bridge” the insulation envelope, providing excellent thermal performance. The panels are pre-fabricated in a factory and then assembled on the job site, which allows for extremely fast erection with only a few workers. High R-value, fast construction, good quality control, and material efficiency make these products well suited for cold regions, especially in remote areas. The most common materials for fabricating SIPs is oriented-strand-board (OSB) skins with an expanded-polystyrene foam (EPS) core. However, SIPs with plywood skins and closed-cell polyurethane (PU) foam provides better structural performance and moisture durability. The increased cost of PU and Plywood could be offset by their higher strength, stiffness, and much higher R-values, if their structural behavior is understood.

Given that the core and skins are made of synthetic and natural polymers, respectively, the panels will experience load-induced, time-dependent deformations, such as creep. Data exists on the time-dependent performance of each material, but little information is available on the bending behavior of the composite, which involves complex interaction of the components. This study investigates the bending creep behavior of full-size Plywood-PU foam SIP panels with an 8-foot (2.4 m) span tested at three different load levels: 30psf, 60psf, 120 psf (1400 Pa, 2800 Pa, 5600 Pa). Load was applied and deflection recorded for 90 days, followed by a minimum of 60 days of recovery. It was found that the creep behavior can be accurately characterized using the Power Law, and that after 60 days of recovery, the panels had recovered approximately half of their maximum 90 day creep deformation.

# Emergency Water Refill for Northern Village of Kangiqsualujjuaq, Nunavik Region, Northern Quebec, Canada

Chris Keung,<sup>1</sup> Luc Malo,<sup>2</sup> Ken Johnson,<sup>3</sup> Hossein Shafeghati,<sup>4</sup> and Alfred Tsui<sup>5</sup>

<sup>1</sup>EXP, 101-8616 51 Ave NW, Edmonton AB Canada T6E 6E6; email:

*christopher.keung@exp.com*

<sup>2</sup>EXP, 1355, rue Daniel-Johnson Ouest, Saint-Hyacinthe QC J2S 8W7; email:

*luc.malo@exp.com*

<sup>3</sup>EXP, 101-8616 51 Ave NW, Edmonton AB Canada T6E 6E6; email: *ken.johnson@exp.com*

<sup>4</sup>Kativik Regional Government, P.O. Box 9, Kuujjuaq QC J0M 1C0; email: *hshafeghati@krg.ca*

<sup>5</sup>Kativik Regional Government, P.O. Box 9, Kuujjuaq QC J0M 1C0; email: *atsui@krg.ca*

## Abstract

In 2023, the Kativik Regional Government of the Nunavik Region of Northern Quebec experienced a water supply emergency in the remote Arctic community of Kangiqsualujjuaq (latitude 58.7 degrees north) due to the unexpected drawdown of the community's water supply lake reservoir. The late summer identification of this emergency led to the execution of a hasty plan to accomplish a 100,000 m<sup>3</sup> refill of the reservoir before the onset of winter in October. A nearby lake was selected as a water source. Two pumps and 1,550 metres of 200-mm flexible hose were mobilized 1,600 km north to the community by airlifting and sealifting as the community has no road access. A 1,300-metre trail for the hose was constructed between the two lakes. Pumping began in late September 2023 and the refill was successfully completed 35 days later.

**Keywords:** Arctic, emergency, water refill

## Introduction

The Kativik Region Government of the Nunavik Region of Northern Quebec observed low water levels in the water supply lake reservoir in the remote Canadian Arctic community of Kangiqsualujjuaq in May 2023. Kangiqsualujjuaq's current water source is an elevated water supply lake north of the community with a capacity of 360,000 m<sup>3</sup> at an elevation of approximately 140 m above sea level.

Upon inspection in July 2023, it was determined that the lake reservoir had lost a significant quantity of its stored volume through a loss from the water recirculation pipeline. The loss was not observed because the discharge occurred under the snowpack. It was determined that the resulting low lake level would not be sufficient to provide the overwinter water supply to the community. It was estimated that the lake would need a supplementary recharge of approximately 100,000 m<sup>3</sup>.

This situation created a water supply emergency in the community. EXP Services Inc. (EXP) was retained by the Kativik Regional Government (KRG) to plan, engineer and assist in the execution of an emergency water reservoir refill. After the consideration of several water sources in reasonable proximity to the lake, Lake Ellasie was selected as the most appropriate source for the refill. The refill of the lake reservoir was executed with a diesel pump and a pipeline that was mobilized to the community.

## Methodology

Following the source selection, the emergency was presented to the Province of Quebec Ministry of the Environment. Considering that temporary and non-recurring water withdrawals carried out in an emergency or for humanitarian or civil security purposes are exempt from authorization from the



Ministry, the project was exempt from having to submit an official authorization request, which would have caused delays of several months. An informal request was submitted to the Ministry which approved the request.

Efforts focused on the logistics for executing the refill, which was up against the coming Arctic winter, where October temperatures can fall to minus 10°C. The refill from Lake Ellasie could require a pumping system and a 1,300 m overland piping system that would have to be mobilized by air and sea to this remote Arctic community. The community is not accessible by road. As the project progressed at the end of the summer, the sealift (a scheduled cargo ship) was not an option. In addition, the community airfield in Kangiqsualujjuaq is not long enough for larger aircraft. Further research was undertaken to determine what pumping and piping equipment could be mobilized with an aircraft capable of landing in the community. Given the mobilization limitations, a system comprised of flexible piping and diesel pumps was selected, but the equipment airlift mobilization could only be taken as far north as a community with Boeing 737 landing capability.

Based on 30 days of 24/7 operation, the pumping system would require a flow rate of approximately 2,200 LPM and would need to overcome approximately 65 m of static head. Various equipment suppliers were contacted to locate pumping equipment that was available and could be procured and transported given the numerous logistical challenges. Two high-head pumps, 1,550 m of flexible 200 mm hose and associated materials were procured. Concurrently, discussions occurred with various cargo and logistic companies to organize transportation options. As the final solution, a Boeing 737 cargo plane was chartered from southern Quebec to the nearby community of Kuujjuaq, which has a longer airfield. From Kuujjuaq, the equipment and materials were transferred to a commercial fishing boat and transported 200 km to Kangiqsualujjuaq.

Once the equipment was on site, the challenge was to install the flexible pipe along a hastily constructed trail from Lake Ellasie to the water supply lake reservoir. Other site works included the construction of a pad for the pumps; provision of fuel supply; installation of the fuel tank; and maintenance and operation of the pumps.

### **Findings or Results**

The pumping progressed according to schedule with minor adjustments. A 10,000 L fuel tank was installed very close to the pump to avoid potential damage during the necessary daily fuel fillings. Employees inspected the pumping system and discharge line several times a day throughout the project. Daily readings of pumping system parameters and levels of each lake were recorded. No notable change (less than 25 mm) in the level of Lake Ellasie was observed throughout the duration of the pumping. No discernible reduction in flow was observed in the outlet of Lake Ellasie, and therefore it is reasonable to conclude that no significant impact to the lake occurred.

Halfway through the pumping phase, there was a mechanical breakdown at pump #1, which was quickly replaced by replacement pump #2. The decision to bring two pumps to the site was therefore very appropriate for completing the project. Pumping began in late September 2023 and the refill was completed 35 days later.

### **Conclusions**

- An emergency lake reservoir refill was successfully executed for the Arctic community of Kangiqsualujjuaq, Nunavik Region, Northern Quebec with significant challenges.
- A water source for the refill was quickly selected and approved by the regulatory authorities.
- The selection of the appropriate equipment for the refill was completed concurrently with the mobilization logistics in consideration of the equipment selected.
- Site works for the refill pipeline were also completed concurrently and the refill was underway

shortly after the equipment arrived on site.

- Pumping began in late September 2023 and the refill was completed 35 days later.



Photo 1: Kangiqsualujjuaq refill emergency pipeline laid out of constructed trail – source lake (Lake Ellsie) in the background with the pump visible on the shore.



Photo 2: Arrival of pump at Kangiqsualujjuaq on fishing boat after 200 km voyage from Kuujjuaq - pump was airlifted to Kuujjuaq.





Photo 3: Pump and intake system in place on source lake (Lake Ellasie) with connection to the refill pipeline.



Photo 4: Discharge into Kangiqsualujjuaq water supply lake (Imirtaviup Tasinga Lake) at the start of the refill.

# Measuring Depth to Ice-Bonded Permafrost using Surface Waves: Challenges and Recommendations from Field Measurements in Eagle Summit, Alaska

Joseph P. Vantassel, Ph.D., A.M.ASCE<sup>1</sup> and Abhijeet Acharjee Jeet, S.M.ASCE<sup>2</sup>

<sup>1</sup>750 Drillfield Drive, Department of Civil and Environmental Engineering, Virginia Polytechnic Institute and State University, Blacksburg, VA 24061; email: [jpvantassel@vt.edu](mailto:jpvantassel@vt.edu)

<sup>2</sup>750 Drillfield Drive, Department of Civil and Environmental Engineering, Virginia Polytechnic Institute and State University, Blacksburg, VA 24061; email: [abhijeet@vt.edu](mailto:abhijeet@vt.edu)

## Abstract

The depth to ice-bonded permafrost is a critical piece of information for engineering design in cold regions. The use of non-invasive methods allows depth measurements to be made more rapidly than using traditional invasive methods resulting in project savings. However, while non-invasive methods may be faster than invasive techniques, non-invasive techniques must be carefully analyzed to produce meaningful results. Here we present the analysis of a unique surface wave dataset acquired in August 2023 in Eagle Summit, Alaska. Measurements followed a dynamic data acquisition methodology that resulted in multichannel analysis of surface waves (MASW) data from arrays of different lengths (23 m and 2.3 m) and waveforms associated with different surface waves (i.e., Rayleigh and Love) and particle motion directions (i.e., Rayleigh-vertical, Rayleigh-inline, and Love-crossline). The Eagle Summit site (65.4621N, 145.4349W) is of particular interest because of the challenges associated with the data acquisition and interpretation. These challenges include the presence of thick near-surface organic material, obfuscating near-field effects, and ambiguous multi-mode dispersion trends. Yet, despite these challenges, the authors were successful in characterizing the shear wave velocity ( $V_s$ ) to a depth of 5 m and identifying the top of ice-bonded permafrost at approximately 0.45 m. The authors hope that by presenting this unique and challenging dataset to highlight key challenges and provide recommendations for performing seismic measurements at permafrost sites.

# Accounting for Permafrost Degradation in Site-Specific Ground Motion Procedures for Building Design

Matthew D. Joyner, Ph.D.<sup>1</sup>, Rosa Affleck, Ph.D.<sup>2</sup>, Kevin Bjella, P.E.<sup>3</sup>, John Thornley, Ph.D., P.E.<sup>4</sup>, and Jeffrey Cegan<sup>1</sup>

<sup>1</sup>*U.S. Army Engineer Research and Development Center, Environmental Laboratory, Concord, MA; email: matthew.d.joyner@usace.army.mil*

<sup>2</sup>*U.S. Army Engineer Research and Development Center, Cold Regions Research and Engineering Laboratory, Hanover, NH; email: rosa.t.affleck@usace.army.mil*

<sup>3</sup>*U.S. Army Engineer Research and Development Center, Cold Regions Research and Engineering Laboratory – Alaska Research Office, Fairbanks, AK; email: kevin.bjella@usace.army.mil*

<sup>4</sup>*WSP, Geotechnical, Permafrost, and Earthquake Engineering, Anchorage, AK; email: john.thornley@wsp.com*

## Abstract

Permafrost degradation in the Arctic and Subarctic is expected to continue due to global warming. This poses various issues for building structures in these regions: sites containing ice-rich, thaw-unstable permafrost carry significant risk of differential settlement—due to thawing—and liquefaction, in the event of an earthquake. Many sites, however, lie on ice-poor, thaw-stable permafrost, which comes with its own unique challenges for seismic hazard. On these sites, while the settlement may be of lesser concern, liquefaction and the additional risk associated with changing soil amplification are of importance. Given that the shear wave velocity (which governs soil amplification) of a frozen soil can be several times greater than that of the same soil in its thawed state, the change in amplification over the life of a structure is an important consideration in light of permafrost degradation. Additionally, the thickness of the unfrozen soil overlaying the permafrost may also play a role in the predominant period of the ground motion, interacting with structures differently based on their period. This paper proposes modified risk targets to be used in site-specific ground motion procedures for design to address the effects of climate-driven permafrost thawing—based on global climate models. Results from nonlinear site response analysis under a selected set of hazard-representative ground motions are used to develop new design ground motions targeting alternative collapse risk levels for a site in central Alaska.

**Keywords:** seismic risk; permafrost; risk targeting; seismic design; earthquake design; site response analysis

## Introduction

Thawing permafrost driven by global warming can lead to various problems for Arctic structures—including differential settlement, foundation instability, and other issues (Yu et al., 2020; Liew et al., 2022). In seismic regions of the Arctic and Subarctic, these issues can be compounded by earthquake risks, leading to increased liquefaction risk and changes in site amplification—this paper addresses the latter. The risk-targeted design ground motions used as the basis for designing modern structures in the US do not account for potential amplification due to permafrost thaw, despite research pointing to the potential impacts (Yang et al., 2011; Chen et al., 2018; Yu et al., 2022). Given the rate at which permafrost is expected to thaw over the next 50 years due to global warming, this may pose a significant threat to buildings in Alaska. This paper builds upon research described in Joyner et al. (2024), which explores the impact of permafrost thaw on the conditional and 50-year collapse probabilities associated with design ground motions for a site in Fairbanks, AK. The results of that investigation showed 50% and 21% increases in the 50-year collapse probability under the RCP8.5



climate scenario—the worst-case warming trend where emissions continue largely unchanged; and the RCP4.5 climate scenario—a more likely intermediate scenario where emissions begin declining in 2045, respectively. Conditional collapse probabilities increased by factors of 4.5 and 3.1 correspondingly. Given these considerable deviations from ASCE risk targets of 1%-in-50-years and 10% conditional, this paper proposes a strategy for selecting more appropriate design ground motions on permafrost sites to include the effects of potential thawing.

### Methodology

Originally proposed by Luco et al. (2007), the process for calibrating design ground motions to achieve stated targets can be explained starting with the following formulation of annual collapse probability:

$$P_{cA} = \int (1 - F_D) f_C dS_a \quad (1)$$

where  $F_D$  is the cumulative distribution function (CDF) of demand,  $f_C$  is the probability density function (PDF) of capacity, and both are functions of the intensity measure,  $S_a$ .  $F_D$  can be defined on an annual basis for a given site through probabilistic seismic hazard analysis (PSHA), and  $f_C$  is simply the PDF associated with a given structure's collapse fragility. The following equation is used to translate  $P_{cA}$  from an annual basis to a 50-year collapse probability:

$$P_{c50} = 1 - (1 - P_{cA})^{50} \quad (2)$$

Hazard at the site, and therefore  $F_D$ , can be established based on published hazard data provided by the US Geological Survey (USGS, 2023). The calibration, then, operates through iterative alteration of  $f_C$ , which can be fully defined by two parameters: 1) an uncertainty parameter; and 2) a given percentile  $S_a$ . Luco et al. (2007) suggested a lognormal distribution with a logarithmic standard deviation of  $\beta = 0.8$ —based partly on analyses conducted by the ATC-63 project: “Quantification of

Building System Performance and Response Parameters”. By selecting the 10th percentile spectral acceleration capacity,  $S_{a10}$ , as the remaining parameter,  $f_C$  is iteratively changed through alteration of  $S_{a10}$ , each time calculating  $P_{c50}$  [Eqs. (1) and (2)], until it is equal to 1%. The resulting value of  $S_{a10}$  is then taken as the risk-targeted maximum considered earthquake ground motion,  $MCE_R$ , resulting in an  $f_C$  that is simultaneously calibrated to achieve both the 10% conditional collapse probability at  $MCE_R$  level shaking and a 1% collapse probability over a 50-year lifespan. This procedure was adopted by ASCE 7, with a modified  $\beta$  value of 0.6, for site-specific ground motion calculation starting in 2010 as an optional alternative (ASCE, 2010), and then as a requirement in 2022 (ASCE, 2022).

Implicit in Eq. (2) is the assumption that site soil conditions remain constant over a structure's 50-year life. This means that the conditional collapse probabilities also remain constant—i.e.,

$$P_{c,condnl} = F_C(S_{a10}) = 10\% \quad (\text{where } F_C \text{ is the cumulative distribution function associated with } f_C).$$

Since this is not the case for sites with thawing permafrost, modifications are needed to these relationships to assess collapse risk. As described in Joyner et al. (2024), these modifications can be made by 1) Selecting a group of ground motion records to represent bedrock seismic hazard at the site—done using a modified version of the Conditional Spectrum method (Baker and Lee, 2018); 2) Performing nonlinear site response analysis under selected ground motions for a range of permafrost depths, oscillator periods, and hazard levels using the SeismoSoil software (Asimaki and Shi, 2017); and 3) Carrying out statistical analysis of the resulting spectral accelerations. The results can be translated to projected time series using forecasts of the depth to permafrost over time at the site, obtained from the GIPL2-MPI/GCM model, developed by the Geophysical Institute Permafrost Lab (GIPL) of the University of Alaska Fairbanks (Marchenko et al., 2001 & 2008; Nicolsky et al., 2017; Nicolsky and Romanovsky, 2018; and Jafarov et al., 2012).

The resulting 50-year collapse probability,  $\hat{P}_{c50}$ , and its conditional counterpart,  $\hat{P}_{c,Cndnl}$ , directly account for permafrost thaw over the structure's life, and can be used to define more appropriate risk targets and associated design ground motions for the site. Risk targeting with these modified relationships, however, must contend with two complicating factors: First  $\hat{P}_{c,Cndnl}$  is now a function of time, since it depends on the depth to the permafrost table, which is increasing. Second,  $\hat{P}_{c50}$  and  $\hat{P}_{c,Cndnl}$  cannot be simultaneously calibrated to target values, as is done with  $P_{c50}$  and  $P_{c,Cndnl}$  to meet ASCE 7 targets. Thus, new risk targets are needed. In this paper, the following three alternatives will be explored and compared with the collapse probabilities corresponding to current design standards: 1) limit  $\hat{P}_{c50}$  to 1%; 2) limit  $\max(\hat{P}_{c,Cndnl})$  to 10%; and 3) limit  $\text{mean}(\hat{P}_{c,Cndnl})$  to 10%. Each of these targets is matched through numerical solution of the following relationship for  $S_{a10}$ :

$$\hat{P}_c(S_{a10}) - R_t = 0 \quad (3)$$

where  $\hat{P}_c$  is either  $\hat{P}_{c50}$  or  $\hat{P}_{c,Cndnl}$ ;  $S_{a10}$  is the 10<sup>th</sup> percentile structural capacity in terms of spectral acceleration; and  $R_t$  is the risk target—in this case either 10% or 1%. While the current paper only considers these three risk target alternatives, any number of alternatives could be defined and targeted using the same approach. In practice, selection of the appropriate target for a given building should consider a range of objectives including not only safety, but also cost, functionality, and resilience. Since the 50-year collapse probability and conditional collapse probability indicate fundamentally different things about a design's capacity, such a decision would depend to some extent on the risk tolerance of the decision maker(s). It should also be noted that all three alternatives meet or exceed the current seismic design standards of ASCE 7 (2022), which do not address permafrost thaw.

## Results

The findings in Joyner et al. (2024) demonstrate that the greatest site amplification—and therefore collapse probability increases—occurred at shorter building periods close to the characteristic site period of 0.215 sec. In this paper, a building period of  $T_b = 0.2$  sec will be assumed for risk targeting with Eq. (3), in order to highlight the extent to which permafrost thaw may affect design ground motions. It should be noted, however, that for longer periods approaching 1 sec, the analyses found that amplification was minimal, leading to values of  $\hat{P}_{c50}$  and  $\max(\hat{P}_{c,Cndnl})$  that were close to the 1% and 10% ASCE 7 targets, respectively. Table 1 lists the design ground motions, in terms of  $S_a$ , resulting from the proposed risk targeting approach, and Figure 1 summarizes the resulting collapse probabilities.

Table 1 - Design ground motion values needed to meet risk targets of ASCE 7 standards and each of the three alternatives. Results correspond to a building period of 0.2 sec.

Design Basis	Collapse Risk Target	Permafrost Thawing Considered?	Design $S_a$ (g)*	
			RCP8.5	RCP4.5
ASCE 7	1%-in-50-yrs and 10% Conditional	No	1.19	1.19
Alternative 1	1%-in-50-yrs	Yes	1.29	1.22
Alternative 2	10% Mean Conditional	Yes	1.52	1.33
Alternative 3	10% Max Conditional	Yes	2.40	1.88

\*the design  $S_a$  is defined as the 10th percentile value of the building's capacity distribution,  $f_c$

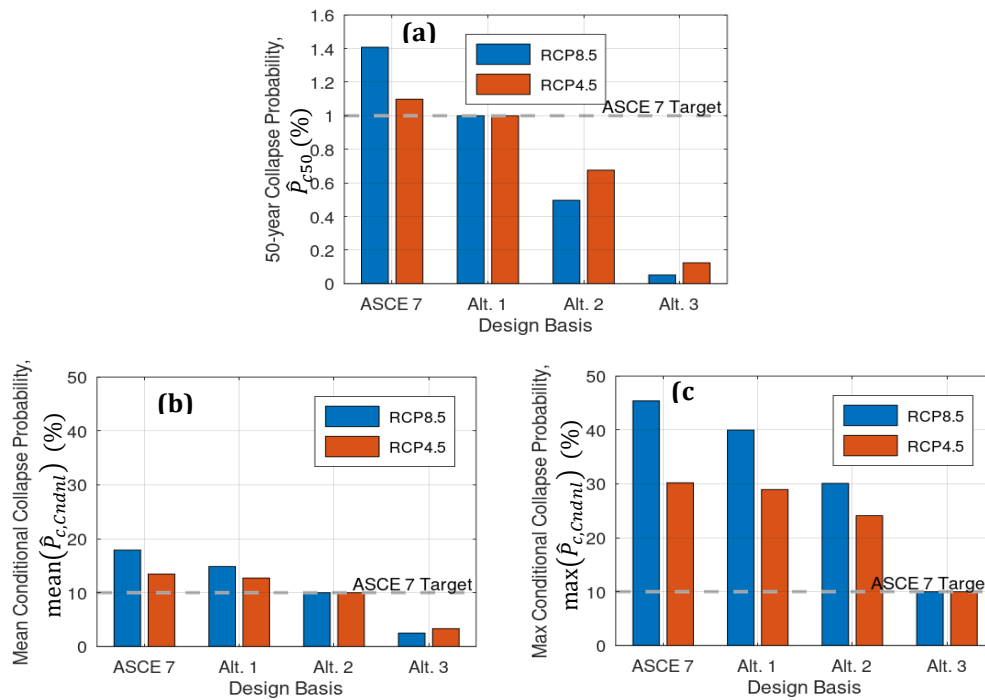


Figure 1 - 50-year and conditional collapse probabilities for each alternative's design ground motion, as listed in Table 1.

## Discussion and Conclusions

This paper proposes alternative collapse risk targets for a building on a permafrost site in central Alaska where current ASCE 7 design ground motions are inadequate to meet stated targets. Using results from nonlinear site response analysis under scaled ground motions representing the hazard, the 50-year and conditional collapse probabilities are estimated with direct consideration of the change in permafrost table depth caused by global warming. These climate-informed collapse probabilities are then used as the basis for calibrating new design ground motions for proposed alternative targets.

The results in Figure 1 show that the standard ASCE 7 design ground motions do not meet either of the stated risk targets for the selected site. Of the three alternatives considered, the only one which meets or exceeds both of the current ASCE 7 risk targets is Alternative 3. As shown in Table 1, under the worst-case warming scenario, RCP8.5, meeting this target would require a 100% increase in the design ground motion, whereas the more likely RCP4.5 scenario would only require a 58% increase. This design, however, could be seen as overly conservative, given that its 50-year collapse probability is only 5% and 12% of the allowable 1% (see Figure 1a). Alternative 1 meets the 1%-in-50-years target exactly (see Figure 1a) but overshoots the maximum conditional collapse probability by factors of 3.9 and 2.9 for RCP8.5 and RCP4.5, respectively (see Figure 1c). Considering the potential infeasibility of Alternative 3 design ground motions from a cost perspective, and the high risk of Alternative 1, Alternative 2 may be more acceptable. As shown in Figure 1b, the average conditional probability over the life of the building is 10% for Alternative 2, and the 50-year collapse probability is well under the 1% limit for both climate scenarios. The only question is whether or not the maximum conditional collapse probability of 30% and 24%—for RCP8.5 and RCP4.5, respectively (see Figure 1c)—are acceptable. Ultimately, the final selection should be made through an appropriately rigorous decision analysis process, which is beyond the scope of this paper.

## References

ASCE (2010). ASCE/SEI 7-10. Minimum design loads for buildings and other structures. American Society of Civil Engineers, Reston, VA.

ASCE (2022). ASCE/SEI 7-22. Minimum design loads for buildings and other structures. American

Society of Civil Engineers, Reston, VA.

Asimaki D., Shi J. (2017) "SeismoSoil User Manual, v1.3"

Baker, J. W., & Lee, C. (2018). "An improved algorithm for selecting ground motions to match a conditional spectrum." *Journal of Earthquake Engineering*, 22(4), 708-723.

Chen T., Ma W., Zhou G. (2018). "Numerical analysis of ground motion characteristics in permafrost regions along the Qinghai-Tibet Railway." *Cold Regions Science and Technology*, 148, 88-95.

Jafarov E.E., Marchenko S., Romanovsky V.E. (2012). "Numerical Modeling of Permafrost Dynamics in Alaska Using a High Spatial Resolution Dataset." *The Cryosphere*, 6(3), 613-624.

Joyner M.D., Affleck R., Bjella K., Thornley J., and Cegan J.C. (2024). "Risk-Targeted Ground Motions on Sites with Thawing Permafrost." In proceedings of The 18<sup>th</sup> World Conference on Earthquake Engineering. Milan, Italy. Forthcoming.

Liew M., Ji X., Xiao M., Farquharson L., Nicolsky D., Romanovsky V., Bray M., Zhang X., McComb C. (2022). "Synthesis of physical processes of permafrost degradation and geophysical and geomechanical properties of permafrost." *Cold Regions Science and Technology*, 198, 103522.

Luco N., Ellingwood B.R., Hamburger R.O., Hooper J.D., Kimball J.K., Kircher C.A. (2007). "Risk-targeted versus current seismic design maps for the conterminous United States." *Proceedings of SEAOC 2007 Convention*. Squaw Creek, California.

Marchenko S. S. (2001). "A model of permafrost formation and occurrences in the intracontinental mountains." *Norsk Geografisk Tidsskrift - Norwegian Journal of Geography*, 55(4), 230-234.

Marchenko S., Romanovsky V. Tipenko G. (2008). "Numerical Modeling of Spatial Permafrost Dynamics in Alaska." *Proceedings of the Ninth International Conference on Permafrost*, University of Alaska Fairbanks.

Nicolsky D.J., Romanovsky V.E. (2018). "Modeling Long-Term Permafrost Degradation." *Journal of Geophysical Research: Earth Surface*, 123(8), 1756-1771.

Nicolsky D.J., Romanovsky V.E., Panda S.K., Marchenko S.S. Muskett R.R. (2017). "Applicability of the ecosystem type approach to model permafrost dynamics across the Alaska North Slope." *Journal of Geophysical Research: Earth Surface*, 122(1), 50-75.

U.S. Geological Survey (2023). Unified Hazard Tool. Accessed October 1, 2023 at URL <https://earthquake.usgs.gov/hazards/interactive/>

Yang Z.J., Dutta U., Xu G., Hazirbaba K., Marx E.E. (2011). "Numerical analysis of permafrost effects on the seismic site response." *Soil Dynamics and Earthquake Engineering*, 31(3), 282-290.

Yu W., Zhang T., Lu Y., Han F., Zhou Y., Hu D. (2020). "Engineering risk analysis in cold regions: State of the art and perspectives." *Cold Regions Science and Technology*, 171, 102963.

Yu X., Zhang R., Cheng Y., Hu Y. (2022). "Monte Carlo seismic response analysis of permafrost sites: a case study." *Natural Hazards*, 113(1), 237-259.

# Shallow Buried Fuel Gas Line: Stability Maintenance in the Arctic

Donald G. (Greg) Kinney, P.E.<sup>1</sup>, and Larry Mosley<sup>1</sup>

<sup>1</sup>*Alyeska Pipeline Service Company, Fairbanks, AK 99701*

## **Abstract**

Alyeska Pipeline Service Company (APSC), operator of the Trans-Alaska Pipeline System (TAPS) maintains a supporting fuel gas line (FGL) extending 148.4 miles south of Prudhoe Bay. This line, which is 10” nominal diameter for the first 33.9 miles and 8” diameter beyond that, has supplied natural gas since 1977 to three pump stations south of Pump Station 1. The FGL was originally buried a minimum of 36 inches below ground surface (within the active layer of an ice-rich permafrost regime); it runs primarily along the Dalton Highway as buried piping, with two above-ground highway crossings and one elevated bridge crossing. Its route includes both thaw-stable and thaw-unstable segments, some of which have proven vulnerable to thermokarst formation. In addition, the FGL is subject to water infiltration and erosion from seasonal surface water overflow, which also can contribute to or cause loss of cover materials. Because of these dynamics, Alyeska has developed a set of monitoring methods for the FGL. These include use of in-line curvature and corrosion inspection tools, field surveys, periodic “linewalk” surveillance, and LIDAR interpretation. This paper describes these tools, as well as the maintenance approaches that Alyeska has developed over the last 46 years to maintain line stability and protection.



# Slipstream Heat Addition on the Trans-Alaska Pipeline: Thermal Risk Mitigation Strategies and Lessons Learned

Donald G (Greg) Kinney, P.E.<sup>1</sup>, and David Roberts, P.E.<sup>1</sup>

<sup>1</sup>*Alyeska Pipeline Service Company, Anchorage, AK 99503*

## **Abstract**

The Trans Alaska Pipeline System (TAPS), designed for a peak throughput of over 2 million barrels per day, operates at an average of less than 470,000 barrels per day (2023). At peak flow, the transit time from Prudhoe Bay to the Valdez Marine Terminal was 4.3 days; it is now more than 18 days. Frictional heating is now negligible, and the extended time in transit assures significant heat loss along the line which can become operationally critical in winter months. This paper describes the development of a strategy by the pipeline operator, Alyeska Pipeline Service Company (APSC), to mitigate ice formation risks. This effort began in the mid-2000s and continues to this date.

The paper details the mechanisms behind heat loss on the pipeline, the TAPS temperature gradient model, establishment of risk critical temperature thresholds, evaluation of heating methods (bulk vs slipstream), and the operation and performance of the three major “heating kits” and supplementary heating methods along TAPS. Finally, the paper will offer lessons learned to date, and how the lessons are being applied to improve future operations.

# The Lone Peak Tram

Cooper Knarr<sup>1</sup> and Dr. Colin Shaw<sup>2</sup>

<sup>1</sup>*Department of Mechanical Engineering, Harvard University, 150 Western Ave, Boston, MA 02134; email: cknarr@college.harvard.edu*

<sup>2</sup>*Department of Earth Sciences, Montana State University, Culbertson Hall, 100, Bozeman, MT 59717; email: cashaw@montana.edu*

## Abstract

Big Sky Ski Resort is one of the largest, most popular ski resorts in the United States. It's most sought-after lift to ride, the Tram, takes the most advanced skiers several thousand meters above sea level. What many tourists and most locals do not know is that the ground upon which the base of the Tram sits is a rock glacier. This paper examines the impact of thermal conduction between the lower terminal building and the rock glacier. Temperature profiles are contextualized using soil strength equations along with the terminal's observed vertical displacement. The scope of this paper is restricted to the conductive heat transfer between the building's insulation, soil, and the rock glacier between 2005 and 2014. Temperature profiles of the rock glacier from 0 to 10 meters below the surface are modeled using COMSOL Multiphysics®. Geotechnical data of the Lone Peak Rock Glacier and monthly temperature profiles in Big Sky, Montana are used as inputs. Results indicate that the creep strain and creep strain rate in 2014 was 27 times larger than the creep strain and creep strain rate in 2005. Between January 2005 and January 2006, the internal temperature 2 meters below the surface increased from -2°C to -.7°C. From 2005 to 2014, the temperature .61 meters subsurface increased 4°C. The junction between the building insulation and the surface reaches 6.5°C in December 2014 compared to 1.4°C in January 2005. Furthermore, results show greater temperature disparities during the winter months. As such, the negative vertical displacement previously may be attributed to conductive heat transfer between the building and the glacier.

## Introduction

Before its 2023 reconstruction, Big Sky Ski Resort's most popular lift, the Lone Peak Tram was an anomaly: The lower terminal sits on an active rock glacier, meaning the building moves with the ground beneath it. Consequently, the terminal has experienced several meters of vertical and horizontal displacement, movement which partially influenced the new location of the 2023 renovations. Although extensive research by Montana State University has examined the base's horizontal and vertical movement, minimal research has examined the heat transfer relationship between the building and the rock glacier it sits upon. Since 2001, the base of Lone Peak Tram has moved several meters. [1] 1 Gaston Engineering, of Bozeman, has recorded data regarding the movement of the Tram's base and the underlying glacier. This data was analyzed by Dr. Colin Shaw of Montana State University in, who clarified that although the Tram was built to move with the glacier, the original plans included a passive refrigeration system of thermosyphons that would act to decrease glacial melt due to the tram's structure. However, this plan was scrapped. Although no substantive research has been conducted on the thermal impacts of the environment on the glacier's melting, there are indications in Dr. Shaw's research that there is a higher rate of glacial melting underneath the large Tram-base structure. The design of the tram does consider thermal conduction from the structure to the glacier: underneath the concrete pad upon which the structure sits is an eight inch foam insulation.[2] Due to the cost of thermosyphons, which would decrease the amount of conduction between the building and the glacier, the design does not include them but rather tubes in the insulation that can be easily turned into thermosyphons. [2] Thermosyphons, before being used on the Tram design, were used mainly in permafrost locations.[2] This research project aims to identify the impact of thermal conduction on the

---

<sup>1</sup> Data also comes from LiDaR analysis of the Lone Peak Rock Glacier conducted by Dr. Colin Shaw

structure of the tram-base. This will be done by simulating the heat transfer from the atmosphere through the building and into the glacier on COMSOL for the years 1995 to 2022. The temperature and weather data can be downloaded under public domain from the national weather service. The project will use the basics of conduction and heat transfer to explain the depth at which the heat would penetrate the glacier and the results of the projections of the COMSOL simulation. Such analysis provides insight into the changing structure of the Lone Peak Tram base, which was ultimately moved from the glacier in 2023.

Research published in July 2023 by Alessandro Rotta Loria at Northwestern University, utilized COMSOL to simulate how the change in Chicago ground temperature has and may impact Chicago’s building foundations. Although Rotta Loria’s paper was published after the completion of the Lone Peak Tram COMSOL simulation, Rotta Loria’s work acts not only as a useful resource for future iterations of this project but also supports the usage of COMSOL to evaluate how a building interacts with its surroundings.

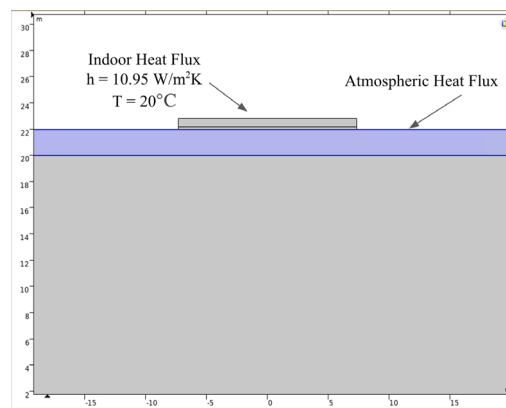


Figure 1: Display of the COMSOL geometry.

## Methodology

### COMSOL Geometric Setup

The geometric setup of the COMSOL simulation is displayed in figure 1. The top layer is a .6096m concrete slab, which utilized the pre-programmed COMSOL concrete thermal properties. Below the concrete slab is a 8 inch layer of DOW High-load 60 Insulation. The blue layer represents an approximate 1.8 meter layer of top soil, estimated from [3] 2011 findings during excavation. Underneath the top soil layer is the rock glacier. Thermal properties used in the analysis are displayed in Table 1. The density of the soil comes from the density of the debris as stated in [4]. The density of the glacier was calculated using a weighted average of debris and ice following the weighted percentages reported in Florentine’s 2014 paper on the geography around the Lone Peak Tram [4].

Material Properties					
Material	Resistivity (m <sup>2</sup> K/W)	Thermal Conductivity (W/mK)	Heat Capacity (J/kgK)	Density (kg/m <sup>3</sup> )	Initial Temperature (°C)
Insulation (DOW Blue Highload 60)	.88 [5]	.025[6]	1450 <sup>3</sup>	35 (estimated)[7]	9.85
Ice/Gravel	NA	2.22[8]	2050[8]	1747.85[4]	-2
Soil	NA	1.5[9]	700[9]	2600[9]	0

Table 1: Material properties input into the COMSOL simulation.

Heat fluxes were simulated inside the building structure and along the soil outside. The indoor heat convection coefficient was estimated as 10.95 (W/m<sup>2</sup>K), as this is a reasonable heat flux value for an indoor environment. It was assumed that the building was temperature controlled at 20°C. The initial

temperature of the insulation was 9.85°C and the initial glacial temperature was simulated as -2°C.

An outside atmospheric heat flux was also simulated, with heat convection coefficients corresponding to the atmospheric temperature, calculated using Equation 1.

Month by month average temperature values between 2005 and 2014 were used and collected from [10]. May 2005 was missing a temperature value and was inferred as 45°F. The heat convection coefficient of the ground was calculated by month using the following equation from [11]:

$$H_s = 1.72(T_s - T_a)^{0.33} \quad (1)$$

$T_s$  is the surface temperature of the ground, and  $T_a$  is the atmospheric temperature.

After examining the temperature change overtime, the creep strain and creep strain rate ratios were calculated to examine how the increase in temperature impacted the soil underneath the building.

To compare the creep and creep rates for two temperatures  $\theta_1$  and  $\theta_2$ , the following equation from [12] is used:

$$\frac{E_{1,\theta_1}}{E_{2,\theta_2}} = \left( \frac{\theta_1 + \theta_0}{\theta_2 + \theta_0} \right)^{-mn} \quad (2)$$

<sup>2</sup>Dimensions from unpublished technical data

Where  $w$  is the temperature exponent and is generally less than or equal to one.  $n$  is the creep exponent of stress.  $\theta_1$  is the temperature in 2005.  $\theta_2$  is the temperature in 2014.  $\theta_0$  is set at  $1^\circ\text{C}$ .

### Results

Horizontal Cross Section: 2 meters below the surface displayed a total temperature change of  $4^\circ\text{C}$ , increasing from  $-2$  to  $2^\circ\text{C}$ . Sensitivity testing was done by adjusting the glacier's initial temperature to  $0^\circ\text{C}$ . When the glacier's initial temperature was adjusted to  $0^\circ\text{C}$ , temperature increased  $3.6^\circ\text{C}$ . Assuming  $w = 1$  and  $n = 3$  in Equation 2, a temperature change of  $4^\circ$  increases the ratio by 27 times. Figure 2 c and d shows how the temperature from the base of the insulation to 10 meters below the surface has changed from 2005 to 2014 during December, January, and February. The largest temperature differences appear to occur between 2 and 6 meters below the surface, emphasizing the importance of heat regulation near the contact areas between the building and the glacier.

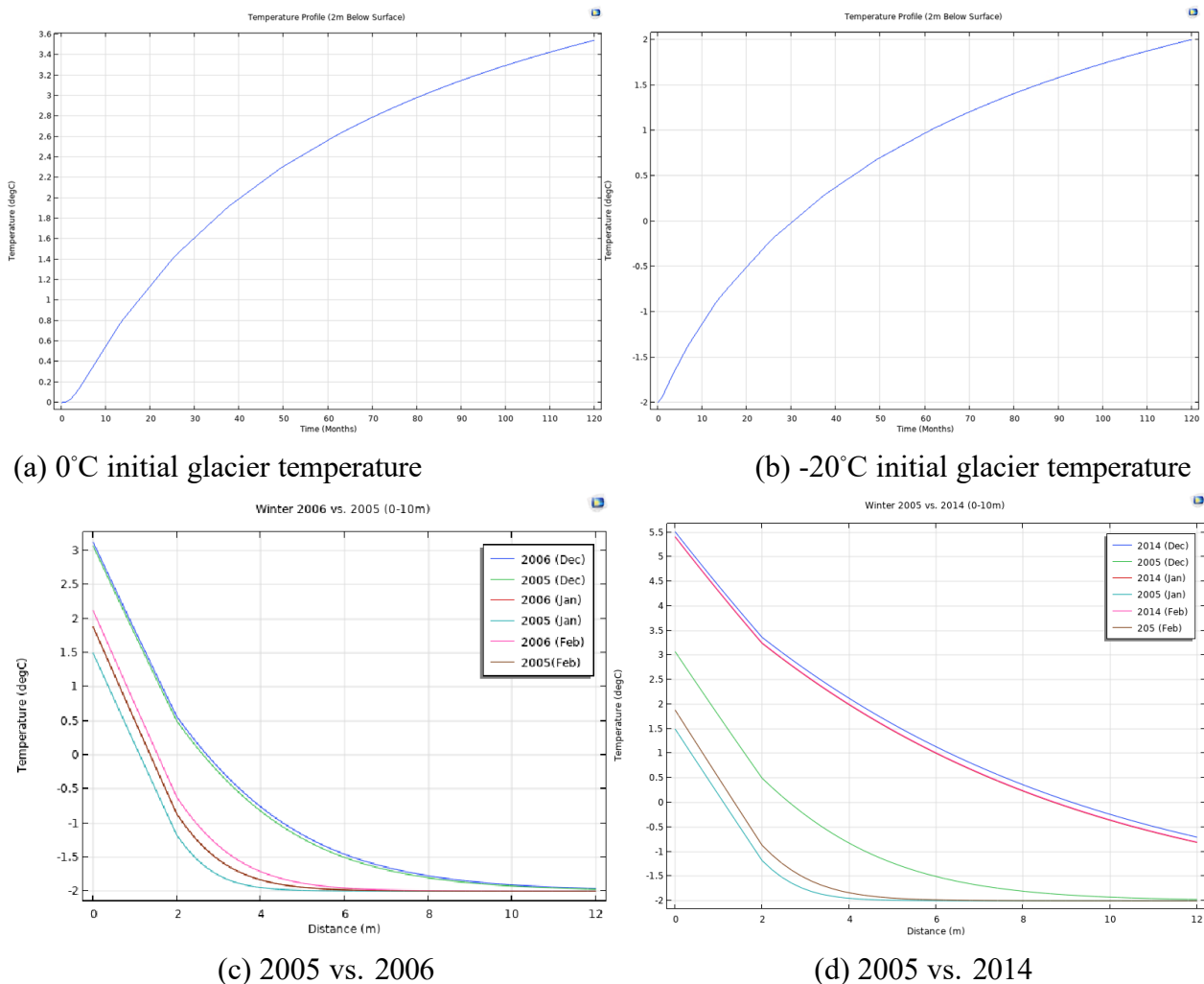


Figure 2: a and b) Temperature profile 2m subsurface at different initial glacial temperature. c and d) Change in temperature from 0-10m subsurface during the winter months.

### Limitations

Heat flow into/out of a glacier is complicated due to difference freezing indices, convection, radiation, etc. Which makes it hard to model in COMSOL, though future iterations of the project should consider the more intricate glacial movements and heat movement. Furthermore, it was difficult to account for the melted portions of the ice, as this required more geotechnical data and assumptions. Furthermore, frost heave was not considered in the simulation, but might be an important consideration. Although outside the scope of this project, future iterations should consider modeling the heat transfer under the addition of thermosyphons, which were introduced in the original design. Because Rotta Loria's paper [13] was published after the original COMSOL simulations, their method of including how the ground heaved/sunk in Chicago was not included in this analysis but methods should be considered in future explorations of simulations exploring how ground temperature impacts a building's foundation.

## **Conclusions**

From this analysis, the usage of COMSOL to examine how a building transfers heat to its surroundings is explored. This analysis showed that between 2005 and 2014, heat transfer between the Lone Peak Tram displayed a theoretical increase of 4°C in glacial temperature at 2m below the surface when the initial glacial temperature is -2°C. Such modeling suggests that the insulation layer between the Lone Peak Tram and the rock glacier might have had increased effectively with additional heat control parameters, such as thermosyphons. Calculations suggest that the building's creep and creep rate ratio in 2014 was 27 times the same ratio in 2006. Overall, this paper aims to explore how COMSOL can be utilized to examine infrastructure in dynamic temperature regions of the world.

## **References**

Yellowstone-Bighorn Research Association. Ybra uplift 2018. Annual Newsletter of the Yellowstone-Bighorn Research Association, 2018.

Douglas K. Hamre, David, Erwin L. McCarty, Edward Long, and Yarkmak Jr. Ice engineering for rock glaciers. page 433, 2000.

Caitlyn Florentine. Regional context, internal structure, and microbiological investigation of the lone peak rock glacier, big sky, montana. Master's thesis, Montana State University, 2011.

Caitlyn Florentine, Mark Skidmore, Marvin Speece, Curtis Link, and Colin A. Shaw. Geophysical analysis of transverse ridges and internal structure at lone peak rock glacier, big sky, montana, usa. Journal of glaciology, 60(221):453–462, 2014.

DOW. Styrofoam™ highload 40, 60 and 100 extruded polystyrene insulation. BestMaterials.com. Accessed: 5-3-2023.

DOW. Styrofoam blue extruded polystyrene foam. DOW Building Solutions. Accessed: 5-3-2023.

Aqua Calc. Density of styrofoam highload 60 insulation (material). AVCalc LLC. Accessed: 5-3-2023.

The Engineering Tool Box. Ice - thermal properties. The Engineering Tool Box. Accessed: 5-1-2023.



Michael J. Heap, Alexandra R.L. Kushnir, J'ér'emie Vasseur, Fabian B. Wadsworth, Pauline Harl'e, Patrick Baud, Ben M. Kennedy, Valentin R. Troll, and Frances M. Deegan. The thermal properties of porous andesite. *Journal of volcanology and geothermal research*, 398:106901, 2020.

National Weather Service. Nowdata - noaa online weather data. National Oceanic and Atmospheric Administration. Accessed: 5-1-2023.

M.R. Granados, S. Bonachela, J. Hern'andez, J.C. L'opez, J.J. P'erez-Parra, E.J. Baeza, and J.J. Mag'an. Measurement of the soil-air convective heat transfer coefficient from a greenhouse mulch soil. In *Acta horticulturae*, number 893, pages 539–544. International Society for Horticultural Science (ISHS), 2011.

Orlando B Andersland. *Frozen ground engineering*. J. Wiley [with] American Society of Civil Engineers, Hoboken, N.J., 2nd ed. edition, 2004.

Alessandro F. Rotta Loria. The silent impact of underground climate change on civil infrastructure. *Communications engineering*, 2(1):44, 2023.

## Case study of the thermal regime of permafrost underneath the airstrips near Hudson Bay coast, Canada

Xiangbing Kong, Ph.D<sup>1</sup> and Guy Doré, Ph.D, P.Eng<sup>2</sup>

<sup>1</sup> *Department of Mathematics, Computer Science and Engineering, Université du Québec à Rimouski, 300, allée des Ursulines, Rimouski, QC, Canada; email: xiangbing\_kong@uqar.ca*

<sup>2</sup> *Department of Civil and Water Engineering, Université Laval, 2325, rue de l'Université, Québec City, QC, Canada; email: Guy.Dore@gci.ulaval.ca*

### **Abstract**

Transportation infrastructure is of vital importance to the local communities in Nunavik, Quebec, Canada. Permafrost degradation results in infrastructure failures and affects social, economic development. The case study of airstrip embankment at Salluit was selected to help improve the understanding of ground thermal conditions in Nunavik. This paper presents the analysis of thermal data collected at the Salluit airstrip and one two-dimensional geothermal model developed to reproduce the subsurface thermal regime under the centerline of airstrip embankment. The measured embankment dimension and air temperature were used as the inputs to improve the model accuracy. Field measurement of ground temperatures for a two-year monitoring period from 2016 to 2018 was used to calibrate the model developed. This study provided valuable information to investigate the vulnerability of the airstrips using the simulation approach in response to climate warming effects, in Nunavik.

## Study on the thermal regime of permafrost underneath the Tasiujaq airstrip near Ungava Bay coast, Northern Quebec

Xiangbing Kong, Ph.D<sup>1</sup> and Guy Doré, Ph.D, P.Eng<sup>2</sup>

<sup>1</sup> *Department of Mathematics, Computer Science and Engineering, Université du Québec à Rimouski, 300, allée des Ursulines, Rimouski, QC, Canada; email: xiangbing\_kong@uqar.ca*

<sup>2</sup> *Department of Civil and Water Engineering, Université Laval, 2325, rue de l'Université, Québec City, QC, Canada; email: Guy.Dore@gci.ulaval.ca*

### **Abstract**

Observed and projected climate warming affects the thermal stability of airstrip foundation in Nunavik, Canada. Intensive maintenance is needed to keep a reasonable service level. The paper focus on a case study of permafrost beneath the airstrip embankment at Tasiujaq, Nunavik. Field measurements of 6 years thermal data have been used to calibrate a 2D finite element model developed to reproduce the thermal condition of airstrip foundation and simulate soil temperatures. The model developed was well calibrated to the measured temperature data, supporting the reasonable accuracy of developed model. Specific interest was paid to the side slope, where rapid permafrost degradation was expected. One adaptation solution was also proposed, based on documented thermal stabilization approach.

# Assessing the use, utility, and spatial accuracy of 3-D camera tools for the measurement and visualization of permafrost thaw impact on road and bridge infrastructure in rural Alaskan Communities

Olaf Kuhlke, Ph.D.<sup>1</sup> and Steven Rowell<sup>2</sup>

<sup>1</sup> *Professor, Minneapolis College of Art and Design. Email: okuhlke@mcad.edu*

<sup>2</sup> *Post-graduate Researcher, Minneapolis College of Art and Design. Email: srowell@mcad.edu*

## **Abstract**

In this paper, we demonstrate the use, utility, and spatial accuracy of the Matterport Pro-3 camera tool and the Apple Vision Pro for the measurement and 3-D visualization of permafrost thaw and its impact on road and bridge infrastructure in rural Alaska communities. Permafrost thaw is having an increasingly noticeable effect on public infrastructure degradation in remote Alaskan communities. To document the subsidence and other engineering concerns associated with roads and bridges, we utilized two different devices and workflows to map and visualize sites in Nome, Circle, and Utqiagvik, AK, including roads, bridges, and revetments. The MCAD team deployed a tripod-mounted Matterport Pro3 LiDAR camera with the proprietary Matterport platform. This paper assesses the use of this camera technology (user-friendliness, cost, user experience), utility (capability and variety of visualization functions, software integration), and spatial resolution (accuracy of spatial measurements) and its potential application and replicability in future field research in the Arctic. Furthermore, will examine and demonstrate the interoperability of the Matterport system with the recently released Apple Vision Pro VR headset for visualization of the captured imagery.

# Low Impact Sustainable Gravel Mining on the Sagavanirktok River Floodplain

Alexandre Lai <sup>1</sup>

*<sup>1</sup> Sr. Civil Integrity Engineer, Alyeska Pipeline Service Company. Email: alexandre.lai@alyeska-pipeline.com*

## **Abstract**

Gravel mining along river systems have a negative reputation due to past practices that resulted in adverse impacts on the environment. Cases cited in the literature of negative environmental impacts are typically large commercial operations with continuous high volume mining were extraction likely exceeded natural recharge rates of the river system.

A three year pilot program by Alyeska Pipeline Service Company on the Sagavanirktok River shows that with appropriate controls, gravel extraction can be done in a sustainable and environmentally responsible manner.

Infrastructure maintenance and development on the North Slope of Alaska such as the Dalton Highway and the Trans- Alaska Pipeline require substantial quantities of gravel material. If gravel can be mined locally on suitable stream reaches, it can reduce overall costs by shortening haul distances, increase road travel safety and reduce vehicle emissions.



# Impact of Glacier Outburst Floods on Stream Stability at the Tazlina River Trans-Alaska Pipeline Crossing

Alexandre Lai <sup>1</sup>

*<sup>1</sup> Sr. Civil Integrity Engineer, Alyeska Pipeline Service Company. Email: alexandre.lai@alyeska-pipeline.com*

## **Abstract**

The Tazlina River is subject to periodic Glacier Lake Outburst Floods (GLOF) when water from marginal lakes blocked by the glacier is suddenly released. These floods can damage infrastructure, threaten life and property of affected communities, and destabilize stream reaches for many years. This paper analyzes the affects of GLOFs on the Trans-Alaska Pipeline crossing at the Tazlina River and actions taken to reduce risk to Pipeline integrity.

## Preliminary Finite-Element Modeling of Floating Sea Ice Impacting Vertical Piles with Accreted Ice

Jasmine Langmann, E.I.T., M.S., M. ASCE, & Scott Hamel, P.E., Ph.D., M. ASCE

### **Abstract**

The current approach to calculate ice design forces on coastal structural elements is to apply the crushing strength of thick sea ice over the width of the structural element, plus the width of any accreted ice bonded to the element. To evaluate the accuracy of this method, accreted ice samples from the Port of Alaska were harvested and tested for shear and compression strength. The resulting data was then used to calibrate a preliminary finite-element (FE) material model in Abaqus CAE 2022 using a concrete damaged plasticity model. Three simulations were created and evaluated: A uniaxial compression model of a cylindrical sample to verify the material model against the experimental results; a bare pile and ice floe interaction model; and an interaction model consisting of a vertical pile, accreted ice, and ice floe. Model results showed the modeled ice floes were extremely stiff, causing excessively large ice forces that greatly exceeded the design capacity of the pile. The model provided valuable insight into the complexities of numerical modeling of ice-ice-structure interaction, and demonstrated that more sophisticated ice material models are needed for the ice floe.

# Estimation of bed shear stress distribution using ADCP data in ice-covered streams

Berkay Koyuncu and Trung Bao Le

*Department of Civil and Environmental Engineering, North Dakota State University, Fargo, ND 58102, Email: trung.le@ndsu.edu*

## **Abstract**

We study cross-stream distribution of bed shear stress in ice-covered streams. Bed shear stress is a critical factor in regulating the evolution of natural streams, especially during spring floods. However, there have been limited numbers of studies on the link between ice coverage and bed shear stress. In this study, we investigate the impact of ice cover on the three-dimensional flow structures and the bed shear velocity in a trapezoidal channel. We investigate both fully-covered and partially covered (symmetrical shore ice) conditions using numerical simulation (Large Eddy Simulation) and analytical method. Our analytical and numerical results agree well with the corresponding experimental data. Finally, we derive a novel theoretical model to explain the pattern of the bed shear stress distribution in natural streams.

# Prediction of Mid-Winter Breakup of Ice Cover on Canadian Rivers

Zoe Li, Ph.D., P.Eng, M.ASCE<sup>1</sup> and Michael De Coste, Ph.D.<sup>2</sup>

<sup>1</sup> *Department of Civil Engineering McMaster University, Hamilton, L8S 4L7, ON, Canada; email: zoeli@mcmaster.ca*

<sup>2</sup> *School of Engineering, Okanagan Campus, The University of British Columbia, Kelowna, V1V 1V7, BC, Canada; email: michael.decoste@ubc.ca*

## Abstract

Mid-Winter Breakups (MWBs) are the early melt of river ice cover outside of the typical spring breakup season. These events can lead to severe flooding especially when the breakups trigger the formation of ice jams. MWBs are usually caused by periods of unseasonably high temperatures, which are becoming more common in Canada as a result of climate change. They are difficult to predict, as they involve complex river ice dynamics and there are very limited data. In this study, a machine learning (ML) framework based on binary classification was developed to predict MWBs based on a Canada-wide river ice dataset. The proposed framework consists of several ML algorithms, including Adaptive Boosting, k-Nearest Neighbors (KNN), Class Switching, and Adaptive Resampling and Combining X4 (ArcX4). The models were trained using 452 MWB events across Canada during 1955 to 2015. The developed models were demonstrated to be reliable and efficient for predicting MWBs. This study was the first successful attempt to utilize ML in MWB prediction on a national scale. It can provide useful technical support for further applications in other similar cold regions.

**Keywords:** Mid-Winter Breakup, machine learning, binary classification, Canadian Rivers

## Introduction

Mid-Winter Breakup (MWB) is the early breakup of ice cover outside of the typical spring season. Recently, it has been noted that many rivers in cold regions have become vulnerable to MWBs [1,2]. MWBs often lead to the risk of river ice jam formation, which can trigger severe flooding [3]. To reduce such risks and their cascading impacts on the affected communities, robust and effective prediction of MWBs is of great importance. However, previous studies on MWB prediction have faced constraints related to both the effectiveness of the methodology and the availability of data [3]. In this study, a two-level modeling approach was first developed for the prediction of MWBs. An MWB Ontology was then developed and integrated with the two-level modeling approach to establish a hybrid modeling framework to further enhance prediction accuracy.

## Methodology

In the two-level modeling approach, the first level models predict MWB occurrence within a given period (e.g., one month, two weeks, one week) and the second level models predict the timing of an MWB occurrence within that period [3]. The adopted ML algorithms for binary classification and prediction (i.e., YES or NO MWB) included Adaptive Boosting, k-Nearest Neighbors (KNN), Class Switching, and Adaptive Resampling and Combining X4 (ArcX4). An MWB Ontology, which effectively organizes and analyzes MWB data, events, and relationships in an ice season, was developed and integrated with the two-level modeling approach for MWB prediction [2].

The river ice data for this study were extracted from the Canadian River Ice Database (CRID) (<https://open.canada.ca/data/en/dataset/c5b58ccd-0011-4a80-8f24-034c86cbc14d>). The CRID, developed by Environment and Climate Change Canada, provides river ice data from 196 Canada's National Hydrometric Program sites within the period of 1894 to 2015. River ice data at 52 gauges affected by MWBs were extracted from the original CRID. A total of 452 MWB events occurred during 1955 to 2015 were included. Climate data, including daily maximum and minimum temperature and precipitation, were obtained from National Resources Canada. Accumulated Freezing Degree Days (AFDD) with a reference date of October 1st, as well as total precipitation cumulatively summed from the freeze-up date of river ice cover, were also calculated and used.

## Results

Multiple configurations of the two-level modeling approach, with different period lengths, input variables and classification algorithms, were tested for the dataset consisting of 452 MWB events. The best performing configuration used a biweekly time period for the first level and a daily resolution for the second level. The overall accuracies were 80.1% and 77.6% for the first and second level models, respectively [3]. The hybrid model framework was able to further enhance prediction accuracy. The best configuration had a mean absolute error of 12.47 days for MWB prediction [2]. The results demonstrated the effectiveness of the proposed machine learning and hybrid approaches. More results can be found in [2] and [3].

## Conclusions

The new machine learning and hybrid modeling approaches provided new and easy-to-use tools capable of predicting MWBs across Canada. The methodology can be extended and transferred to other cold regions including locations that have not yet experienced MWBs. This study can provide valuable decision-making support to rivers and communities vulnerable to the risks of MWBs.

## Acknowledgments

This study was supported by Natural Sciences and Engineering Research Council of Canada (NSERC).

## References

- M. De Coste, Z. Li and R. Khedri (2024). A hybrid ontology-based semantic and machine learning model for the prediction of spring breakup. *Computer-Aided Civil and Infrastructure Engineering*, 39(2): 264-280.
- M. De Coste and Z. Li (2023). The prediction of mid-winter and spring breakups of ice cover on Canadian rivers using a hybrid ontology-based and machine learning model. *Environmental Modelling and Software*, 160: 105577.
- M. De Coste, Z. Li and Y. Dibike (2022). Machine-learning approach for predicting the occurrence and timing of mid-winter ice breakups on Canadian rivers. *Environmental Modelling & Software*, 152: 105402.
- M. De Coste, Z. Li and Y. Dibike (2022). Assessing and predicting the severity of mid-winter breakups based on Canada-wide river ice data. *Journal of Hydrology*, 127550.

M. De Coste, Z. Li, D. Pupek and W. Sun (2021). A hybrid ensemble modelling framework for the prediction of breakup ice jams on northern rivers. *Cold Regions Science and Technology*, 189: 103302.

### 3D Coordinates Determination for the Featured Points Based on close-up photogrammetric Method

Zhanhe Li,<sup>1</sup> Chuang Lin,<sup>1\*</sup> Han Zhao,<sup>2</sup> Decheng Feng,<sup>1</sup> and Feng Zhang.<sup>1\*</sup>

<sup>1</sup>*School of Transportation Science and Engineering, Harbin Institute of Technology, Harbin 150001, China; email: linchuang@hit.edu.cn*

<sup>2</sup>*Jilin Traffic Planning and Design Institute, Changchun 130000, China; email: mzm1755709496@163.com*

#### **Abstract**

Aiming at the many shortcomings of the current traditional monitoring methods, such as high cost, inability of real-time solving, and high requirements for the monitoring environment, we propose a three-dimensional coordinate calculation method of feature points based on the close-up photogrammetry technology, and analyze and research on the calibration of the camera parameters, identification and localization of markers, and calculation of the coordinates of feature points. Firstly, the calibration method is selected for camera calibration test, and the internal and external parameters of the camera are calculated; secondly, artificial markers are selected, target detection algorithm is used to identify the markers, and the marker images are preprocessed to obtain the 2D coordinates of the feature points; lastly, the matrix transformation of the image under the spatial system is analyzed through the projective geometric transformation, and the mathematical characterization of the relationship between the 2D coordinates of feature point pixels and the actual 3D coordinates is established.



# Study of the properties of wicking geotextile-mudstone mixed soil subgrade in cold regions

Xingmao Su,<sup>1</sup> Chuang Lin,<sup>1\*</sup> Decheng Feng,<sup>1</sup> and Feng Zhang.<sup>1\*</sup>

<sup>1</sup>*School of Transportation Science and Engineering, Harbin Institute of Technology, Harbin 150001, China; email: [linchuang@hit.edu.cn](mailto:linchuang@hit.edu.cn)*

## Abstract

Mudstone mixed soil is a kind of mixed soil formed by the mixture of mudstone and surface soil. The disintegration properties of mudstone in contact with water have led to a significant decrease in the weak stability of mudstone mixed soil, so it is often treated as a kind of construction solid waste in engineering construction. In order to promote the process of resource utilization of construction waste, improve the mechanical and stability of mudstone mixed soil, and make it meet the road performance requirements of subgrade in cold areas, the benefits of the wicking geotextile were quantified via numerical simulations. The performances were compared for road embankments with and without the wicking geotextile. The results showed that Wicking geotextiles can effectively reduce the moisture content of the subgrade, and the moisture content of the bottom layer of the upper road bed and the bottom layer of the lower road bed are reduced by 45.4% and 41.6%. Maximizes subgrade performance when wicking geotextiles are placed at the bottom of the roadbed. Based on research results, the mudstone soil mixture, as a solid waste, can be used as a filling material in cold regions with the application of the wicking geotextile.

## Quantification of influence factors in the studded tire wear using the Prall device

D. Loaiza-Monsalve<sup>1</sup>, J.-P Bilodeau<sup>2</sup>, Fournier. B<sup>3</sup>, F. Doucet<sup>4</sup> and S. Chabchoub<sup>5</sup>

<sup>1</sup>*Department of Civil and Water Engineering, Laval University, Quebec, QC G1V 0A6, Canada; email: dayani-senedy.loaiza-monsalve.1@ulaval.ca*

<sup>2</sup>*Department of Civil and Water Engineering, Laval University, Quebec, QC G1V 0A6, Canada; email: jean-pascal.bilodeau@gci.ulaval.ca*

<sup>3</sup>*Department of Geology and Geological Engineering, Laval University, Quebec, QC G1V 0A6, Canada; email: benoit.fournier@ggl.ulaval.ca*

<sup>4</sup>*Asphalt Mixes section, Ministry of Transportation and Sustainable Mobility, Quebec, QC G1P 4C7, email: felix.doucet@transport.gouv.qc.ca*

<sup>5</sup>*Department of Civil and Water Engineering, Laval University, Quebec, QC G1V 0A6, Canada; email: syrine.chabchoub.1@ulaval.ca*

### Abstract

Studded tire wear is widely considered to be a critical aspect that conditions the ride quality in cold regions. This research provides a comparative analysis of the influence of certain factors on pavement wear caused by studded tires. Abrasion resistance measurements were conducted on aggregates and asphalt specimens, using the Nordic Ball Mill apparatus and the Prall apparatus, respectively. This approach ensures an understanding of the interaction between these variables and the resultant wear response of the asphalt mixture. Tests relied on three different types of asphalt mixtures (ESG, dense-graded asphalt; EG, coarse-graded asphalt; and SMA, Stone Matrix Asphalt), different percentages of reclaimed asphalt pavement (0%, 10%, and 20%), and different aggregate hardness. Image analysis methodology was used to assess the coarse-sectional area of the sample covered by coarse aggregates. The results showcased that harder coarse aggregates were less prone to wear. Comparisons indicate that the SMA10 yields higher abrasion resistance than the remaining mixtures used in this study. The percentage of the cross-sectional area covered by coarse aggregate influences the mixture abrasion value.

## Multiscale characterization of cracking resistance in asphalt: Link between binder and mixture tests

Blaise Elliott, Jianmin Ma <sup>✉</sup>, Hanwalle M.C. Nawarathna, Chandra S. Mohanta, Simon A.M. Hesp <sup>✉</sup>

*Department of Chemistry, Queen's University, Kingston, Ontario K7L 3N6, Canada*

*✉ email: jianmin.ma@queensu.ca; simon.hesp@chem.queensu.ca*

### **Abstract**

Establishing a link between low temperature cracking resistance results for binder and mixture tests has proven challenging. This study aims to investigate the underlying factors that impact this correlation. A diverse set of loose asphalt mixture samples was collected from user agencies around North America, allowing for the extraction and recovery of asphalt binder as well as the preparation of semi-circular bend (SCB) specimens. Subsequently, extended bending beam rheometer (EBBR) and double edge notched tension (DENT) tests were conducted on the recovered binder. SCB tests were performed on asphalt mixture specimens before and after low-temperature conditioning. The analysis of correlations between binder and mixture test results revealed that considering thermo-reversible aging significantly improves the correlation between the two sets of data. Additionally, the presence of oil exudation was identified as another confounding factor for the correlation exercise.

# Comparative analysis of tension-compression and shear oscillatory loading on the rheological response of asphalt binders from a Northern Ontario pavement trial

Emily Garvin, Jianmin Ma <sup>✉</sup>, Simon A.M. Hesp <sup>✉</sup>

*Department of Chemistry, Queen's University, Kingston, Ontario K7L 3N6, Canada*

*✉ email: jianmin.ma@queensu.ca; simon.hesp@chem.queensu.ca*

## **Abstract**

This study explores the rheological behavior of asphalt binders under two distinct loading conditions: oscillatory shear and cyclic tension-compression. Notably, the longitudinal complex modulus of asphalt binders was found to be lower in oscillatory shear compared to cyclic tension-compression loading. Furthermore, a reduction in asphalt film thickness during tension-compression loading led to an increase in longitudinal complex modulus. Phase angle master curves of asphalt binder in tension-compression loading show rheologically complex behavior. Interestingly, alterations in asphalt film thickness had minimal influence on the phase angle master curve for tension-compression, while the phase angle master curve under oscillatory shear exhibited higher values at high frequencies or low temperatures. Additionally, the study discovered that the limiting phase angle temperature was lower in oscillatory shear than in tension-compression. A decrease in asphalt film thickness leads to an increase in the limiting phase angle temperature.

## Effect of Salt Concentrations on the Freeze-Thaw Behavior of Soils

Mohammad Wasif Naqvi<sup>1</sup>, Md Fyaz Sadiq<sup>2</sup>, Bora Cetin<sup>3</sup>, Micheal Uduebor<sup>4</sup>, John Daniels<sup>5</sup>,

<sup>1</sup>Graduate Research Assistant, Department of Civil, Construction and Environmental Engineering, Michigan State University, East Lansing, MI 48824; Email: [naqvimo1@msu.edu](mailto:naqvimo1@msu.edu)

<sup>2</sup>Graduate Research Assistant, Department of Civil, Construction, and Environmental Engineering, Michigan State University, East Lansing, MI 48824; Email: [sadiqmd@msu.edu](mailto:sadiqmd@msu.edu)

<sup>3</sup>Associate Professor, Department of Civil and Environmental Engineering, Michigan State University, East Lansing, MI 48824; Email: [cetinbor@msu.edu](mailto:cetinbor@msu.edu) (Corresponding Author)

<sup>4</sup>Lecturer, Department of Civil Engineering, Florida Gulf Coast University, Fort Myers, FL 33965; Email: [muduebor@fgcu.edu](mailto:muduebor@fgcu.edu)

<sup>5</sup>Professor, Department of Civil and Environmental Engineering, UNC Charlotte, Charlotte, NC 28223; Email: [john.daniels@charlotte.edu](mailto:john.daniels@charlotte.edu)

### Abstract

Freeze-thaw cycles in the soil can lead to negative effects like frost heave and decreased stiffness during thawing. The frost action in soils can be influenced by the salt concentration in soils, which is altered due to road deicing operations during the winter. Salt concentrations in soils cause freezing point reduction (FPD), which reduces the development of ice in the soil. Simultaneously, a high level of salt causes osmotic suction due to the movement of ions toward the freezing front as ice forms. These two phenomena can potentially result in either a decrease or an increase in the vulnerability of soils to frost action. The present study aims to examine the influence of varying salt concentrations on the freeze-thaw susceptibility of soil. The soil samples were treated with salt concentrations of 0.2%, 1%, and 5% NaCl solutions, as well as a control prepared with deionized water only. The FPD caused by the presence of salt was measured, and it was noted that the extent of depression increased in proportion to the salt concentration. The specimens were subjected to a unidirectional freeze-thaw test. During the experiment, measurements were taken for heave, temperature, and water intake. Additionally, the moisture contents and pore water salinities were measured at different depths of the specimen following the freeze-thaw test. The findings indicated that specimens subjected to salt treatment displayed a decrease in the maximum heave of up to 31% compared to the control prepared with deionized water only, attributed to reduced ice segregation. The water migration in the soil was found to be lower in soils treated with salt. The moisture content and pore water electrical conductivity increase with the height of the specimen. It can be concluded that the FPD exerted a greater influence compared to osmotic suction, resulting in a decrease in the formation of ice within soils. Hence, the presence of salt can aid in the mitigation of freeze-thaw damage in soils.

# Feasibility of SAA to Monitor Freeze-Thaw Performance of Pavement Foundations in Cold Regions

Md Fyaz Sadiq<sup>1</sup>, Mohammad Wasif Naqvi<sup>2</sup>, Joseph Podolsky, Ph.D., P.E.<sup>3</sup>, Raul Velasquez, Ph.D., P.E.<sup>4</sup>

<sup>1</sup>Graduate Research Assistant, Department of Civil and Environmental Engineering, Michigan State University, East Lansing, MI 48824; Email: [sadiqmd@msu.edu](mailto:sadiqmd@msu.edu)

<sup>2</sup>Graduate Research Assistant, Department of Civil and Environmental Engineering, Michigan State University, East Lansing, MI 48824; Email: [naqvimo1@msu.edu](mailto:naqvimo1@msu.edu)

<sup>3</sup>MnROAD Data Science Expert, Minnesota Department of Transportation (MnDOT), Maplewood, MN 55109; Email: [joseph.podolsky@state.mn.us](mailto:joseph.podolsky@state.mn.us)

<sup>4</sup>Geomechanics Research Engineer, Minnesota Department of Transportation (MnDOT), Office of Materials and Road Research (OMRR), Maplewood, MN 55109; Email: [raul.velasquez@state.mn.us](mailto:raul.velasquez@state.mn.us)

## Abstract

Frost heave and thaw weakening have a significant impact on the performance of pavement foundations in cold regions, leading to structural damage. Road Agencies use different approaches, including seasonal load restrictions (SLR), to minimize the impact of this damage. Accurate and continuous measurement of displacements caused by frost action is crucial for agencies to assess the condition and behavior of pavement foundations. Existing methods, such as vehicle-mounted laser sensors and surveying equipment, have limitations in capturing the temporal distribution of displacement in roadways. Shape Array Accelerometers (SAA) can measure the ground's displacement in real-time and come with temperature sensors that provide temperature measurements at its location. This study discusses the installation procedure and evaluates the effectiveness of SAA in characterizing frost heave-thaw settlement of flexible pavements. SAA was installed along the cross-section of a flexible pavement within the Minnesota Road Research Facility (MnROAD) mainline on Westbound I-94 near Albertville, Minnesota. Minnesota falls in the wet-freeze climatic region, making it highly susceptible to freeze-thaw damage. The collected displacement and temperature dataset for the 2022-23 freeze-thaw season was analyzed, and maximum settlement of 3.5 mm and 10.3 mm were observed in the shoulder and passing lane, respectively. The temperature data indicated that the ground started to settle when thermocouple readings went below freezing, suggesting ice lens formation, resulting in the contraction of the soil structure. After the spring thaw, a maximum residual settlement of 6.6 mm remained along the wheel paths, but the ground eventually stabilized once the thawing was complete. The efficacy of SAA in capturing real-time displacement data indicates its potential for broader implementation in similar climatic conditions.



# Analysis for Arctic Climatic Typing (ACT)

Michelle L. Michaels,<sup>1, a</sup> Rosa T. Affleck, Ph.D.,<sup>1, b</sup> Kevin Bjella, P.E.,<sup>2, c</sup> Brendon Hoch,<sup>1, d</sup>  
Paige Toebben<sup>2, e</sup>

<sup>1</sup>*U.S. Army Corps of Engineers, Engineer Research and Development Center (ERDC), Cold Regions Research and Engineering Laboratory (CRREL), 72 Lyme Rd, Hanover, NH 03755;*

<sup>a</sup>*michelle.l.michaels@erdc.dren.mil;* <sup>b</sup>*rosa.t.affleck@usace.army.mil;*

<sup>d</sup>*brendon.hoch@erdc.dren.mil*

<sup>2</sup>*U.S. Army Corps of Engineers, Engineer Research and Development Center (ERDC), Cold Regions Research and Engineering Laboratory (CRREL), 4070 9<sup>th</sup> Street, Fort Wainwright, AK 99703;* <sup>c</sup>*kevin.bjella@usace.army.mil;* <sup>e</sup>*paige.m.toebben@usace.army.mil*

## Abstract

The Army maintains stringent requirements for equipment in the Arctic operational environment and expresses concerns of risk to mission failure for sustaining the forces at temperatures down to -65°F, wind speeds greater than 100 mph, and 25 lb/ft<sup>2</sup> snow load. However, these conditions may only be encountered on rare occasions, and in certain subregions of the Arctic. The Arctic environment has wide climatic variations, and the climatic conditions have vast divergence between the coastal areas and interior locations because of latitude, circulation patterns, and elevation. As such, there is a need to refine the Arctic climate zones with additional environmental parameters to delineate where these climatic conditions can be found.

**Keywords:** weather, climate, Arctic operations, resilience

## Introduction

In this new start project, we explore refining the Arctic climatic zones characterization relative to the design thresholds of temperatures down to -65°F, wind speeds greater than 100 mph, and 25 lb/ft<sup>2</sup> snow load. This includes identifying the circumpolar north climate breaks for environmental parameters to narrow the contingency, logistics and resources needed, and develop site-focused requirements for the Department of Defense to operate across the region. To accomplish this, we intend to include three climate characteristics (air temperature extremes, snow depth and wind speed limits) to the currently defined climate zones and conduct analysis against materiel and equipment exposure thresholds. This will provide mission critical data and information for installation operations managers to make better risk-informed decisions and to operate equipment, materiel, and force projection in the circumpolar region. Incorporating these climate characteristics with various operation exposure thresholds will provide realistic and practical environmental parameters to decisively apply the right resources and capability for DoD operations.

Our analysis is driven by these main guiding questions:

- Are all Arctic materiel solutions required to operate at -65°F?
- Are there existing capabilities and solutions that can operate at -65°F?
- Are there existing capabilities that don't meet the -65°F requirement that can be used anywhere else in the Arctic?
- Do some subregions of the Arctic never experience 100+ mph winds or 25 lb/ft<sup>2</sup> of

snowload?

## Methodology

Both the Army Technical Manual (TM 4-33.31, *Cold Weather Maintenance Operations*) and the Army Regulation 70-38 (AR 70-38) outline climatic categories according to the general principles and technical guidance on the effects and hazards in a cold environment that impact mission functions including planning, design, operation, and maintenance of equipment. TM 4-33.31 categorizes cold temperatures based on absolute minimum values into five groups (wet-cold, dry-cold, intense-cold, extreme-cold, and hazardous-cold), and mainly generalizes the effects of snow and ice conditions. The AR 70-38 delineates climatic categories into four elements (basic cold, cold, severe cold, and extreme cold) and incorporates to some degree the design conditions based on limits of continuous time exposure with ambient air temperature, snow surface temperature, wind speed, and relative humidity tending towards saturation. This is the current status of the identification of climate zones in the circumpolar north that is referenced by DoD.

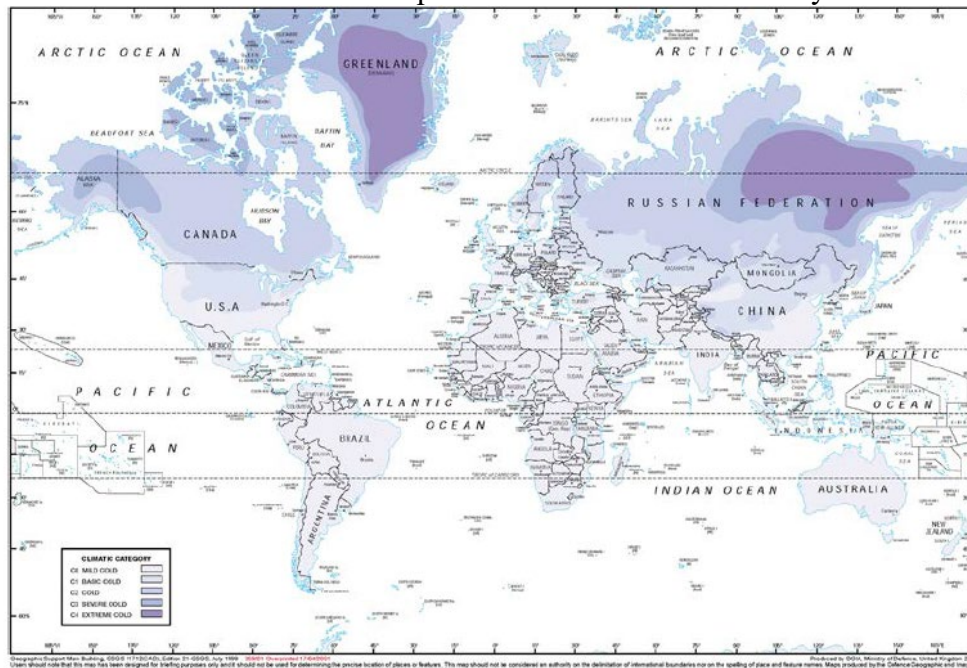


Figure 1. An excerpt from AR 70-38 with the current identification of cold and severe cold climatic categories.

The objective of this proposed work is to further identify and refine the climate zones in the circumpolar north identified in TM 4-33.31 and AR 70-38 to include three climate characteristics (air temperature extremes, snow depth and wind speed limits) and map against material and equipment exposure thresholds. Our outline of tasks and methods for accomplishing our project objectives are below.

### *Compile climate information.*

Climate information is gathered and compiled from the U.S. Air Force (USAF) 14th Weather Squadron (14<sup>th</sup> WS), USAF 3<sup>rd</sup> Weather Squadron, Detachment 3 (DET3), USAF 611<sup>th</sup> Air Operations Center, US Army Testing and Evaluation Center - Cold Regions Test Center, and other

sources.

*Generate climate conditions limits and thresholds.*

Arctic materiel is identified, and inventory is represented against critical infrastructure and resources required for movement and maneuver, protection, and sustainment.

Operational climate conditions limits and thresholds are generated based on a collaborative approach for scoping the various thresholds and operation requirements by working with the US Army Cold Regions Test Center, DoD climate experts, NORAD/ NORTHCOM, and other DoD personnel.

*Generate new Arctic climate operational classification maps.*

Maps generated from the climate information data analyses performed in Tasks 1 and 2 include a circumpolar map leveraging gridded reanalysis data for historical climate conditions, and regional maps with higher resolution data based on station observations. Tables will be generated listing conditions at key population and installation centers with analysis on specific or selected operational parameters.

*Document findings and results in a report.*

Results will tentatively be incorporated in the Unified Facilities Criteria (UFC) 3-130-01 on Arctic and Subarctic Construction and into a resilience technical report that will summarize the project goals, outcomes, and results.

## **Findings**

Due to the recent start of this project and acceptance of funding, the project team is currently working on gathering and compiling climate information as outlined in task 1. There are no major findings or results yet to report. We are actively collaborating with members of the USAF 14<sup>th</sup> WS and are evaluating the suitability of data acquired from a support request for the purposes of our analysis. We are investigating numerous sources of global gridded reanalysis data for our analysis of the circumpolar north climate breaks and determining the best available data as well as processing requirements.

## **Conclusions**

At the current status of our project, we have begun identifying suitable data sources for use in our Arctic climate typing analysis and collaborating with our partners at the USAF 14<sup>th</sup> WS for data collection and gathering. We have established the goals and scope for our two discrete analyses – one for the circumpolar north using global gridded historical reanalysis data and one for regional analyses to be conducted at higher resolution for a localized area using local station observations. The regional analyses will be cross-referenced with the collected materiel and equipment inventory and used to create the tables outlining operational parameters for the Arctic environment. Any limitations to our completion of the analyses are expected to be from a potentially limited collected materiel and equipment inventory, or limited knowledge of the status of current operational parameters. Barring none, the implications of this work are to provide mission critical data and information and assist installation operations managers in making better risk-informed decisions to operate in the circumpolar region.

## **Acknowledgements**

The research team would like to acknowledge the Environmental Security Technology Certification

Program (ESTCP), under the Assistant Secretary of Defense, Energy, Installations, and Environment, for funding this work.

The research team would like to acknowledge the USAF 14<sup>th</sup> Weather Squadron and the US Army Cold Regions Test Center for their assistance to this project.

### **References**

AR70-38, 2020, Research, Development, Test and Evaluation of Materiel for Worldwide Use.

## **How climate change is changing bridge design in Alaska**

Murray, Nicholas W

### **Abstract**

This presentation explores the profound impact of climate change on the design and engineering of bridges and other infrastructure in Alaska. With rising temperatures altering precipitation patterns, thawing permafrost, and intensifying weather events, the structural integrity and longevity of bridges face unprecedented challenges. Coupled with high seismicity throughout the state, engineers today need to be cognizant of future scenarios that may impact infrastructure. Traditional bridge design principles must evolve to contend with these changing conditions and innovative strategies need to be employed in adapting to the Alaskan climate to enhance resilience and durability.

# **Quantifying Structural Snow Loads using the Finite Area Element Method: A Comparison Between Physical Wind Tunnel and Computational Fluid Dynamics Input Data**

Christopher Oreskovic<sup>1</sup>, Timothy Wiechers<sup>1</sup>, Jan Christopher Dale<sup>1</sup>, Sreeyuth Lal<sup>2</sup>

<sup>1</sup>Rowan Williams Davies and Irwin, Inc. (RWDI), Guelph Ontario, Canada

<sup>2</sup>Canadian Nuclear Laboratories (CNL), Chalk River, Ontario, Canada

## **Abstract**

For current structural snow loading modeling, scale model wind tunnel tests are commonly conducted to gather bulk wind flow data across building roofs. While the wind tunnel data is reliable, collecting high-resolution data is constrained by the size of wind sensors and building geometry. This study employs computational fluid dynamics simulations, specifically using the Reynolds Averaged Navier Stokes (RANS) turbulence model, to develop a cost-effective method for generating high-resolution input flow fields for RWDI's snow loading software. A well-understood building with bluff body aerodynamics was chosen, and both a scale model wind tunnel test and a numerical model RANS simulation was conducted. The computational fluid dynamics model attains higher-resolution data than wind tunnel by directly resolving the mean flow at every grid node, correcting some post-processing artifacts. Snow-related structural loads are generally within 10% in most areas. Limitations in the computational fluid dynamics method include discrepancies in snow loads in regions with strong wind recirculation, to be addressed in future Large Eddy Simulation computations.



## **Spit Recycling: the Default Nature-based Solution at Shaktoolik, Alaska**

Phil Osborne, Principal, Senior Geomorphologist, Northwest Hydraulic Consultants Isaac Pearson, Senior Civil Engineer, Bristol Engineering Services Company LLC

### **Abstract**

A sandspit (spit) is a depositional coastal landform that forms where downdrift deposition of alongshore transport ends in deep water (e.g., at the point of shoreline re-entrance). Spit stability is achieved through continued supply of sediment, by the establishment of size grading, or the development of a counteractive cell (e.g., natural recycling) (Carter, 1988). Spits often extend alongshore at the same time as moving onshore and may become unstable when the original sediment supply is interrupted or cut off, or spit elongation leads to net withdrawal of material from the proximal end leading to thinning and sometimes breaching (e.g., Nicholls & Webber, 1987). The process of elongation, thinning, and onshore migration accelerates under rising sea levels. Shaktoolik, Alaska, a remote village of 260 people located 125 miles (~200 km) east of Nome, on a narrow spit of land between the Tagoomenik River and the Bering Sea, facing significant challenges for long-term protection of infrastructure due to the progression of natural spit processes. The village has been relocated twice in the past; however, a recent assessment concluded that the current location now also faces increasing flooding risk from both sides of the spit, and erosion from waves and storm surges, with potential to damage infrastructure. Sandspits have often been inhabited by Indigenous communities like Shaktoolik due to proximity to subsistence food sources, and an abundance of flat land that makes them attractive for the construction of airports, and municipal and residential infrastructure. Thus, in the short to medium term, the community has made the decision to stay and defend in place for as long as they can hold out. Out of necessity, Shaktoolik have adopted a nature-based approach, known as spit recycling that involves borrowing sediment from the distal end of the spit where a sediment surplus exists, transporting and placing the sediment in a berm in front of the community to provide protection. Although the berm provides protection from erosion and flooding, the structure is frequently reshaped by waves requiring seasonal reconstruction. In 2022 alone, the berm was impacted by two storms in July and September which caused significant reshaping and redistribution of the sediment and resulted in the need to reconstruct twice in the same season. Although the berm recycling option is relatively low cost the community now questions the sustainability of the approach, given available sand resources and ongoing maintenance requirements and is considering other options. In this presentation we summarize Shaktoolik's experience with the nature-based spit recycling option and progress with the exploration of other nature-based and grey protection options for the community.

### **References**

Carter, R.W.G., 1988. Coastal Environments. Academic Press Ltd., London, UK, ISBN 0-12-161856-0.

Nicholls, R.J. and Webber, N.B. (1987) The past, present and future evolution of Hurst Castle spit, Hampshire. *Progress in Oceanography*, 18 (1-4), 119-137. (doi:10.1016/0079-6611(87)90029-2).

## **Performance assessment of a CO<sub>2</sub>-based demand-controlled frost resilient dual-core energy recovery ventilation system for northern housing**

Boualem Ouazia, Ph.D.,<sup>1</sup> Chantal Arsenault<sup>1</sup>, Sador Brhane<sup>1</sup>, Daniel Lefebvre<sup>1</sup>, Patrique Tardif<sup>1</sup>, Sandra Mancini<sup>1</sup>, Greg Burns<sup>1</sup>

<sup>1</sup>*Construction Research Centre, National Research Council Canada, 1200 Montreal Road Ottawa, Ontario K1A 0R6 Canada; email: [Boualem.ouazia@nrc-cnrc.gc.ca](mailto:Boualem.ouazia@nrc-cnrc.gc.ca)*

### **Abstract**

To better address indoor air quality (IAQ) and mold issues in northern housing experiencing varying occupancies and indoor conditions, ventilation needs to become demand-controlled. Currently, heat/energy recovery ventilators (HRVs/ERVs) are commonly installed in northern communities and they offer constant or globally controlled airflows. Overcrowded homes are then under-ventilated, leading to higher indoor pollutants and moisture that need to be controlled. This study examines a method for providing adequate ventilation through control of ventilation based on occupancy and modulation of ventilation fans. This paper presents results from a side-by-side testing of a CO<sub>2</sub>-based demand-controlled dual-core ERV versus conventional single-core ERV with constant flow using twin houses with simulated occupancies. The implemented strategy based on a CO<sub>2</sub> sensor network connected with a dual-core ERV continuously exhausting stale air from the kitchen and bathrooms was simple and efficient in adjusting ventilation rate based on occupancy rate. The potential of the CO<sub>2</sub>-based demand-controlled dual-core ERV system was evaluated based on its capability to control indoor CO<sub>2</sub> levels, percentage of time kept below 1000 ppm and power consumption.

## Natural and Nature Based Solutions in Alaska and the Arctic

Thomas A. Douglas, U.S. Army Cold Regions Research and Engineering Laboratory Jacquelyn Overbeck, NOAA Office for Coastal Management Alaska Regional Geospatial Coordinator;

### Abstract

Increasingly, Natural or Nature Based Solutions (NNBS) are being applied as part of engineering solutions for a variety of projects. Very few examples of successful NNBS projects exist for Alaskan and Arctic regions where environmental conditions and social systems are different from the contiguous US. Most applications of NNBS use vegetation and dredged sediments that may not be viable in cold regions. Understanding the definition and constraints around what makes a project part of the NNBS portfolio is critical for communities and decision makers. Government resources intended to support communities in becoming resilient to climate change and hazards are guided in part by public policy in which NNBS is frequently referenced (for example: Executive Order 14072, National Strategy on the Arctic, and National Coastal Resilience Fund). National and international forums have placed definitions and guidance in regard to NNBS applications (IUCN, 2020; White House Council on Environmental Quality, 2022). Even with this guidance, implementation of solutions is still open ended and best informed by what has worked before. This leaves communities uncertain in how to use NNBS terminology and in what solutions can succeed in the Arctic. Not only that, critical components of ensuring NNBS are based on inclusive, transparent, and empowering governance processes requires local governance input. NNBS concepts are also common constructs of Indigenous culture and values which are representative of millennia of place-based adaptive management or stewardship of ecosystems which is not typically represented in NNBS guidance documentation. We plan two sessions, 1. a scientific and engineering session of relevant NNBS projects and 2. a panel session to describe current state-of-the-science, discuss existing policy, and identify gaps in guidance related to Alaskan and Arctic NNBS and why it is relevant to engineering in the Arctic and the future of project development for community resilience. Tribal partners are invited to discuss an ongoing project to define NNBS for their regions to come to shared terminology and understanding with existing public policy and provide guidance to government programs and engineers on the application of NNBS in Alaska.

### References

Executive Order 14072, Executive Order on Strengthening the Nation's Forests, Communities, and Local Economies, <https://www.whitehouse.gov/briefing-room/presidential-actions/2022/04/22/executive-order-on-strengthening-the-nations-forests-communities-and-local-economies/>

IUCN (2020). Global Standard for Nature-based Solutions. A user-friendly framework for the verification, design and scaling up of NbS. First edition. Gland, Switzerland: IUCN. <https://portals.iucn.org/library/sites/library/files/documents/2020-020-En.pdf>

The White House, National Strategy For The Arctic Region (October 2022), <https://www.whitehouse.gov/wp-content/uploads/2022/10/National-Strategy-for-the-Arctic-Region.pdf>

White House Council on Environmental Quality, White House Office of Science and Technology Policy, White House Domestic Climate Policy Office, 2022. Opportunities for Accelerating Nature-Based Solutions: A Roadmap for Climate Progress, Thriving Nature, Equity, and Prosperity. Report to the National Climate Task Force. Washington, D.C. <https://www.whitehouse.gov/wp-content/uploads/2022/11/Nature-Based-Solutions-Roadmap.pdf>

# Design of Electrically Conductive Asphalt Pavement for Self-Deicing Applications in Cold Regions

Ashith Marath<sup>1</sup>, Ahmed Saidi, Ph.D.<sup>2</sup>, Yusuf Mehta, Ph.D., P.E.<sup>3</sup>.

<sup>1</sup>*Center for Research and Education in Advanced Transportation Engineering Systems (CREATES), Rowan University, New Jersey 08028, USA, email: [marath42@students.rowan.edu](mailto:marath42@students.rowan.edu)*

<sup>2</sup>*Center for Research and Education in Advanced Transportation Engineering Systems (CREATES), Rowan University, New Jersey 08028, USA, email: [ahmeds@rowan.edu](mailto:ahmeds@rowan.edu)*

<sup>3</sup>*Center for Research and Education in Advanced Transportation Engineering Systems (CREATES), Rowan University, New Jersey 08028, USA, email: [mehta@rowan.edu](mailto:mehta@rowan.edu)*

## Abstract

Electrically Conductive Asphalt (ECA) pavements have emerged as a promising technology for deicing applications in cold regions. This innovative system comprises three key components: an electrically conductive asphalt layer, transverse steel electrodes, and an electrical power supply unit. The design of these components, effectively and economically, is crucial to achieving the desired deicing performance of asphalt pavements in extreme cold climates. This paper proposes a design approach for ECA pavements by determining the thermal power output required to raise and maintain the temperature of the pavement surface above the freezing point of water. Through a combination of experiments and finite element modeling, a design chart that recommends the required thermal power output for ECA pavements under ambient conditions in cold regions was developed. Based on the required thermal power output, the optimum design components of ECA pavements (thickness of the ECA layer and spacing of transverse steel electrodes) were determined.

# Preliminary Numerical Analysis of the Impact of Heterogeneity on Seepage in Frozen Soils

Zakary Picard,<sup>1</sup> Simon Dumais,<sup>2</sup> Élise Devoie<sup>3</sup> and John Molson<sup>4</sup>

<sup>1</sup>Centre d'études nordiques, Département du génie des mines, de la métallurgie et des matériaux, Université Laval, Québec, Québec, Canada

<sup>2</sup>Centre d'études nordiques, Département du génie des mines, de la métallurgie et des matériaux, Université Laval, Québec, Québec, Canada

<sup>3</sup>Civil Engineering, Queen's University, Kingston, Ontario, Canada

<sup>4</sup>Centre d'études nordiques, Département de géologie et de génie géologique, Université Laval, Québec, Québec, Canada

## Abstract

A standard practice in seepage analyses for mining dams with frozen components is to apply homogeneous hydraulic properties, although soil is inherently heterogeneous. In this study, a basic numerical model was developed to evaluate the impact of soil heterogeneity on seepage analyses. Sixteen combinations of soil type and heterogeneity distributions at 12 sub-zero temperatures ranging from  $-0.1^{\circ}\text{C}$  to  $-5^{\circ}\text{C}$  were analysed. The results of the heterogeneous cases are compared to a reference case considering equivalent homogeneous conditions. The findings suggest that homogeneous cases generally underestimate seepage and preferential water flow compared to heterogeneous cases. This research is a first step in evaluating shortcomings of the current engineering practice when modelling frozen soil water flow.

## Investigating the Impact of Freeze-Thaw Damage on Chloride Ingress in Concrete

Md Hasibul Hasan Rahat, MSc., MBA, SM. ASCE,<sup>1</sup> Thien Q. Tran, MSc., SM. ASCE,<sup>2</sup> Brendan D.J.E. Love,<sup>3</sup> Amir Behravan, Ph.D., P.E.,<sup>4</sup> and Alexander S. Brand, Ph.D., P.E., M.ASCE<sup>5</sup>

<sup>1</sup>Graduate Research Assistant, Charles E. Via, Jr. Department of Civil and Environmental Engineering; Virginia Tech, USA; rahatm21@vt.edu; +1-252-3279397

<sup>2</sup>Graduate Research Assistant, Charles E. Via, Jr. Department of Civil and Environmental Engineering; Virginia Tech, USA; tqthien@vt.edu; +1-540-391-1606

<sup>3</sup>Undergraduate Student, The Bradley Department of Electrical and Computer Engineering; Virginia Tech, USA; BrendanLove@vt.edu; +1-804-525-0812

<sup>4</sup>Research Scientist, Virginia Transportation Research Council; Virginia Department of Transportation (VDOT); USA; amir.behravan@vdot.virginia.gov; +1-434-293-1953

<sup>5</sup>Assistant Professor, Charles E. Via, Jr. Department of Civil and Environmental Engineering; Virginia Tech; USA; asbrand@vt.edu; +1-540-232-8726

### Abstract

This study investigates the impact of freeze-thaw (F-T) cycles on chloride ingress in concrete. Two air-entrained concretes, conventional (Group A) and fiber-reinforced (Group B), were investigated using Transmission X-ray Microscopy to determine the time-dependent diffusion coefficients before and after 125 F-T cycles. Performance metrics, including ultrasonic pulse velocity, surface resistivity, mass loss, and relative dynamic modulus of elasticity, were evaluated. Key findings indicated that both concretes were resistant to 125 F-T cycles, with Group A demonstrating slightly better performance. Group A showed a lower mass loss than Group B, which is consistent with the literature. Relative dynamic modulus values (99.7% for Group A and 99.3% for Group B) confirmed the improved F-T resistance. After 125 F-T cycles, diffusion coefficients remained similar, which suggests that F-T damage does not impact chloride diffusion at low numbers of F-T cycles. The findings of this study will facilitate the design of reinforced concrete structures coastal environments in cold regions with combined chloride and F-T exposure.



# Utilizing Machine Learning to Enhance Infrastructure Resilience in Cold Regions

Md Shohel Rana, Ph.D.,<sup>1</sup> Charan Gudla, Ph.D.,<sup>2</sup> Feroz Ahmed, Ph.D.,<sup>3</sup> and Mohammad Nur Nobi, Ph.D.<sup>4</sup>

<sup>1</sup>*Department of Computing and Software Engineering, Florida Gulf Coast University, Fort Myers, FL 33967; email: mrana@fgcu.edu*

<sup>2</sup>*Department of Computer Science and Engineering, Mississippi State University, Starkville, MS 39762; email: gudla@cse.msstate.edu*

<sup>3</sup>*Prediction 3D Technologies, Biloxi, MS 39531; email: feroz.ahmed@prediction3d.com*

<sup>4</sup>*Department of Computer Science, University of Texas at San Antonio, San Antonio, TX 78249; email: mohammadnur.nobi@utsa.edu*

## Abstract

In the challenging domain of engineering, where cold regions present formidable challenges, we confront the relentless forces of nature. From sub-zero temperatures to the unpredictable dance of snowfall and the silent buildup of ice, these regions demand innovative solutions to fortify the resilience of critical infrastructures. This initiative harnesses the potential of cutting-edge technology and leverages the extensive historical weather data tapestry. It introduces a pioneering strategy by integrating machine learning algorithms with extensive weather data, steering Cold Region Engineering into an era defined by foresight and adaptability. This paper studies a transformative approach designed to forecast, prevent, and ultimately enhance infrastructure resilience in the face of rigid cold. Addressing the distinct challenges of cold region engineering, arising from harsh winter conditions such as extreme cold temperature, snowfall, and ice accumulation, we offer a comprehensive study using machine learning algorithms applied to historical weather data to construct a deeper analysis model capable of highlighting adverse weather effects. This, in turn, covers the way for optimized resource allocation, streamlined maintenance planning, and design enhancements. Our proposed study follows a systematic process, encompassing meticulous data collection, appropriate feature selection, and aiming seamless integration of the model into existing infrastructure management systems. Additionally, it facilitates the implementation of efficient and proactive measures to mitigate the impact of severe weather conditions on infrastructure. The paper also conducts three different hypotheses testing: Temperature Impact Hypothesis, Precipitation Influence Hypothesis, and Ice Accumulation and Infrastructure Resilience Hypothesis, propelling engineering practices to new heights, particularly in the face of challenging cold environments.

# Controlling Arctic Coastal Erosion with Thermal and Mechanical Measures

Thomas M. Ravens, Ph.D.,<sup>1</sup> Yamin Man,<sup>1</sup> Anna C. Miller<sup>1</sup>

<sup>1</sup>*Department of Civil Engineering, University of Alaska Anchorage*

## Abstract

Coastal erosion in the Arctic occurs due to both thermal and mechanical processes. On the Alaska Beaufort Sea coast and on much of the Chukchi Sea coast, the dominant coastal erosion mechanism is bluff face thaw / slump or thermal denudation. This erosion mechanism is a two-step process. In the first step, the bluff face thaws due to multiple heat fluxes and then slumps to the beach face. In the second step, storm surge events with their aggressive waves transport material offshore. This two-step sequence is repeated multiple times during the open water period. In this paper, using data from both Foggy Island Bay on the Alaska Beaufort Sea, we develop a process-based model of bluff face thaw / slump erosion and validate calculations with observations. Secondly, using the same model, we explore and integrate thermal and mechanical approaches to slowing coastal erosion.

## **The Ethics of Competence: A Moving Target**

Rebecca Bowman, Esq., P.E., D.F.E., M. ASCE<sup>1</sup>

<sup>1</sup> *Sr. Dir., Ethics and Professional Practice. National Society of Professional Engineers. Email: rbowmanesq@verizon.net*

### **Abstract**

Technology continues to move at an accelerating pace. Traditional design pressures have been exacerbated by dramatic changes in societal expectations and demands, whether in terms of resilience and sustainability or in terms of social justice and inclusion. It is no longer enough to know what we knew, even if we're getting better at it. The ethical standard of competence is a moving target. If we're not keeping up, we're falling behind. Participants will examine several of the moving competence targets and how to assure that they're keeping up.

## **Encounters with Relict Permafrost in the Anchorage Alaska Area**

James w. Rooney, P.E.(Retired) and Charles H. Riddle, CPG (Retired)

### **Abstract**

As a hazard, permafrost degradation was never considered to be of concern until the more active Anchorage development period began after the 1960's. A number of relict permafrost incidents have occurred at various locations since that time. Some of these adverse impacts involved significant economic repair or removal costs. The Anchorage Area Borough then established formal procedures for site evaluation and development in areas of potential relict permafrost. Am not aware of any more recent encounters since the Alaska Railroad proposed realignment study near Eagle River occurred back in 2004!

## **Personal Career Experiences with Permafrost**

James W. Rooney, P.E. (Retired)

### **Abstract**

My early exposure to permafrost terrain and foundation related issues began in 1965 while working for the Alaska Department of Highways in Valdez, Alaska. The projects involved cut and fill slope failures involving thawing permafrost. In 1966 we moved to Fairbanks and I, while working for the State Materials lab located at the university, became exposed to all the university and government permafrost study efforts that were then in progress! In early March, 1969, I became involved in the Trans Alaska Pipeline original geotechnical route study at the request of Ralph Migliaccio. We then formed our company during this initial project effort! During my career with R&M Consultants, I then participated in many challenging projects requiring special treatment of foundation conditions involving frozen and thawing ground.

# Long-Term Evaluation of Permafrost Passive Cooling Features in Interior Alaska

Douglas J. Goering, PE, PhD,<sup>1</sup> Steve Saboundjian, PE, PhD, M. ASCE<sup>2</sup>

<sup>1</sup>*Department of Mechanical Engineering, P.O. Box 755905, University of Alaska Fairbanks, Fairbanks, AK 99775, USA, djgoering@alaska.edu*

<sup>2</sup>*Alaska Department of Transportation and Public Facilities, 5800 East Tudor Road, Anchorage, AK 99507, USA, steve.saboundjian@alaska.gov*

## Abstract

In 2003, the Alaska Department of Transportation and Public Facilities began a new road building project near Fairbanks, Alaska. The project (now known as Thompson Drive) contains three different types of passive cooling systems aimed at maintaining the thermal stability of underlying permafrost. The cooling systems utilize air convection embankment layers, ventilated shoulders, and two-phase thermosyphons in three different configurations. Each of these systems provide a passive cooling effect by enhancing the winter-time cooling of the embankment and underlying foundation soils, thus helping to preserve underlying permafrost and maintain the structural integrity of the roadway.

In this paper we provide a summary of the performance data for Thompson Drive over a 15-year period extending from 2005 to 2020. Each of the systems included in the project have demonstrated effective cooling of the underlying soil layers despite a string of very warm years (2014-2019) in the Fairbanks area. In the present paper we focus on the performance of Test Section #1 of the project, which includes a combined system of hairpin thermosyphons and ventilated shoulders. Temperature time series for a number of key locations within the test section show the cooling progress during the test period. In addition, contour plots of mean yearly temperatures provide a spatial indication of the effectiveness of both the thermosyphon and ventilated shoulder features.



# Development of a High-performance Asphalt Concrete with Enhanced Low-Temperature Performance

Mohamed Saleh<sup>1</sup>, Nirob Ahmed<sup>1</sup>, Renee Penetrante<sup>1</sup>, Taher Baghaee Moghaddam<sup>1</sup>, and Leila Hashemian<sup>1,2</sup>

<sup>1</sup>*Department of Civil & Environmental Engineering, University of Alberta*

<sup>2</sup>*Corresponding author; email: hashemia@ualberta.ca*

## Abstract

This study aims to develop a high-performance asphalt concrete (HPAC) by using waste asphaltenes to modify the binder and incorporating polyethylene terephthalate (PET) fibres to enhance the performance of asphalt mix at low temperature. As such, a method is proposed to reduce the cracking potential of HPAC mixtures composed of asphaltenes-modified binders by the addition of PET fibres. First, performance properties of a crude oil binder modified with 12% asphaltenes are evaluated by artificially short-term and long-term aging of the binder using rolling thin-film oven (RTFO) and pressure aging vessel (PAV) procedures, respectively. Superpave binder tests are conducted on the binders through a rotational viscometer, dynamic shear rheometer, and bending beam rheometer. For modifying the HPAC mixture, 6mm long PET fibres are used at a concentration of 0.15% where it is first tested for compactibility, reflecting field practical considerations. Then, two performance tests, namely dynamic modulus and indirect tensile strength test at low temperatures (-20, -10, and 0 °C), are conducted for an effective mechanical evaluation of the mixture modifications. The results of binder performance grading tests reveal that when the base binder, with continuous PG 70.2-25.9, is modified with 12% asphaltenes, it achieves a continuous PG 82.9-21.8 with a high PG that is suitable for demanding asphalt applications. Although the addition of asphaltenes increases binder stiffness, resulting in a decrease in low-temperature grading, the overall improvement in high-temperature performance outweighs this drawback. Additionally, compactibility tests demonstrate that mixes with 0.15% PET fibres exhibit acceptable compactibility and meet the prescribed air void requirements of a maximum 6%. Furthermore, the incorporation of PET fibres in HPAC mixes increase stiffness by 63% at a 15°C and 10 Hz loading frequency, with no negative impact on the anticipated response. Compared to control mixes where no asphaltenes or fibres are used, the asphaltenes modification and PET fibre incorporation increase fracture energy by up to 27% at -10°C, indicating lower cracking potential and improved low-temperature performance. Moreover, tensile strength is enhanced by up to 18% at 0°C, demonstrating an efficient combined effect of both modifications.

# Volumetric Behavior of Unsaturated Silty Soil Subject to Freeze and Thaw Cycles

Zihao Shang<sup>1</sup>, Bohan Zhou<sup>2</sup>, Marcelo Sanchez<sup>3</sup>

<sup>1</sup>*Department of Civil and Environmental Engineering, Texas A&M University, 3136 TAMU, College Station, TX 77843; email: zihaoshang@tamu.edu*

<sup>2</sup>*Department of Civil and Environmental Engineering, Texas A&M University, 3136 TAMU, College Station, TX 77843. Currently at Hydro China Huadong Engineering Cooperation, 22, Chaowang Road, Xiacheng District, Hangzhou, Zhejiang Province, China; email: zhou\_bh2@hdec.com*

<sup>3</sup>*Department of Civil and Environmental Engineering, Texas A&M University, 3136 TAMU, College Station, TX 77843; email: [msanchez@civil.tamu.edu](mailto:msanchez@civil.tamu.edu)*

## Abstract

This paper presents an experimental investigation related to the effect of Freezing-Thawing (Fr-Th) cycles on the volumetric behavior of unsaturated silty soils. A reconstituted specimen made up from silt collected from Virginia was subjected to Fr-Th cycles in a 1D cell manufactured in a 3D-printer. The soil specimens were prepared at different degrees of saturation from fully saturated and to as low as 60%, and the tests were conducted under open system conditions inside an environmental chamber. Volume changes were recorded using displacement sensor during cyclic F-T. The test results show that the impact of degree of saturation decides the contract or expansion of soil during the freezing. It shows that high degree saturation soil has more accumulated deformation after Fr- Th cycles. In the contrary, low degree saturation soil has less deformation after Fr-Th cycles. The study also shows that stress-history of the soil has a significant influence on the volumetric behavior of soils subjected to Fr-Th cycles.

**Keywords:** Freeze-Thaw, Unsaturated, Volumetric behavior

## Introduction

In the Northern Hemisphere, seasonally frozen ground (SFG) plays a significant role in the Earth's system by influencing freeze-thaw (Fr-Th) cycles. These annual cycles alter the thermal, hydraulic, and mechanical properties of the soil, leading to repeated frost heave and thaw settlement of the surface soil. These phenomena can result in engineering and natural issues such as foundation failure, damage to superstructures, pile jacking, and slope failure. A comprehensive study is essential for understanding the behavior of soil subjected to Fr-Th cycles.

One crucial aspect of studying frozen soil is the water content within its pores, encompassing both the solid and liquid phases. A portion of the water remains unfrozen due to capillary action, adsorption forces, and salinity. The physical properties of ice and liquid water vary significantly, such as elastic properties, thermal conductivity, and electrical conductivity etc. Researchers have also determined that the volume expansion from water to ice is 9%. Consequently, the quantity of unfrozen water content play a pivotal role in assessing the volumetric behavior of frozen soil, as it signifies the extent to which water has transitioned into ice.

Regarding cyclic Fr-Th tests, most experimental investigations focus on studying the behavior of specimens previously subjected to Fr-Th cycles (either in the laboratory or in the field) and comparing their

responses against untreated soils. Konrad (1989) noted that over-consolidated clays tend to expand when subjected to Fr-Th cycles, with this tendency becoming more pronounced as the Over Consolidation Ratio (OCR) increases. Viklander (1998) observed that both Normally Consolidated (NC) and Over Consolidated (OC) soil samples tend toward a residual void ratio after a certain number of cycles. However, current knowledge on the volumetric behavior of frozen soils considering loading history, stress level and degree of saturation remains limited.

As for unsaturated frozen soil, Eigenbrod et al. (1996) reported no net volume changes after Fr-Th cycles in Normally Consolidated (NC) samples with water content close to the plastic limit. Dagesse (2010) reported that soils with  $S_r$  lower than 63-70% exhibit a volumetric decrease, while an expansion was found for soil with  $S_r$  larger than this level. Liu et al. (2019) concluded that the frictional angle does not change much for unsaturated silty clay upon freezing, while cohesion increases significantly, which they attributed to ice cementation and capillary cohesion. They also reported a critical degree of saturation at which frost shrinkage turns into frost expansion. Wang et al. (2022) also state that there is a critical degree of saturation that distinguishes soil properties between frost heave and frost shrinkage. Frost heave or frost shrinkage of soil depends on the freezing of pore water or the thinning of adsorbed water. It is evident that the degree of saturation affects the volumetric behavior and mechanical properties of frozen soil. However, studies on the behavior of unsaturated soil under Fr-Th cycles are limited.

A study related to the effect of stress history and Fr-Th cycles on silt has been conducted by Zhou et al (2023). He concluded that NC soils subjected to Fr-Th cycles tend to accumulate plastic strains with a net contraction while OC soils tend to expand after Fr-Th cycles.

This paper presents an experimental campaign aimed at investigating behavior of unsaturated soil through a series of cyclic Fr-Th tests conducted in an environmental chamber. The objective of the experiment is to generate a new set of high-quality experimental data related to the volume change of unsaturated and saturated soils undergoing freezing-thawing cycles. These data will contribute to a deeper understanding of soil behavior under these intricate conditions.

## **Methodology**

### *Test Material*

The experimental study of the mechanical behavior of frozen soils has been generally based on reconstituted specimens. This is because gathering frozen undisturbed samples from the field is challenging and expensive. (Arenson et al. 2004). The silt collected from Virginia was utilized for this experiment. This silt, characterized by its brown color, underwent routine geotechnical tests to ascertain its fundamental properties. The liquid limit of the sample was determined to be 33.3%. Notably, this material did not demonstrate plastic behavior. The selected initial water content, approximately 1.2 times the liquid limit, was standardized at 40%. The specific gravity of this soil measured 2.72. Initial saturation was at 100%, and the initial void ratio was 1.09. A layer of water is presented on the top of soil surface under one day equilibrium.

### *Experimental program*

All the cyclic freezing-thawing tests are performed with the same equipment and device which was developed by Zhou (2023) to study saturated silt subjected to Fr-Th cycles. The consolidation cell connects to a metal cell filled with water to allow water exchange and keep sample saturated. For unsaturated soil samples, the drainage pipe from the base connects to a valve to control drainage.

The movement of soil sample during Fr-Th cycle is measured by a LVDT on the top of plunger.

The sample was prepared by mixing soils and water to achieve an initial water content of 40%. The mixture was poured into consolidation cell making sure that there were no visible air bubbles. For the saturated sample, the top of the consolidation cell was connected to the pipe used to saturate the sample. As for the unsaturated sample, the slurry was exposed to the laboratory environmental conditions. The change in weight was tracked until the target weight was achieved. The top of the consolidation cell was sealed and kept for one day to reach equilibrium. Then, the cell was placed inside the chamber, the target load was applied and the changes in height were tracked using the LVDT. Once consolidation ended, the sample was subjected to freezing-thawing cycles and the displacements were tracked using the LVDT. Once the test was completed, the sample height and final water content were measured.

Table 1 lists the tests conducted using this setup including the different loading steps and Fr-Th cycles.

Test #	Initial sample condition (Pre-consolidated pressure)	Initial degree of saturation	Step 1 (Vertical load)	Step 2 (Vertical load)	Step 3 (Vertical load)
1	NC soil (10kPa)	100%	8 Fr-Th cycles (10 kPa)	8 Fr-Th cycles (100 kPa)	8 Fr-Th cycles (10 kPa)
2	NC soil (10kPa)	93%	8 Fr-Th cycles (10 kPa)	8 Fr-Th cycles (100 kPa)	8 Fr-Th cycles (10 kPa)
3	NC soil (10kPa)	59%	8 Fr-Th cycles (10 kPa)	8 Fr-Th cycles (100 kPa)	8 Fr-Th cycles (10 kPa)

## Results

As for loose soil sample with high initial degree of saturation ( $S_r = 93\%$ ), the test with a pre-consolidation pressure of 10 kPa before cycling is done firstly, and the consolidation curve under combined cyclic freezing-thawing and three different loading steps is shown in Figure 1a. The load steps are 10 kPa-Cycling-100 kPa-Cycling-10 kPa-Cycling. C will be used as Cycling for short in the following illustration. The test of the saturated soil sample subjected to the same load step is conducted at the same time to compare with the unsaturated one. Void ratio changes with cyclic freezing-thawing processes under different pressure conditions are shown in Figure 1b below.

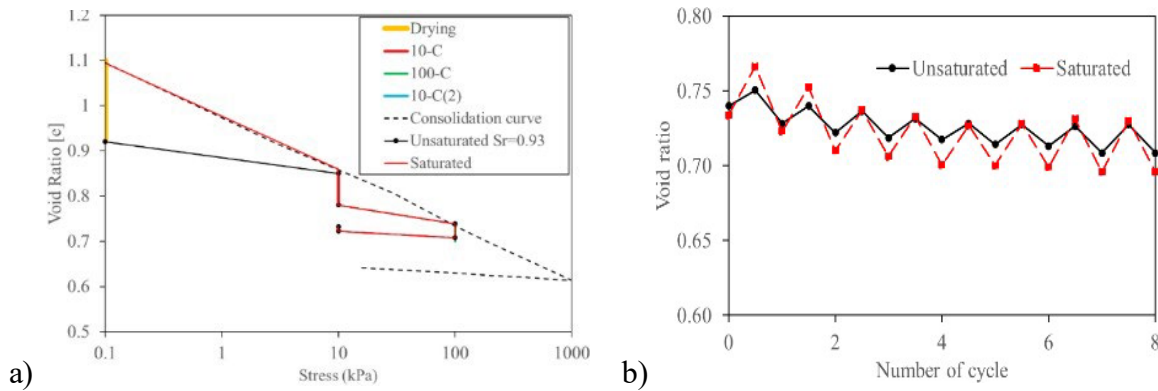


Figure 1a) Loose Soil Sample with  $S_r=93\%$ , Void Ratio versus Freezing-thawing Cycles of Test 2: b) first 10 kPa vertical stress (NC soil);

It can be observed from the Figure that volume change will finally get stable after eight cycles when a residual value is reached. When soil sample cycles at 10 kPa and 100 kPa as normally consolidated soil, it shows a behavior of compaction for both saturated and unsaturated soil samples. While the frost heave for unsaturated one is smaller than that of saturated one. After unloading to 10 kPa, it becomes over consolidated soil, and it shows a behavior of expansion.

*Low degree of saturation sample*

For loose soil with an initial 59% degree of saturation, under the same pre-consolidation pressure of 10 kPa, the cyclic test is conducted with load steps of 10 kPa-C-100 kPa-C-10 kPa-C. The consolidation curve which shows volume changes after cyclic freezing-thawing under three different loading steps is shown in Figure 2a). Void ratio changes with cyclic freezing-thawing processes under different pressure conditions are shown in Figure below.

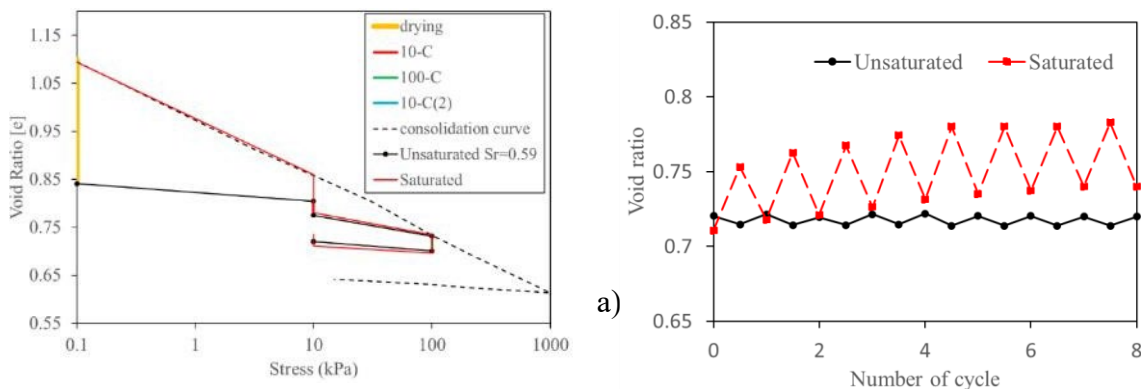


Figure 2 a) Loose Soil Sample with pre-10 kPa  $S_r = 59\%$  and  $S_r = 100\%$ ; Void Ratio versus Freezing-thawing Cycles of Test 3: b) second 10kPa vertical stress (OC soil)

Unlike soil with high degree of saturation, soil with low degrees of saturation does not expand when it is frozen. In the contrary, the soil sample would shrink as temperature going down. And soil sample would expand as temperature going up. As degree of saturation is 59%, volume change of water from liquid phase to solid phase does not cause volume change of entire soil sample, as the ice cannot fill the entire void space. But for normally consolidated soil, it shows a behavior of compaction after cycle and became stable after 7-8 cycle while compaction is much less than saturated sample and soil sample with high degree of saturation ( $S_r = 93\%$ ). Increasing vertical load 10kPa to 100 kPa induces compression of soil sample. Therefore, the degree of saturation of increase during second load step. For over-consolidated soil sample, it will show minor tendency of expansion after cycle which suggest less particle movement during the Fr-Th cycles. With less initial degree of saturation, soil will not have significant volume change. The reason is that

there is less water present in the soil and more water in the void remains unfrozen during freezing, soil particles will have minor rearrangement during temperature change.

## **Conclusions**

This experimental study has help to understand better the volumetric characteristics of frozen soils under varied loading histories and degrees of saturation throughout Fr-Th cycles. The effect of initial degree saturation on soils subjected to Fr-Th cycles was analyzed in terms of the volumetric behavior when comparing the samples prepared at  $S_r = 100\%$ ,  $S_r = 93\%$ , and  $S_r = 59\%$ . Upon freezing the water change from liquid to solid phase, with the corresponding volume expansion. A net expansion of the sample was observed during freezing in all the experiments. As expected, the volume changes increased with the increase of the degree of saturation. The unsaturated samples expanded less because of different factors, there is less water engaged in the phase transformation process, capillary effects restrain phase change and the presence of air in the soil allows the ice to grow into the voids without impacting significantly on the volume change during freezing.

This study collectively provide a valuable insight into the complex behavior of unsaturated frozen soil and emphasizes the relevance of considering the effect of water saturation on the response of soils subjected to freeze-thaw cycles.

## **Acknowledgments**

This project is funded by the National Science Foundation, award number:2034204, Project title: "Coupled Thermo-Hydro-Mechanical Behavior of Soils Subjected to Freeze-Thaw Cycles."

## **References**

- Arenson, L.U., Johansen, M.M., Springman, S.M. (2004) Effects of volumetric ice content and strain rate on shear strength under triaxial conditions for frozen soil samples. *Permafrost Periglac Process.* 15, 261–271.
- Dagesse, D. F. (2010). Freezing-induced bulk soil volume changes. *Canadian Journal of Soil Science*, 90(3), 389-401.
- Eigenbrod K., Knutsson, S., Sheng, D. (1996) Pore-Water Pressures in Freezing and Thawing Fine- Grained Soils. *Journal of Cold Regions Engineering*, 10, 77-92.
- Konrad, J. (1989) Effect of freeze-thaw cycles on the freezing characteristics of a clayey silt at various overconsolidation ratios. *Canada Geotechnical Journal*, 26, 217-226.
- Liu, Z., Liu, J., Li, X., Fang, J.,(2019). Experimental study on the volume and strength change of an unsaturated silty clay upon freezing, *Cold Regions Science and Technology*,157,1-12.
- Wang, H., Wu, Y., Wang, M., & Li, X. (2022). Influence of fines content and degree of saturation on the freezing deformation characteristics of unsaturated soils. *Cold Regions Science and Technology*, 201, 103610.
- Viklander, P. (1998) Permeability and volume changes in till due to cyclic freeze-thaw. *Canada Geotechnical Journal*, 35(3), 471-477.



Zhou, B., Shang, Z., and Sanchez, M. (2023). Effects of Temperature on Volumetric Behavior of Soil Subjected to Freezing-Thawing Cycles. Geo congress 2023,

# Improved Prediction of Frost Depth Penetration using Recurrent Neural Networks

Scott Michael Slone<sup>1</sup>, Zachary Zody<sup>1</sup>, Robert Ibey<sup>1</sup>, Wade A. Lein, P.E.<sup>1</sup>

<sup>1</sup>*Cold Regions Research and Engineering Laboratory, Engineer Research and Development Center, US Army Corps of Engineers, 72 Lyme Road, Hanover, NH 03755; email: scott.m.slone@usace.army.mil*

## Abstract

Frost effects, such as frost heave and thaw weakening, can significantly degrade pavements. Effective mitigation relies on accurate prediction of frost penetration depth. Current prediction methods use empirical equations or finite element analysis, with recent progress using machine learning. One potentially appropriate machine learning model may be a recurrent neural network, which takes in present data as input, and outputs an estimation of future data, which can then be fed back into the model recursively to make further predictions. Using this method and training data from Hill Air Force Base, Utah and Air Force Academy, Colorado, we were able to forecast soil parameters including temperature, thermal conductivity, and moisture content for frost susceptible soils, with a deviation from experimental values of no more than 10%, with the most significant contributions to accuracy being the use of Gated Recurrent Unit neurons and the incorporation of multiple soil parameters.

# Ground Freezing for Deep Shaft Excavation in New York City

Joseph Sopko<sup>1</sup>

<sup>1</sup> *Director of Ground Freezing, Keller North America. Email: JASopko@keller-na.com*

## Abstract

Two shafts were constructed as part of the New York City Water Tunnel No. 3 water distribution project. The shafts required excavation through overburden soils ranging from 130 to 230 feet and then to approximately 700 in the underlying bedrock. Artificial ground freezing was specified as the method to provide temporary earth support and ground water control until a final lining could be installed.

The project required a comprehensive Supplemental Geotechnical Investigation the required extensive frozen soil testing. This paper discusses the details of the testing program as well as the design methods. Design challenges included minimizing time dependent creep deformation during excavation and the freezing process in multiple strata with varying thermal properties.

# Variability of Geotechnical Properties in Arctic Coastal and Shelf Regions with regards to Sediment Dynamics

Nina Stark, Ph.D., M.ASCE<sup>1</sup> Nicola C. Brillì, Ph.D.,<sup>2</sup> Elise Hummel, M.Sc,<sup>2</sup> Emily Eidam, Ph.D.,<sup>3</sup> and Jaap Nienhuis, Ph.D.,<sup>4</sup>

<sup>1</sup>University of Florida, Engineering School of Sustainable Infrastructure and Environment, 365 Weil Hall, Gainesville, FL 32611; email: [nina.stark@essie.ufl.edu](mailto:nina.stark@essie.ufl.edu)

<sup>2</sup>Virginia Tech, Charles E. Via, Jr. Department of Civil and Environmental Engineering, Patton Hall, Blacksburg, VA 24061, email: [nickb96@vt.edu](mailto:nickb96@vt.edu), [ehummel@vt.edu](mailto:ehummel@vt.edu)

<sup>3</sup>Oregon State University, College of Earth, Ocean, and Atmospheric Sciences, Corvallis, OR97331, email: [Emily.eidam@oregonstate.edu](mailto:Emily.eidam@oregonstate.edu)

<sup>4</sup>Utrecht University, Department of Physical Geography, 8a Princetonlaan, Utrecht 3584, the Netherlands; email: [j.h.nienhuis@uu.nl](mailto:j.h.nienhuis@uu.nl)

## Abstract

Geotechnical properties of seabed sediments can vary significantly in coastal and shelf regions in response to sedimentation processes, sediment dynamics, as well as possible applied stresses and loads. In cold regions, ice dynamics influence these governing processes, possibly leading to further changes with climatic shifts. Geotechnical properties of seabed sediments affect local erodibility, benthic processes, and are relevant for coastal and offshore engineering. However, despite the relevance, few geotechnical data sets exist in Arctic coastal and shelf regions. Recently, portable free fall penetrometers have been introduced as a rapid and convenient means to test sediment strength of seabed sediments in Arctic coastal and shelf regions. Results obtained during two field expeditions to Harrison Bay, Alaska and initial measurements near Quinhagak, Alaska revealed a wide range of sediment strength related to sediment type and geomorphology. Initial testing of sediment erodibility of co-located sediment cores suggested that variations in sediment strength also relate to variations in erodibility particularly in the case of fine-grained sediments. In summary, portable free fall penetrometers have proven suitable for in-situ geotechnical seabed surface characterization in the Arctic. Variability of seabed sediment strength of the uppermost meter of the seabed surface is significant and relevant for engineering applications, as well as local sediment dynamics.

**Keywords:** geotechnics, coastal sediments, site investigation, portable free fall penetrometer

## Introduction

Arctic coastal dynamics often include significant morphodynamic changes, erosion, and complex drivers affected by climate change (e.g., MacDonald et al. 2015). Soil mechanics are also exceptionally complex in Arctic coastal environments resulting from a wide range of abundant sediment types, sediment dynamics, and from permafrost thaw and freeze-thaw processes (Stark et al. 2017). At the same time, comprehensive data sets are few, and sometimes, become outdated rapidly due to rapid erosion and changes in geomorphology, as well as by extreme storm and flood events. This results from environmental and logistical challenges that drive up costs or even make site investigations just unfeasible using traditional geotechnical site investigation methods, particularly in Arctic coastal environments (Stark et al. 2022). This drives the need for novel solutions for geotechnical site investigation. Portable free fall penetrometers have emerged as a reliable tool for the rapid characterization of seabed surface sediment in dynamic coastal environments, including in the Arctic (Stark et al. 2017). In this study, we discuss preliminary results of portable free fall penetrometer data from two Alaskan Arctic coastal environments, Harrison Bay and Quinhagak.

## Methodology

Portable free fall penetrometer measurements were carried out in Harrison Bay, Prudhoe Bay, Alaska in 2021 and 2022, and in Quinhagak, Alaska in 2023. The goals for the respective studies were to relate geotechnical properties to geomorphodynamics in and near the Colville Delta in Harrison Bay, and to test the feasibility of portable free fall penetrometer (PFFP) testing for coastal and riverine infrastructure risk assessment in Quinhagak. In both studies, the PFFP BlueDrop by BlueCDesigns was used. The PFFP has a weight of approximately 8 kg and a length of 64 cm, enabling manual deployment and recovery from any vessel of opportunity. The same probe was previously successfully used in a study of nearshore environments of Herschel Island, Southern Beaufort Sea, Yukon Territory, Canada (Stark et al. 2017). In Harrison Bay, the PFFP was deployed from the R/V Upik in conjunction with seabed coring, bathymetric mapping, and seabed stratigraphy scanning using chirp sonar. In Quinhagak, the PFFP was deployed from skiffs operated by local navigators targeting the lower reach and inlet of the Kanektok River and the lower reach of the Arolik River (Fig. 1) and on the beach and tidal mudflat by walking out (Fig. 2). Deployment locations were chosen based on bathymetric maps in Harrison Bay and based on vicinity to infrastructure systems in Quinhagak.

## Initial Results

For the Harrison Bay data set, a classification scheme was developed based on the PFFP measurements differentiating between cohesive and non-cohesive sediments associated with a threshold fines content of 30%. Strength properties were then calculated for cohesive or non-cohesive sediments, respectively. For non-cohesive sediments, the relative density was estimated from the PFFP results and related to the JET-derived detachment coefficient,  $kd$ , with the critical shear stress being determined via empirical relations. Three categories were assigned for cohesive sediments undrained shear strength derived from PFFP results. An undrained shear strength separator of  $su = 2$  kPa correlated well with groupings of  $kd$  obtained from JET tests performed on gravity core samples, and the third category for the least erosive sediments was developed for  $su$  values greater than 20 kPa. These categories highlighted and related variability in erodibility and sediment strength across Harrison Bay. The classification identified highly erodible and low erodibility sediments in a rapid manner and allowed to correlate the findings to bathymetric features and coastal processes. It showed that recently deposited sediment from bluff erosion and ice-scoured seabed both classified in the highest erodibility group.

PFFP measurements in Quinhagak confirmed highly variable sediments reaching from coarse gravels to soft mud. Figure 3 shows a data example from the lower beach. It shows measured deceleration and derived instrument velocity over the penetration depth into the soil. In Fig. 3 left), the probe only penetrated the soil surface (~5 cm) and reached a maximum deceleration of  $> 30$  g (g being gravitational acceleration) with some irregularities (fluctuations in the profile). In Fig. 3 right), the probe reached a soil depth of ~ 8 cm and reached a maximum deceleration of 24 g. In both cases, an impact velocity of ~ 5 m/s is indicative of a valid deployment and good data quality. Both examples represent fairly stiff soils with the location shown on the right being slightly weaker. The irregularity observed in the left example may be associated with gravel, shells, vegetation, or layering. Surficial bearing strength was about 150 kPa for the left case and only about 40 kPa for the right case, highlighting the difference in stiffness.



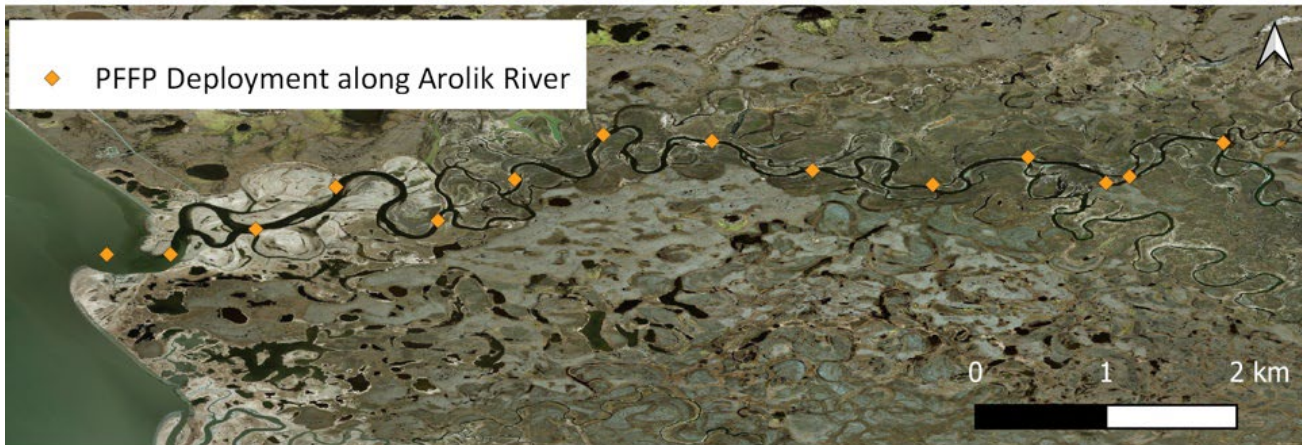
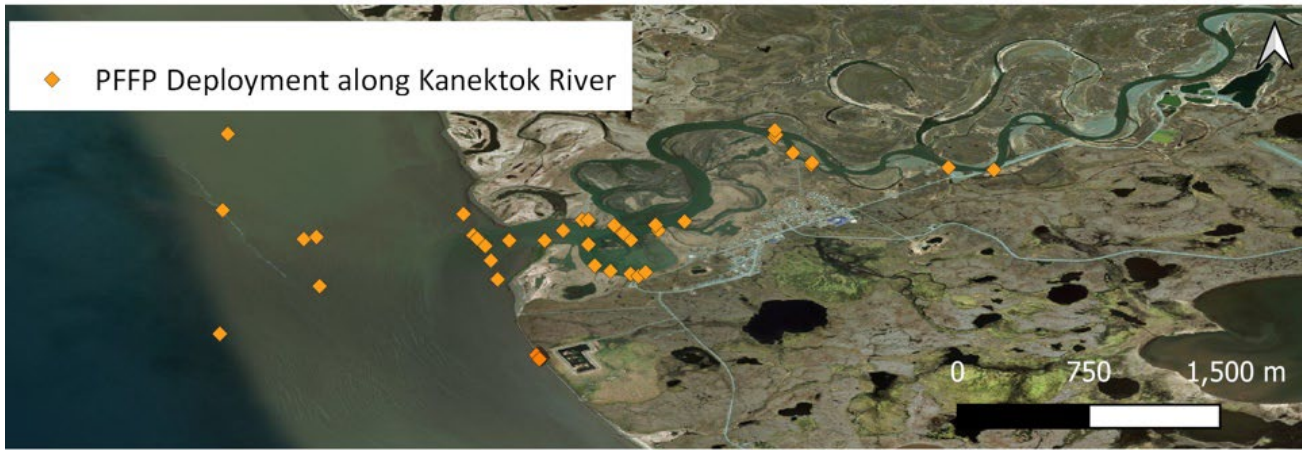


**Fig. 1. PFFP deployment locations in Quinhagak, AK in June 2022.**



**Fig. 2. PFFP deployment at the beach and intertidal zone in Quinhagak, AK in June 2022.**



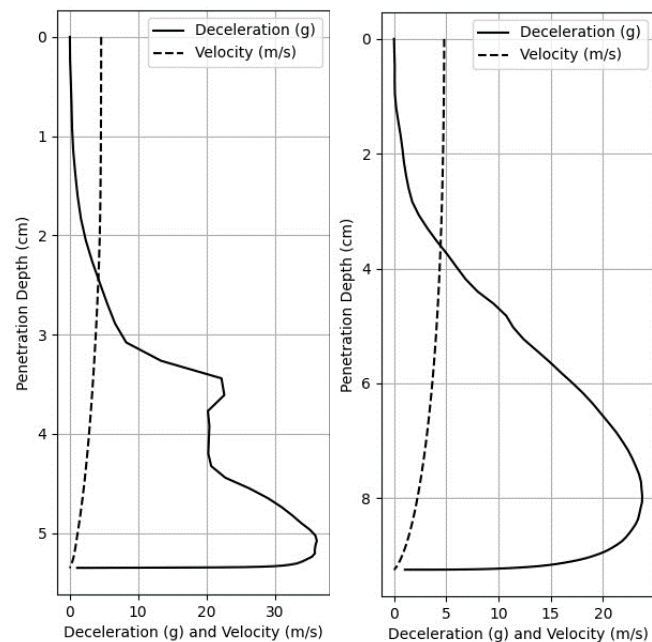


Fig. 3. Two example PFFP measurements showing measured deceleration and derived velocity versus derived soil penetration depth. Please note that a penetration depth of 0 cm indicates the soil surface and a deceleration of 0 represents freefall for these two deployments from the Quinhagak beach near the sewage lagoon.

## Conclusions

Recent developments in coastal geotechnical site investigation methods with focus on surficial sediment testing promote access to and data collection in Arctic areas. These types of data can assist with increasing data coverage of geotechnical sediment properties, and thereby improve the understanding of soil mechanics and sediment dynamics in the Arctic.

## Acknowledgments

This study was funded by the National Science Foundation through grants ICER-2022562 and OPP-1912863. The authors are deeply indebted for the local support during the field measurements by Captain Mike Flemming (R/V Upik), Sean Gleason (Nalaquq Inc.), Lynn Church (Nalaquq Inc.), and Warren Jones (Qanirtuuq Inc.). Any opinions, findings, and conclusions or recommendations expressed in this material are those of the author(s) and do not necessarily reflect the views of the National Science Foundation

## References

- Macdonald, R. W., Kuzyk, Z. Z. A., & Johannessen, S. C. (2015). The vulnerability of Arctic shelf sediments to climate change. In *Environmental Reviews* (Vol. 23, Issue 4). <https://doi.org/10.1139/er-2015-0040>
- Stark, N., Radosavljevic, B., Quinn, B., & Lantuit, H. (2017). Application of portable free-fall penetrometer for geotechnical investigation of Arctic nearshore zone. *Canadian Geotechnical Journal*, 54(1). <https://doi.org/10.1139/cgj-2016-008>
- Stark, N., Green, B., Brill, N., Eidam, E., Franke, K. W., & Markert, K. (2022). Geotechnical Measurements for the Investigation and Assessment of Arctic Coastal Erosion—A Review and Outlook.

Journal of Marine Science and Engineering, 10(7), 914. <https://doi.org/10.3390/jmse10070914>

## Overview of NASA SnowEx Alaska field campaign in 2022-2023

Svetlana Stuefer<sup>1</sup>, Carrie Vuyovich<sup>2</sup>, HP Marshall<sup>3</sup>, Michael Durand<sup>4</sup>, Dragos Vas<sup>5</sup>, Christopher Larsen<sup>6</sup>, Kelly Elder<sup>7</sup>, Batu Osmanoglu<sup>8</sup>, Megan Mason<sup>9</sup>

<sup>1</sup> Associate Professor. University of Alaska Fairbanks. Email: sveta.stuefer@alaska.edu

<sup>2</sup> National Aeronautics and Space Administration. Email: carrie.m.vuyovich@nasa.gov

<sup>3</sup> Boise State University. Email: hpmarshall@boisestate.edu

<sup>4</sup> Ohio State University. Email: durand.8@osu.edu

<sup>5</sup> Cold Regions Research and Engineering Laboratory. Email: Dragos.A.Vas@erdc.dren.mil

<sup>6</sup> University of Alaska Fairbanks. Email: cflarsen@alaska.edu

<sup>7</sup> U.S. Department of Agriculture Forest Service. Email: elderrmrs@gmail.com

<sup>8</sup> National Aeronautics and Space Administration. Email: batuhan.osmanoglu@nasa.gov

<sup>9</sup> National Aeronautics and Space Administration. Email: megan.a.mason@nasa.gov

### Abstract

Snow depth, snow water equivalent (SWE), and precipitation data are used in several areas of cold regions engineering, including hydrology, transportation, and geotechnical work. Yet, snow data are often prone to measurement errors and are notably sparse in cold regions. This presentation provides an overview of field activities and snow datasets collected during SnowEx campaigns in Northern Alaska in 2022–2023. NASA's SnowEx was initiated by the Terrestrial Hydrology Program in 2017 to study snow remote sensing challenges in different environments in preparation for future satellite mission opportunities to collect snow data from space. SnowEx campaigns have taken place in continental and maritime snowpacks of the western U.S., and in taiga and tundra snowpacks of Alaska. A suite of airborne and ground-based validation measurements was collected in fall 2022 and spring 2023 in northern Alaska at five study sites. Three SnowEx sites were selected in interior Alaska, a boreal forest environment with discontinuous permafrost and seasonal taiga snowpack. Two SnowEx sites were located on the North Slope of Alaska, a region dominated by gentle topography, tundra snowpack, and continuous permafrost. The largest data collection occurred in March 2023: snow characteristics (microstructure, depth, density, SWE, hardness, and liquid water content) were measured at 170 study plots distributed across five SnowEx sites. These ground-based snow measurements were accompanied by two concurrent airborne missions (LiDAR and SWESARR). When taken together, the SnowEx field campaigns provide snow datasets in support of testing and advancement of remote sensing, modeling, and measurements techniques needed for the development of global SWE products. This presentation focuses on the objectives of the boreal forest and tundra SnowEx campaign and presents an overview of SnowEx March 2023 field activities in Alaska.

# Composite Pore Model for Chlorinated Silty Clay under Confining Pressure during Freeze-Thaw Based on NMR Fractal Theory

Yong Tao<sup>1</sup>, Ping Yang,<sup>2</sup> and Yifei Dai<sup>3</sup>

<sup>1</sup> College of Civil Engineering, Nanjing Forestry University, Nanjing 210037, China; email: [taoyongr@njfu.edu.cn](mailto:taoyongr@njfu.edu.cn)

<sup>2</sup> College of Civil Engineering, Nanjing Forestry University, Nanjing 210037, China; email: [yangping@njfu.edu.cn](mailto:yangping@njfu.edu.cn)

<sup>3</sup> College of Civil Engineering, Nanjing Forestry University, Nanjing 210037, China; email: [yundai6210@gmail.com](mailto:yundai6210@gmail.com)

## Abstract

Soil pore is a crucial parameter for the design of an artificial ground freezing (AGF) system, directly affecting soil strength, water potential, hydraulic conductivities, frost heave and thaw settlement. Previous research primarily focused on the pore structure without pressure, while studies on pore morphology under confining pressure remain limited. Through Nuclear Magnetic Resonance (NMR) experiments, this paper investigated the impacts of confining pressure and temperature on the unfrozen water content and pore structure of chlorinated silty clay during a full freeze-thaw cycle. Utilizing NMR-based fractal theory, the fractal characteristics of the pore were characterized. Mesopores and micropores were conceptualized as a three-dimensional capillary model, while macropores were represented as a sphere-cylinder dual structure model, leading to the establishment of a composite pore model. The influence of temperature on unfrozen water content and pore structure was significant, with pronounced hysteresis effects observed in both pore morphology and pore size distribution. Furthermore, a modified model was established to calculate the unfrozen water content under confining pressure.

Keywords: Saline silt clay; Confining pressure; Unfrozen water content; Composite pore model

## Introduction

Artificial ground freezing (AGF) is a widely used technique in construction to temporally reinforce subway connection aisles, as well as the launching and receiving shafts, during construction activities. The soil strength, water potential, and hydraulic conductivities are dependent on the amount of unfrozen water (Xiao et al., 2021). The unfrozen water content of a composite medium relates not only to the freezing temperature, but also to the pore size and shape, type and concentration of electrolyte, and surface characteristics of solid particles (Kurylyk and Watanabe, 2013).

The fractal dimension of soil porosity is essential for understanding soil pore structure complexity and heterogeneity. It improves upon traditional methods, enabling more accurate soil-structure interaction and environmental models (Li et al., 2018). Presently, the evaluation of fractal dimensions relies on six predominant mathematical models, including geometric, two-dimensional capillary, three-dimensional capillary, spherical, thermodynamic, and wetting phase models (Wang et al., 2018).

Existing methods for analyzing soil pore structure include X-ray computed tomography (X-CT) (Hamamoto et al., 2016), mercury intrusion porosimetry (MIP) (Zeng et al., 2017), scanning electron microscopy (SEM) (Darbari et al., 2017) and nuclear magnetic resonance (NMR) (Tao et al., 2023). Compared to other methods, the utilization of NMR, known for its speed, accuracy, and nondestructive nature, is highly recommended (Liu et al., 2020). As a result, NaCl saline soils were adopted in this study to characterize the unfrozen water content and pore fractal dimension under different conditions (i.e., confining pressure and

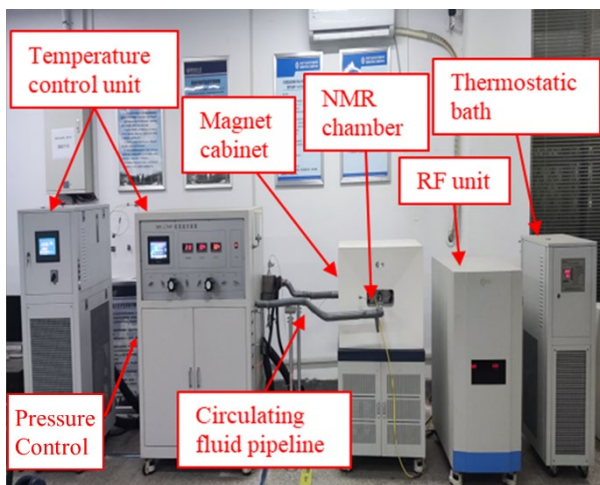
temperature). A modified model was established to calculate the unfrozen water content during freezing under different pressures and temperatures.

### Methodology

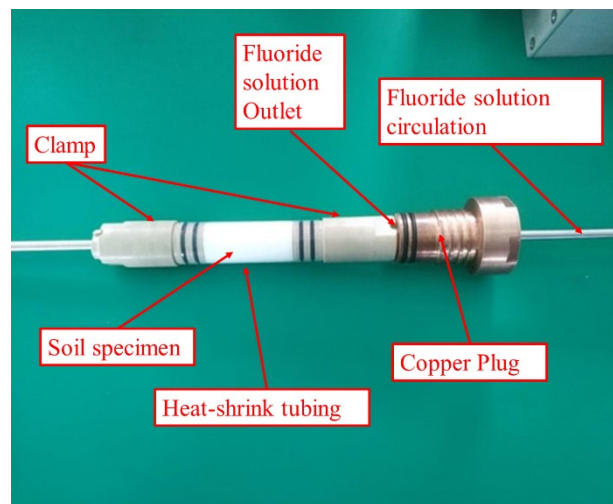
The soil specimens for the study were collected from Ningbo, China. After vacuum saturation, the samples were subjected to consolidation under an applied surcharge pressure of 800 kPa. Post-consolidation, the specimens were evaluated, revealing a water content of 21.5%, with the final dimensions recorded as 25.2 mm in diameter and 74 mm in height. Subsequently, the specimens were placed within the NMR chamber of the MesoMR12-060H-I device (Fig. 1a), pressure was applied to the heat-shrink tubing via the fluoride solution, with the soil specimen wrapped inside the heat-shrink tubing (Fig. 1b). Table 1 shows the MMR measurement scheme aimed at assessing the impacts of varying confining pressures (i.e. 0, 200, 400, 600, and 800 kPa) on the unfrozen water content and pore size distribution in saline silt clay with a 1% NaCl concentration, throughout a full freeze-thaw cycle.

Table 1 NMR measurement scheme

Salt type	Initial water content	Initial salt content	Pressure/kPa	Target measurement temperature/°C	Stable duration of each target temperature/h
NaCl	21.5%	1%	0, 200, 400, 600, and 800	-30, -22.5, -15, -10, -6 -4, and 0 °C	2.5



(a) Integrated NMR system



(b) NMR chamber

Fig. 1 NMR device

The temperature in the NMR chamber after specimen installation was then reduced from 20 °C to -30 °C and raised up to 20 °C to simulate a full freeze-thaw cycle. After temperature stabilization for 2.5 hours, the nuclear magnetic signal of unfrozen water remained constant, which was obtained by activating and deactivating the magnetic field. The unfrozen water content and pore fractal dimension were subsequently calculated through semaphore (Tao et al., 2023).

### Findings or Results

A model presented by Zhou et al. (2018) was validated to be accurate in predicting the unfrozen water content of saline silty clay, as demonstrated below:

$$\frac{dT}{dp_i} = \frac{1-\beta}{\eta} = -0.073\text{K/MPa} \quad (1)$$

Where  $T$  is the soil temperature,  $p_i$  is the overburden pressure (MPa),  $\beta$  and  $\eta$  are the constants in the

generalized Clapeyron equation ( $\beta \approx 1.09$ ,  $\eta \approx 1.23 \text{MPa}/^\circ\text{C}$ ).

Due to the confining pressure acting on the soil sample, a pressure conversion coefficient  $k_p$  ( $k_p = 0.52$ ) was added into:

$$\frac{dT}{dp_j k_p} = \frac{1-\beta}{\eta k_p} = \frac{-0.073}{k_p} \text{K/MPa} \quad (2)$$

Where  $p_j$  is the confining pressure,  $k_p$  is the pressure conversion coefficient.

The freezing point of soil under confining pressure  $p$  can be expressed as:

$$T_f = T_{f0} + \frac{1-\beta}{\eta k_p} p \quad (3)$$

Where  $T_f$  is the soil freezing point,  $T_{f0}$  is the freezing point of the unconfined soil ( $T_{f0} = -3.8^\circ\text{C}$ ). As a function of temperature, unfrozen water content can be obtained as follows (Tao et al. 2023):

$$w = w_0 \left( \frac{T_0 - T_f}{T_0 - T} \right)^k \quad (4)$$

Where  $w$  is the gravimetric unfrozen water content (unit: kg/kg),  $w_0$  is the initial gravimetric unfrozen water content (unit: kg/kg),  $T_0$  is the reference freezing point of water ( $T_0 = 273.15 \text{K}$ ),  $k$  is model coefficient. For confined saline soil, substituting Eq. (3) into Eq. (4):

$$w = w_0 \left( \frac{T_0 - T_{f0} - \frac{1-\beta}{\eta k_p} p}{T_0 - T} \right)^k \quad (5)$$

Through a least-square technique, the best estimation of model coefficients  $k$  was determined as 6.37 during freezing while confined pressure was less than 400kPa. The predictions matched well with the experimental results with a high correlation coefficient. A model coefficient was introduced in Eq. to predict unfrozen water content when confined pressure was more than 400kPa:

$$w = w_0 \left( \frac{T_0 - T_{f0} - k_o \frac{1-\beta}{\eta k_p} p}{T_0 - T} \right)^k \quad (6)$$

Where  $k_o$  is the model coefficient of over-consolidated soil ( $k_o = 1.1$ ).

The fractal dimension characterizes the self-similarity and complexity of irregular bodies, providing a theoretical basis for revealing the geometric characteristics of dense clay porous media. Assuming the pore model as a three-dimensional capillary model, the formula for determining the fractal dimension  $D_c$  using nuclear magnetic resonance is as follows:

$$\lg S_{T_2} = (D_c - 2) \lg \frac{1}{T_2} + C \quad (7)$$

Where  $T_2$  is relaxation time,  $S_{T_2}$  is accumulated signal strength percentage,  $D_c$  is the fractal dimension of three-dimensional capillary model,  $C$  is the model coefficient. Fig. 2a demonstrates the relationship between relaxation time and signal strength at different temperatures during freezing under 0 kPa, with a tripartite fitting curve established at  $-0.2^\circ\text{C}$ . This division categorized porosity into macropore, mesopore, and micropore. It is observed that the fractal dimensions of mesopores and micropores lay between 2 and 3, whereas the fractal dimension of macropores exceeded 3. This phenomenon was due to the significant difference in pore and throat diameters within the macropore system, lacking fractal characteristics. This was considered an oversimplification of "ink bottle" type pores (Lai et al., 2016; Rahimi et al., 2018; Wang et al., 2022). For macropores, the wetting phase model was proposed for calculating the fractal dimension (Zhang and Weller 2014):



$$\lg S_{T_2} = (3 - D_{sc}) \lg T_2 + C \quad (8)$$

Where  $D_{sc}$  is the fractal dimension of the sphere-cylinder model. The macropore included a relatively larger sphere-shaped central pore and two little cylinder-shaped spaces (Fig. 2b). Table 2 shows the model fractal dimension coefficients of three types of soil pore during freezing at  $-29.1^\circ\text{C}$ .

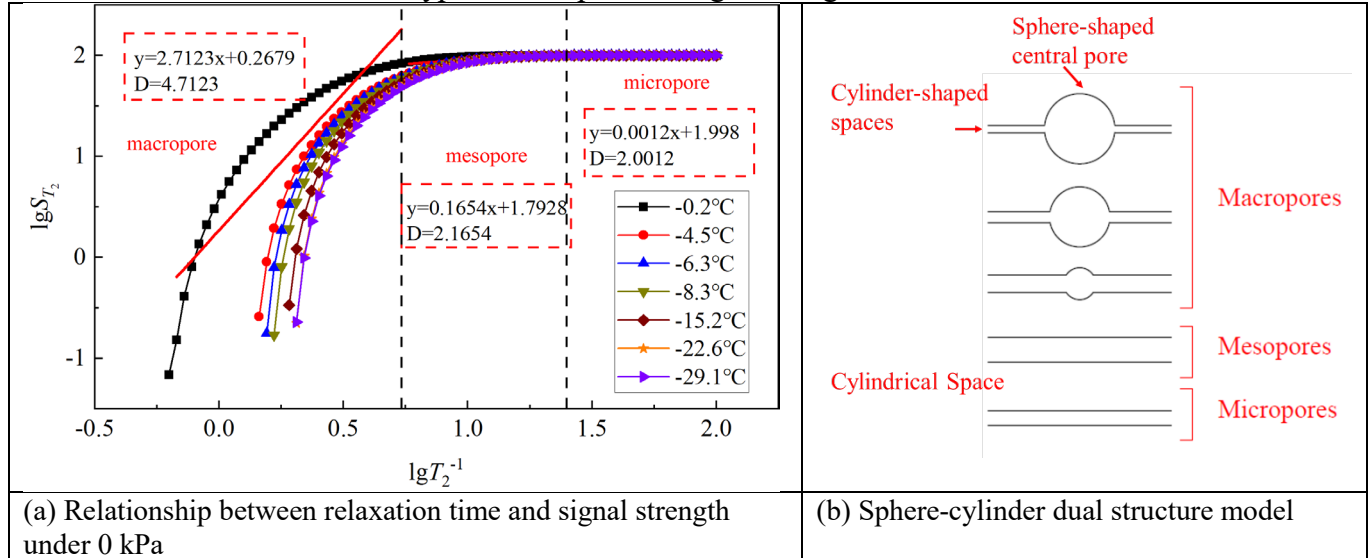


Fig. 2 Pore fractal dimension and structure

Table 2 Model fractal dimension coefficients of three types of soil pore during freezing

Pressure/kPa	Macropore			Mesopore			micropore		
	$a_{ma}$	$b_{ma}$	$D_{sc}$	$a_{me}$	$b_{me}$	$D_c$	$a_{mi}$	$b_{mi}$	$D_c$
0	0.5815	2.221	2.4185	0.4099	1.4846	2.4099	0.0029	1.995	2.0029
200	0.6879	2.2409	2.3121	0.3242	1.5932	2.3242	0.0022	1.9963	2.0022
400	0.6191	2.2051	2.3809	0.3384	1.5749	2.3384	0.0024	1.996	2.0024
600	0.668	2.236	2.332	0.332	1.5833	2.332	0.0022	1.9962	2.0022
800	0.6711	2.2353	2.3289	0.3322	1.5829	2.3322	0.0023	1.9961	2.0023

## Conclusions

This paper evaluated the effects of pressure, temperature on the soil unfrozen water content and pore size structure. Following are the main conclusions:

1. The soil unfrozen water content initially increased rapidly and then grew more slowly as pressure increased. A model was established to calculate the unfrozen water content during freezing under different pressures and temperatures.
2. For over-consolidated soils, the variations in unfrozen water content and pore size fractal dimensions with pressure change rate differed from those of under-consolidated soils. An over-consolidation coefficient ( $k_o$ ) needed to be incorporated to predict the unfrozen water content.
3. For mesopores and micropores, the capillary tube model was used to calculate the fractal dimension. Whereas the structure of macropores differed which included a relatively larger sphere-shaped central pore and two little cylinder-shaped spaces, so a modified wetting phase model was used for calculation.

## Acknowledgments

This study was supported by the National Natural Science Foundation of China (Grant No.52178337).

## References

Darbari Z, Jaradat K A, Abdelaziz S L. Heating–freezing effects on the pore size distribution of a kaolinite

clay[J]. *Environmental earth sciences*, 2017, 76(20): 713.

Hamamoto S, Moldrup P, Kawamoto K, et al. Pore network structure linked by X-ray CT to particle characteristics and transport parameters [J]. *Soils Found*, 2016, 56(4): 676-90.

Kurylyk B L, Watanabe K. The mathematical representation of freezing and thawing processes in variably-saturated, non-deformable soils[J]. *Advances in Water Resources*, 2013, 60: 160-177.

Lai J, Wang G, Fan Z, et al. Insight into the pore structure of tight sandstones using NMR and HPMI measurements[J]. *Energy & Fuels*, 2016, 30(12): 10200-10214.

Li K, Yang H, Han X, et al. Fractal features of soil particle size distributions and their potential as an indicator of *Robinia pseudoacacia* invasion[J]. *Scientific Reports*, 2018, 8(1): 7075.

Liu J, Yang P, Li L, et al. Characterizing the pore size distribution of a chloride silt soil during freeze–thaw processes via nuclear magnetic resonance relaxometry[J]. *Soil Science Society of America Journal*, 2020, 84(5): 1577-1591.

Rahimi R, Bagheri M, Masihi M. Characterization and estimation of reservoir properties in a carbonate reservoir in Southern Iran by fractal methods[J]. *Journal of Petroleum Exploration and Production Technology*, 2018, 8: 31-41.

Tao Y, Yang P, Li L, et al. Characterizing unfrozen water content of saline silty clay during freezing and thawing based on superposition of freezing point reduction[J]. *Cold Regions Science and Technology*, 2023: 103933.

Wang C, Li S, Lai Y, et al. Predicting the Soil Freezing Characteristic From the Particle Size Distribution Based on Micro-Pore Space Geometry[J]. *Water Resources Research*, 2022, 58(1): e2021WR030782.

Wang F, Jiao L, Liu Z, et al. Fractal analysis of pore structures in low permeability sandstones using mercury intrusion porosimetry [J]. *Journal of Porous media*, 2018, 21(11).

Xiao Z, Lai Y, Zhang J. Method for calculating the liquid water fraction of saline soil during the freezing process[J]. *Permafrost and Periglacial Processes*, 2021, 32(1): 92-101.

Zeng L, Cui Y, Conil N, et al. Experimental study on swelling behaviour and microstructure changes of natural stiff Teguline clays upon wetting [J]. *Canadian Geotechnical Journal*, 2017, 54(5): 700-709.

Zhang Z, Weller A. Fractal dimension of pore-space geometry of an Eocene sandstone formation[J]. *Geophysics*, 2014, 79(6): D377-D387.

Zhou J, Wei C, Lai Y, et al. Application of the generalized Clapeyron equation to freezing point depression and unfrozen water content[J]. *Water Resources Research*, 2018, 54(11): 9412-9431.

## **Snowpack Strength and Micromechanics on Grand Mesa, Colorado via the 2017 NASA SnowEx SnowMicroPen dataset**

Molly E. Tedesche<sup>1</sup>, Aaron C. Meyer<sup>2</sup>, and Sergey N. Vecherin<sup>3</sup>

*<sup>1</sup>Cold Regions Research & Engineering Laboratory, Force Projection and Sustainment Branch, US Army Engineer Research & Development Center, Hanover, NH, USA;*

*Molly.E.Tedesche@erdc.dren.mil*

*<sup>2</sup>Cold Regions Research & Engineering Laboratory, Signature Physics Branch, US Army Engineer Research & Development Center, Hanover, NH, USA; Aaron.C.Meyer@erdc.dren.mil*

*<sup>3</sup>Cold Regions Research & Engineering Laboratory, Signature Physics Branch, US Army Engineer Research & Development Center, Hanover, NH, USA;*

*Sergey.N.Vecherin@erdc.dren.mil*

### **Abstract**

This study investigates several of the snowpack micromechanical and microstructural properties which are critical to assessing the engineering capabilities of snow, such as stability. Snow density, compression strength, and microstructural element deflection at rupture, were derived using the 2017 NASA SnowEx SnowMicroPenetrometer datasets from the Grand Mesa, Colorado, USA. Our study employs a comprehensive methodology involving spatial statistical relationships and physically based calculations to assess these microparameters. The SMP force profiles were initially pre-processed to correct signal errors and eliminate non-snow portions. Results from the statistical analyses reveal notable spatial auto- and cross-correlations among compression strength, deflection at rupture, and snow density. Despite non-uniform spacing between the sampling locations, results indicate positive cross-correlations between snow density and compression strength, as well as between snow density and deflection at rupture. Conversely, an observable negative correlation exists between compression strength and the rupture deflection.

## Foundation Performance Evaluation of an At-Grade LNG Storage Tank on Warm Permafrost in Fairbanks, Alaska

John D. Thornley, Ph.D., P.E., D.GE, M. ASCE<sup>1</sup>, Andrew P. Daggett, P.E., M. ASCE<sup>1</sup>, David J. Prusak, P.E. M. ASCE<sup>2</sup>, Mark L. Rockwell, P.E.<sup>3</sup>

<sup>1</sup>*WPS Inc., Anchorage, Alaska, USA*

<sup>2</sup>*Stantec, Fairbanks, Alaska, USA*

<sup>3</sup>*Interior Gas Utility, Fairbanks, Alaska, USA*

### Abstract

In Fairbanks, Alaska, a 5.25-million-gallon LNG storage tank was designed to be an at grade structure with a shallow mat foundation, due to the high seismic setting. Thermal analysis and design was performed to understand the transfer of cold energy from the storage tank foundation to the supporting permafrost below. Mechanical systems were designed to provide control and maintain temperatures that protect the permafrost from aggrading and degrading over the 75-year design life of the structure.

Liquefied natural gas (LNG) storage tanks are often pile-supported structures when located in permafrost regions. This allows for a thermal break between the bottom of tank, where LNG is stored at -160°C and the ground surface. The thermal break provides protection to the permafrost below so that it does not aggrade causing issues such as ice wedge development below the storage tank over time.

It has been more than four years since the construction and beginning of operation of the storage tank and monitoring of systems has been routinely performed. This paper presents the engineering design and construction considerations for the storage tank foundation and provides an evaluation of the operational performance of the foundation system.

Long-term monitoring includes survey measurements of the tank foundation, temperature measurements at the bottom of the concrete foundation and external temperature monitoring. The temperature measurements are performed to control the heating system within the foundation that turn on when the tank foundation gets too cold. External temperature monitoring is described and presented for the permafrost directly below the storage tank and beyond the storage tank footprint. The LNG storage tank is operating according to the design and performance of the structure is as expected, showcasing the potential to use this design methodology for other LNG storage tanks in permafrost regions.

## 3D Printing Ice Composites for Construction in Cold Regions

Kiera Thompson Towell,<sup>1</sup> Megan Kreiger,<sup>2</sup> and Emily Asenath-Smith<sup>3</sup>

<sup>1</sup> *Cold Regions Research and Engineering Laboratory (CRREL), US Army Corps of Engineers Engineer Research & Development Center, 72 Lyme Road, Hanover, NH 03755; email: kiera.l.towell@usace.army.mil*

<sup>2</sup> *Construction Engineering Research Laboratory (CERL), US Army Corps of Engineers Engineer Research & Development Center, 2902 Newmark Dr, Champaign, IL 61822; email: megan.a.kreiger@usace.army.mil*

<sup>3</sup> *Cold Regions Research and Engineering Laboratory (CRREL), US Army Corps of Engineers Engineer Research & Development Center, 72 Lyme Road, Hanover, NH 03755; email: Emily.asenath-smith@usace.army.mil*

In cold regions it is difficult to use conventional construction methods for infrastructure, as the cold temperatures and remote locations hinder the procurement, transportation, and use of typical construction materials, such as concrete and asphalt. On the other hand, ice and snow are abundant natural resources that can be used as building materials if techniques and methodologies are developed. The addition of particles and fibers to ice can significantly increase the strength of ice, particularly in flexural and tensile loading [1], and fibers can inhibit crack propagation through the brittle ice matrix [2]. Cellulose nanofibers (CNFs) have shown promise in reinforcing ice for construction [1, 3], and the tunable nature of the thermal and optical properties of the cellulose reinforced ice [4] make CNFs a compatible second phase material to modify ice for use in cold regions infrastructure.

To enable the construction of complex structures and to reduce the risk of cold injury in the construction process, a method was developed by the Engineer Research & Development Center utilizing 3D printing of reinforced ice by liquid extrusion. The methodology under development is scalable for use in additive construction of reinforced ice to facilitate construction of larger structures. The print material is a solution containing cellulose and other additives is extruded as a fluid that freezes after deposition on a cold surface. The CNF gel used is a complex fluid with a yield stress and shear thinning behavior, resulting in smooth flow and good shape stability after printing.

The resulting ice composite has enhanced ductility and strength, in both flexural and compressive loading, compared to regular ice (Figure 1). During flexural loading there was no delamination or fracture between the layers, demonstrating cohesion between the 3D printed layers as they freeze. Our method has demonstrated the ability to form complex shapes and support multiples layers (Figure 2). Using this system, structures have been printed up to a height of 100 mm so far, with line widths ranging from 3 mm to 10 mm. This demonstrated lab-scale methodology has potential for utilization in additive construction using ice and snow of structures in cold regions.

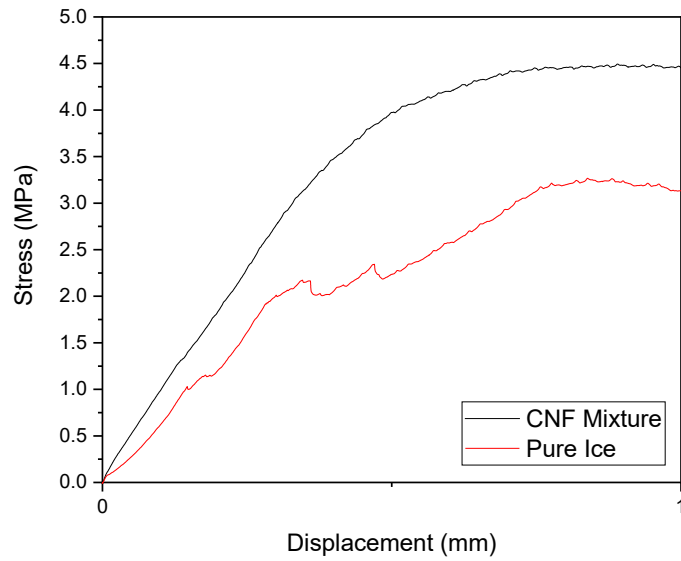


Figure 1. Stress strain curves from compressive testing of frozen CNF gel and pure ice cylinders. The pure ice was frozen in layers to simulate the 3D printed structure.

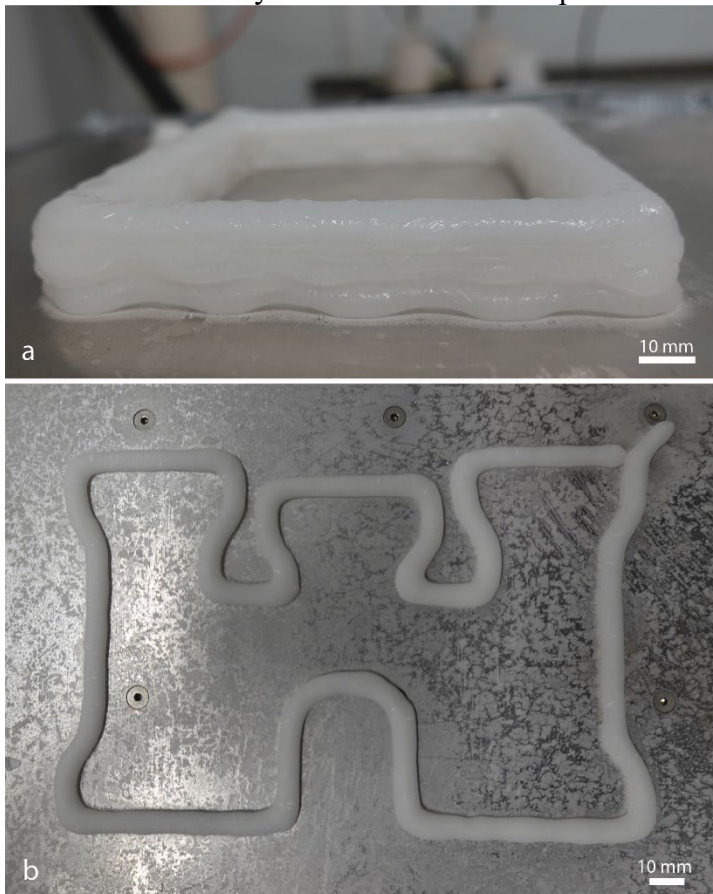


Figure 2. 3D printed ice square (a) and castle (b) made from frozen, extruded, CNF gel with a line thickness of roughly 10 mm and a layer height of 3.5 mm.

**References**

K. Thompson Towell, et al., “Construction and structural analysis of an arched cellulose reinforced ice



bridge for transportation infrastructure in cold regions.” *Cold Regions Science and Technology*, 198, 103508, (2022).

E. Asenath-Smith, et al., “Observation of crack arrest in ice by high aspect ratio particles during uniaxial compression.” *ERDC-CRREL Technical Report*, 22-3, (2022).

N. Vasiliev, et al., “A review on the development of reinforced ice for use as a building material in cold regions.” *Cold Regions Science and Technology*, 115, 56-63, (2015).

K. Thompson Towell, et al., “Cellulose nanofibers tune the mechanical, optical, and thermal properties of ice.” (2024). *In progress*.

# Impact of Engineered Water Repellency on Mechanical Properties of Frost-Susceptible Soils under Repeated Freeze-Thaw Cycles

M. Uduebor, M.Eng, Ph.D., A.M.ASCE<sup>1</sup>, J. Daniels, D.Eng, P.E., F.ASCE<sup>2</sup>, Y. Saulick, Ph.D., M.ASCE<sup>3</sup>, E. Adeyanju, SM.ASCE<sup>4</sup>, A. Familusi SM.ASCE<sup>5</sup>, W. Naqvi, M.S., SM.ASCE<sup>6</sup>, Bora Cetin, Ph.D., M.ASCE<sup>7</sup>

<sup>1</sup>Bio, Civil and Environmental Engineering, Florida Gulf Coast University, 10501 FGCU Blvd. So., Fort Myers, FL 33965-6565; email: [muduebor@fgcu.edu](mailto:muduebor@fgcu.edu)

<sup>2</sup>Civil and Environmental Engineering, The University of North Carolina at Charlotte, 9201 University City Blvd, Charlotte, NC 28223; email: [jodaniel@uncc.edu](mailto:jodaniel@uncc.edu)

<sup>3</sup>Civil and Environmental Engineering, The University of North Carolina at Charlotte, 9201 University City Blvd, Charlotte, NC 28223; email: [ysaulick@uncc.edu](mailto:ysaulick@uncc.edu)

<sup>4</sup>Civil and Environmental Engineering, The University of North Carolina at Charlotte, 9201 University City Blvd, Charlotte, NC 28223; email: [dadeyanj@uncc.edu](mailto:dadeyanj@uncc.edu)

<sup>5</sup>Civil and Environmental Engineering, The University of North Carolina at Charlotte, 9201 University City Blvd, Charlotte, NC 28223; email: [afamilus@uncc.edu](mailto:afamilus@uncc.edu)

<sup>6</sup>Department of Civil and Environmental Engineering, Michigan State University, East Lansing, MI 48824; email: [naqvim1@msu.edu](mailto:naqvim1@msu.edu)

<sup>7</sup>Department of Civil and Environmental Engineering, Michigan State University, East Lansing, MI 48824; email: [cetinbor@msu.edu](mailto:cetinbor@msu.edu)

## Abstract

Frost-susceptible soils, when exposed to seasonal freeze-thaw cycles, undergo significant changes in their deformation, strain, and stress profiles, critically affecting their engineering properties. These changes, which result in frost heaving and thaw weakening, impose profound changes across the soil system's moisture content, stress, and strain dynamics. Engineered Water Repellency (EWR), a novel intervention aimed at inducing hydrophobicity within soils, has shown promise in transforming in-situ soil materials into effective barriers against water transport, thereby mitigating frost heave phenomena. Water repellency in soils can be achieved by combining soils with polymers and other complex organic molecules - water-repellent additives - known as organo-silanes (OS). This technique enhances soil properties, making them suitable for use as moisture barriers in various infrastructures like road pavements, landfills, and tunnels exposed to seasonal wet-dry and freeze-thaw effects. Despite the apparent efficacy of EWR in addressing moisture-induced soil challenges, comprehensive insights into its effects on the mechanical behavior of soils under repeated freeze-thaw cycles remain scarce. Through a comprehensive experimental campaign supported by the U.S. National Science Foundation (Award #1928813), this study embarked on a series of laboratory freezing experiments to investigate the impacts of engineering water repellency on the performance of soil under repeated freeze-thaw conditions. Utilizing frost-susceptible soil from Fairbanks, Alaska, treated with an organosilane, the study assessed the mechanical properties of the soil subjected to multiple freeze-thaw cycles. Assessment tests included Contact Angle and Water Drop Penetration tests to determine the extent of water repellency conferred on treated samples, alongside Unconfined Compressive Strength tests to determine the treatment's influence on soil strength vis-à-vis untreated samples. Both treated and untreated samples were subjected to four freeze-thaw cycles, with subsequent strength testing. The study unveiled that the water-repellent treatment markedly enhanced the contact angles (117.6° air-dried, 127.6° oven-dried) and water drop penetration test times (2875s air-dried, >3600s oven-dried), evidencing the treatment's efficacy in imparting water repellency to the soil. While untreated samples manifested a decrease in unconfined compressive strength, consequent to moisture conditioning and the

expansive action of freezing water within pore spaces after repeated freeze-thaw cycles, treated samples exhibited improved strength post-multiple freeze-thaw cycles, attributed to the enhanced water repellency within the soil matrix. This induced hydrophobicity ensured that the treated samples preserved their unsaturated condition and strength attributes under diverse wetting scenarios, rendering them more apt for construction endeavors where design considerations typically hinge on worst-case subgrade strength scenarios in relation to moisture content. The integration of water repellency into pavement subgrade soils emerges as an innovative technique for achieving more dependable pavement design, enabling reductions in pavement thickness specifications, and improving cost efficiencies in pavement construction endeavors.

# Impact of Salts on Engineered Water Repellency Treatment in Pavement Soils

M. Uduebor, M.Eng, Ph.D., A.M.ASCE<sup>1</sup>, J. Daniels, D.Eng, P.E., F.ASCE<sup>2</sup>, Y. Saulick, Ph.D., M.ASCE<sup>3</sup>, Bora Cetin, Ph.D., M.ASCE<sup>4</sup>

<sup>1</sup>*Bio, Civil and Environmental Engineering, Florida Gulf Coast University, 10501 FGCU Blvd. So., Fort Myers, FL 33965-6565; email: muduebor@fgcu.edu*

<sup>2</sup>*Civil and Environmental Engineering, The University of North Carolina at Charlotte, 9201 University City Blvd, Charlotte, NC 28223; email: jodaniel@uncc.edu*

<sup>3</sup>*Civil and Environmental Engineering, The University of North Carolina at Charlotte, 9201 University City Blvd, Charlotte, NC 28223; email: ysaulick@uncc.edu*

<sup>4</sup>*Department of Civil and Environmental Engineering, Michigan State University, East Lansing, MI 48824; email: cetinbor@msu.edu*

## Abstract

Engineered Water Repellency (EWR) treatment has emerged as a promising solution for managing moisture in soils, with applications in geotechnical and soil engineering. One of its critical use cases is in mitigating frost action in cold climate regions, where freezing and thawing cycles can pose significant challenges to infrastructure and soil stability. EWR treatment, achieved through the process of silanization, involves the bonding of hydrophobic silane molecules to soil particles, creating a water-repellent protective layer. However, the interaction between salt concentrations and EWR treatment in soils remains a largely unexplored area. In regions with cold climates, salt applications are common for road maintenance, which can influence the effectiveness of EWR treatment. Sodium chloride (NaCl) and calcium chloride (CaCl<sub>2</sub>) are frequently used salts, but their impact on EWR treatment and treated soils remains uncertain. Moreover, the relationship between pH levels and the silanization process, which is crucial for EWR treatment efficacy is disrupted by salt concentrations. Natural soils and glass beads were collected and subjected to EWR treatment using different organosilane (OS) dosages. The impact of salt concentration was evaluated in both contact angle measurements and Water Drop Penetration Time (WDPT) tests. Additionally, electrical conductivity (EC) and pH measurements were taken to assess the chemical changes in treated soils. Findings reveal that the presence of salts, leads to decreased contact angles, indicating a loss of water-repellent properties. Only at very high OS concentrations and low salt concentrations were strong repellency characteristics retained. The EC and pH results indicated that the addition of salts significantly altered the chemical properties of the soils, making them less suitable indicators of the optimal EWR treatment concentration for salted soils. The presence of salts had a clear impact on pH levels, affecting the silanization process and the bonding of silane molecules to soil particles. This study highlights the crucial role of salt concentration in influencing the effectiveness of EWR treatment and the necessity of considering salt content, particularly in cold climate regions where salts are commonly applied. Engineers and researchers must carefully evaluate soil salt levels and tailor EWR treatment strategies accordingly to ensure optimal performance.

## Development of a smart-light system for remote rural areas

Vinod Vasudevan, Ph.D., P.E, Mohammad Kapourchali, Ph.D.

**Abstract**

Crashes at isolated intersections are dangerous, and most of the time, they result in fatalities. Studies have found that poor lighting plays a significant role in crashes. Since the rural roads have low volume, especially at night, the drivers do not expect other vehicles. Intersection crashes during nighttime hours may occur because of poor driver visual cognition of conflicting traffic or intersection presence. The lack of alertness may lead to severe crashes. An effective way to reduce the likelihood of crashes at isolated intersections is to warn road users of the intersection. An intelligent lighting system can detect approaching vehicles using sensors and transmit this information to a receiver to illuminate the intersection. By deploying a demand-responsive light, the system is expected to provide adequate warning to motorized and non-motorized road users. This presentation discusses developing and deploying a smart-lighting system at the University of Alaska Anchorage (UAA).

# Life-cycle analysis of LED traffic lights in Alaska

Vinod Vasudevan, Ph.D., P.E.

*University of Alaska Anchorage*

## **Abstract**

Over the last two decades, light-emitting diode (LED) technology has advanced, and LEDs have been identified as a replacement for incandescent bulbs in various applications, including traffic signal heads. LEDs do not fail in the same manner as incandescent bulbs. Instead of complete and abrupt failure, which occurs when the filament in an incandescent bulb burns out or breaks, LEDs degrade gradually over time, causing the quality and intensity of the light emitted to decrease. However, the process of gradual failure has drawbacks. It is apparent when an incandescent bulb fails and stops emitting light. On the other hand, LEDs continue emitting light that may need to meet the minimum specifications for intensity and color. These changes cannot always be distinguished by the naked eye, making it difficult to determine when LEDs must be replaced. Therefore, it is essential to conduct a performance assessment of LED traffic lights. This presentation discusses such an assessment for Alaska. Over 40 intersections from Anchorage and Fairbanks were tested and analyzed using the ITE guidelines for luminous intensity and chromaticity. Under the luminous intensity specification, it was found that the average replacement period range for red lights was 7 to more than 12 years, and for green lights, it was 6 to 13 years at 95% confidence. Based on this range, the average replacement age for red lights is between 7 and 11 years. For green lights, the replacement age is between 6 and 10 years. Based on the chromaticity guidelines, the results showed that red signals improved chromaticity over time, whereas green signals displayed a reduction in chromaticity around the 15-year mark. These results show that luminous intensity is critical, and signals should be replaced based on those conditions.



# Funding for Sustainable Infrastructure Efforts in Alaska and Related Challenges

Wagner, Natalie, P.E., M.ASCE<sup>1</sup>

<sup>1</sup>Alaska State Office, Rural Development, United States Department of Agriculture, 800 E Palmer-Wasilla Hwy, Suite 201, Palmer, Alaska 99645; email: Natalie.wagner@usda.gov

## Abstract

Multiple United States (U.S.) government agencies coordinate to fund sustainable and resilient infrastructure in Alaska. The funding is generally divided between planning and construction phases for projects. Planning documents for these projects now address environmental threats, available energy, workforce and ongoing operation and maintenance funding, in addition to the general technical feasibility. The U.S. Government Accountability Office's recent report (May 2022) on how federal funding is spent related to environmental threats in Alaska by agencies noted elements within each agency's mandate and where more could be done. Overall, coordination and support of projects was encouraged. Construction funding often comes with domestic preference requirements. Federal agencies must work within the domestic preference requirements, the delays and supply shortages, when combined with the remote locations and transport challenges, pose additional obstacles to addressing infrastructure challenges in a timely fashion. These dynamics, combined with the recent significant increases in federal funding available for cold climate infrastructure projects, set the stage for building resilient, sustainable future for rural Alaska. This paper will expand on efforts, funding constraints, as well as examples of collaboration and project coordination.

**Keywords:** Sustainable, Cold/Remote, Water and Wastewater Systems, Collaboration

## Introduction

Alaska, the largest state in the U.S., with a total area of approximately 665,400 square miles as well as most of the U.S. coastline, is one of the least populated areas, with a total population of 732,673 (2021) and a population density of 1.3 people per square mile (cite). In addition, according to the US DOT, Alaska also has the lowest road density in the US (as per 2016 DOT). Alaska is also faced with several challenges for construction and environmental threats. The construction challenges include logistics and shipping, barges required for many deliveries and limited windows for scheduling, a shortened construction season. The environmental threats can be summarized into thawing permafrost, river and coastal erosion, flooding and general seasonal impacts due to geography (significant drifting snow, rainfall, etc.). Alaska's remote community water and wastewater infrastructure is funded and maintained in light of these challenges and environmental threats.

Several agencies collaborate to assist in providing funds for sanitation infrastructure. These include United States Department of Agriculture – Rural Development (USDA-RD), United States Department of Health and Human Services - Indian Health Services (IHS)- Alaska Area, Environmental Protection Agency (EPA), United States Department of Commerce – Economic Development Agency (EDA), the Denali Commission, among others.

USDA focuses on communities with population less than 10,000 people. The Justice 40 Initiative, established by President Biden in Executive Order 14008 on “Tackling the Climate Crisis at Home and Abroad,” “applies to projects targeting ... the development of critical clean water and wastewater infrastructure.” There is also additional focus to address the unmet needs of communities that experience

persistent poverty, are distressed, and have with high-cost energy.

According to the 2021 Government Accountability Office report, “Federal agencies have supported Alaska Native villages’ efforts to address environmental threats, but these threats are expected to worsen in the future because of climate change. With more than 70 Native villages highly threatened by erosion, flooding, or thawing permafrost, significant work remains for Native villages to address imminent threats and determine and implement the best courses of action for building resilience to these threats over the long term. In light of this significant work, and the 2021 executive order on environmental justice, it is critical for federal agencies to continue to identify ways to better provide assistance to Native villages and to target that assistance to the areas facing the most significant threats.” “Because federal agencies work closely with each other and tribal and state government entities, coordination is essential to doing this effectively and efficiently” (GAO report, 2022).

Future projects will be completed considering the updated domestic preference requirements. The Infrastructure Investment and Jobs Act (IIJA), Public Law 117-58 or the Bi-partisan Investment Law (BIL) included the updated Build America and Buy America Act (BABA). As a result, there will likely be procurement and availability challenges, as well as increased use of available waivers. In general, the past several years of American Iron and Steel (AIS) compliance has helped prepare the field for complying with the domestic preference requirements included with infrastructure funding. The federal agencies will be able to assistance funding recipients and to help achieve compliance with pragmatic approaches to meeting the overall intent. Alaska also needs to be considerate of the indigenous population and timing impacts related to the implementation of federal programs and tribal input.

### **Methodology**

The information shared is gathered through several decades of targeted collaboration and coordination among the federal agencies and rural Alaskan communities. There are several methods of coordination and collaboration employed in Alaska. These include monthly coordination meetings with IHS, EPA and ANTHC; IHS SDS funding collaboration; and USDA-RAVG funding with EPA and State of Alaska.

### **Findings or Results**

The collaboration and cooperation of the federal agencies and local organizations have been able to successfully provide critical sanitation infrastructure community wide. Several examples show that improved health and general community parameters result from increased access to clean drinking water. Past collaboration success will lend itself to future projects. The additional funding and projects enabled by the infrastructure investments of the federal government share additional challenges with the volume of projects and the domestic preference requirements.

### **Conclusions**

The related benefit of collaboration is that projects can be funded completely by combing funds from different programs that may individually have limitations that would prevent full funding due to various program eligibility requirements and budget constraints. The related challenges include coordinating timing and funding cycles. Further challenges were present with program variations related to domestic preference, which is in part simplified and intensified with the updated requirements for all federal infrastructure funding. Multi-agency collaboration is essential to provide sustainable sanitation infrastructure to enable rural Alaskans to be healthy.

### **Acknowledgments**

Wish to express sincere gratitude to the rural Alaskan communities that we work with, to USDA and our

partner agencies.

## **References**

Infrastructure Investment and Jobs Act (IIJA), Public Law 117-58

GAO-22-104241, “Federal Agencies Could Enhance Support for Native Village Efforts to Address Environmental Threats,” May, 2022

United States Department of Transportation, 2016. "Table HM-10M - Highway Statistics 2015 – Policy, Federal Highway Administration."

Executive Order 14008, “Tackling the Climate Crisis at Home and Abroad”

Water and Waste Loans and Grants, 7 CFR 1780

Rural Alaskan Village Grants, 7 CFR 1784

Environmental Policies and Procedures, 7 CFR 1970

Emergency Community Water Action Grants, 7 CFR 1778

Preliminary Engineering Reports for the Water and Waste Disposal Program – USDA Bulletin 1780-2

# Fabrication and Characterization of Multiphase Bituminous Materials for Cold Region Pavements

Di Wang, Ph.D.,<sup>1</sup> Augusto Cannone Falchetto, Ph.D., M.ASCE<sup>2</sup>, and Fan Zhang,<sup>3</sup>

<sup>1</sup>*Department of Civil Engineering, University of Ottawa, 161 Louis Pasteur, Ottawa, ON K1N 6N5, Canada; email: wangditubs@gmail.com*

<sup>2</sup>*Department of Civil Engineering, Aalto University, Rakentajanaukio 4, 02150 Espoo, Finland; email: augusto.cannonefalchetto@aalto.fi*

<sup>3</sup>*Department of Civil Engineering, Aalto University, Rakentajanaukio 4, 02150 Espoo, Finland; email: fan.3.zhang@aalto.fi*

## Abstract

In this study, the low temperature creep properties of multiphase bituminous materials (binder, mastic, Fine Aggregate Matrix - FAM, and mixture) were experimentally evaluated, and the impact of size effect on FAM and mixture specimen was also assessed. First, the mix design of mastic and FAM were calculated based on the reference mixture AC 22 TS. The mathematical adaptation to the boundary sieve method was applied to determine the gradation and binder content in FAM. Next, a fabrication method was proposed to produce Fine Aggregate Matrix (FAM) in a laboratory environment, and scale-up slab samples were also fabricated for FAM and mixture specimens to evaluate the size effect phenomenon. Finally, three-point bending (3PB) creep tests were conducted on the multiphase bituminous specimens with different dimensions at -6 °C, -12 °C, and -18 °C with a modified Bending Beam Rheometer (BBR) device and a dynamic loading machine, depending on the sample size. Results indicate that the creep stiffness of the FAM was close to mixtures and much higher than the one observed in binder and mastic. The proposed fabrication approach provides a satisfactory method for preparing a representative FAM phase in the mixture, while the air voids can be easily adjusted during the slab compaction procedure. This study supports the idea of using FAM to discriminate asphalt mixtures for cold regions. The correlation between up-scaled FAM and mixtures specimens is recommended to be further investigated, including different mixture types and corresponding FAM.

**Keywords:** Bituminous materials, cold region, Multiphase, FAM, 3PB tests, Size effect.

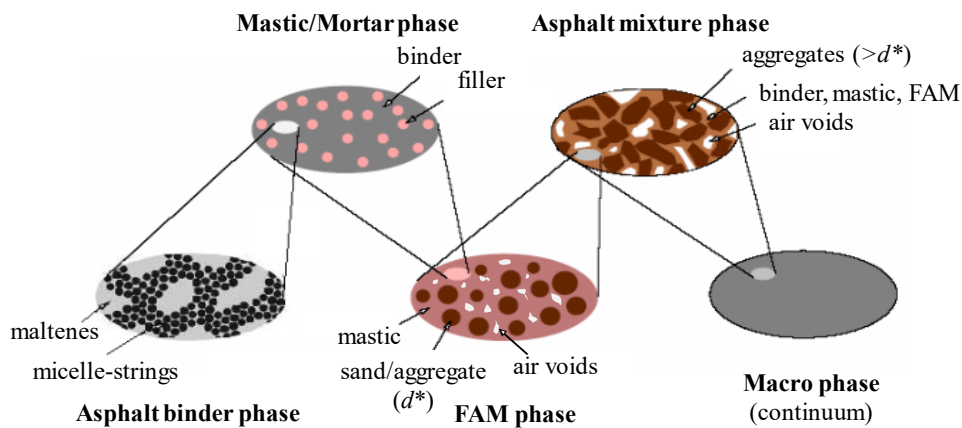
## Introduction

Durable and climate-resilient roads are essential for the infrastructure system in the cold regions, this is especially true for asphalt roads since it is one of the most common road structures globally [1]. Therefore, it is crucial to precisely evaluate the low temperature features of bituminous materials and comprehend how roads distress evolve [2]. Numerous experimental techniques, protocols, and criteria have been developed to evaluate bituminous materials' properties at low temperatures, including three-point bending (3PB) creep test, Direct Tension Tester (DTT), and Asphalt Binder Cracking Device (ABCD) tests for binder phase [3]. And uniaxial tension stress test (UTST), indirect tension tester (IDT), thermal stress restrained specimen test (TSRST), Disc-shaped compact tension (DCT), Semi-Circular Bending (SCB), and notched three-point bending (3PB) for the mixture phase [4,5]. It is crucial to acknowledge the limitations of these experimental procedures even though they were proven to reasonably characterize bituminous materials at low temperatures. There is no experimental protocol was proposed for the intermediate phase (mastic or mortar) of bituminous materials, in which most of the binder remains in mastic status in the mixture [6]. Moreover, in the authors' previous studies, it has been proven that the materials' structure size may significantly affect their nominal strength at low temperatures [7]. This is to say that the currently widely used experimental method may not genuinely capture the low temperature behavior of the asphalt mixture. In this study, the

low temperature creep properties and size effect on multiphase bituminous materials were experimentally characterized and modeled.

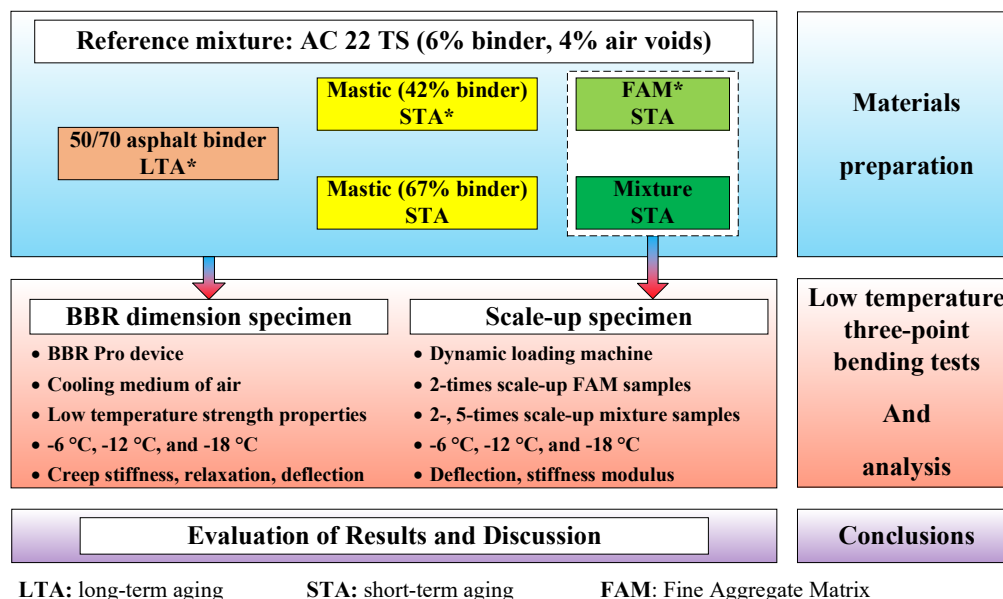
### Methodology

To achieve the aforementioned objective, the following experimental and analysis work were applied. First, the BBR dimension multiphase bituminous materials (Figure 1), binder, mastic, Fine Aggregate Matrix (FAM), and mixture, were fabricated in the laboratory. The base layer dense-graded mixture, AC 22 TS, was selected as the reference material based on TL Asphalt-StB 07. Meanwhile, two different binder contents (one associated with the mixture and the other one with the FAM) were used in mastic to evaluate its effect. Then, scale-up specimens were fabricated for FAM (2x) and mixture (2x, and 5x) in the laboratory. Next, a modified Bending Beam Rheometer (BBR) device was used to characterize the low temperature creep properties of multiphase bituminous materials at BBR size, while a dynamic loading machine was used for scale-up specimens. Finally, comparisons and discussions were conducted regarding the creep stiffness,  $S(60s)$ , relaxation properties,  $m$ -value, and Huet model parameters. Figure 2 provides a summary of the suggested research methodology.



mesh size of filler: 63 $\mu$ m based on European sieving size; 75 $\mu$ m based on the US sieving size.  
 $d^*$ : definition of maximum passing sieving size varied in previous studies.

Figure 1. Multiphase schematic of asphalt road materials [8]



LTA: long-term aging      STA: short-term aging      FAM: Fine Aggregate Matrix

Figure 2. Research approach

To fabricate the FAM sample, its mix design should be determined first. Based on Bailey's approach, the upper threshold sieve size,  $NMAS_{FAM}=1.084$  mm, was determined by using the optimal aggregate size and packing theory (Equation 1) [9], and the nearest sieving size of 1 mm was selected based on the European standard. The gradation of FAM was initially determined by the ideal aggregate size and packing principle, then adjusted by the density of aggregates and filler. The final binder content was determined to be 10.14% by weight, while a target air voids content of 1% was selected. The packing concept was utilized to determine the binder and filler contents for the formulation of mastic materials. The reference materials used were mixture and FAM, where the latter is rich in asphaltene,  $mastic_{FAM}$  has a substantially larger binder content (67%) than  $mastic_{mixture}$  (42%). The determined materials' component was shown in Table 1.

$$FAIB=SCS=PCS\times 0.22=NMA\times 0.222 \quad (1)$$



Table 1. Multiphase bituminous materials and component

BBR dimension beam	Mixture	FAM	Mastic <sub>mixture</sub>	Mastic <sub>FAM</sub>	Binder
Binder content [%]	6	10.14	42	67	100
Air voids [%]	4	1	-	-	-
Scale-up dimension beam	5×Mixture	2×Mixture	2×FAM		
Binder content [%]	6	6	10.14		
Air voids [%]	4	4	1		

The roller sector compactor method [10] was used to fabricate the mixture and FAM specimens. It should be noted that for the FAM specimens, the target air voids were achieved by adjusting the pre-compaction and force-controlled main compression, and by the end, a parafilm-coated method was conducted to validate it. The fabricated specimen was then cutting into the specific dimensions for FAM and mixtures, respectively (Figure 3).

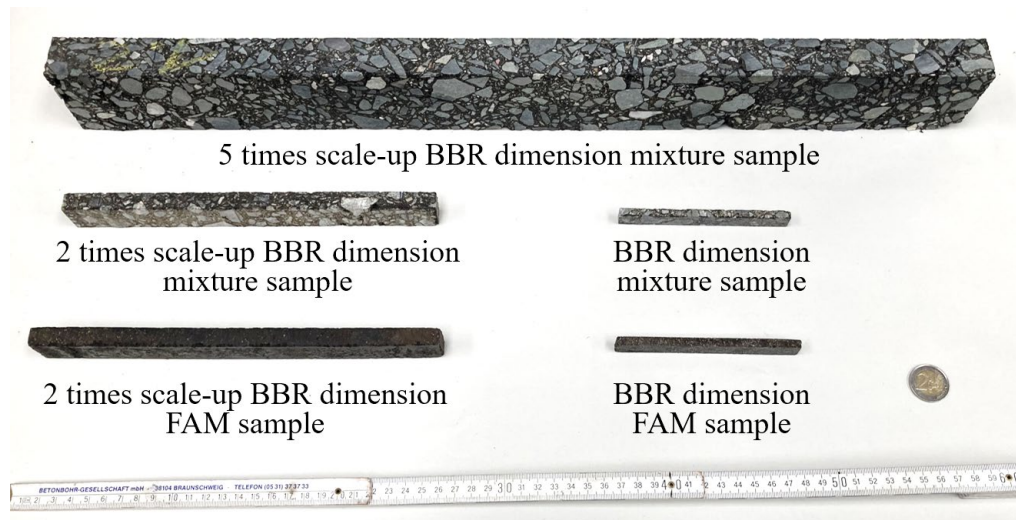


Figure 3. BBR- and scale-up dimensions specimens of asphalt mixture and FAM materials

The modified Bending Beam Rheometer (BBR) device was applied to characterize the low temperature creep properties of multiphase bituminous materials at BBR dimensions at  $-6\text{ }^{\circ}\text{C}$ ,  $-12\text{ }^{\circ}\text{C}$ , and  $-18\text{ }^{\circ}\text{C}$  together with a duration of 1000s. 1N was applied to the binder and mastic phases, while 3N and 4N were conducted to the FAM and mixture phases. For the scale-up samples, a dynamic loading machine was applied. 22N and 26N were determined for 2x BBR dimensions for FAM and mixture, respectively. For the 5x BBR dimension mixture sample, 67 N [11] was applied. A duration of 1000s or a deflection of 1% was used as the threshold. For each condition, at least three replicators were applied.

### Findings or Results

The creep stiffness,  $S(60s)$ , and relaxation characteristics,  $m$ -value (60s), were first calculated for all five multiphase bituminous materials under three testing temperatures (Figure 4). It was observed that the differences in  $S(60s)$  are much larger than the ones in  $m(60s)$  among different phases; such differences were more remarkable at lower temperatures. For  $S(60s)$ , the values increase with the phases. The results of FAM range four to ten times larger than mastic and binder phases; however, they are only about half as high as those obtained on the mixture. An increase of 25% in binder content in mastic leads to a more than 50% (52% to 57%) decrease in the creep stiffness results. It should be noted that the difference between Mastic<sub>FAM</sub> and binder, in comparison, is less than that between Mastic<sub>FAM</sub> and Mastic<sub>mixture</sub>. Therefore, the creep results for FAM and mixes are comparable, whereas the features of the two mastics are comparable to those of the binder. Therefore, FAM materials show very different behaviors from all other phases while

closer to the mixture response than mastics and binders. Hence, FAM appears to exhibit a higher potential to represent mixtures' behavior to discriminate bituminous materials.

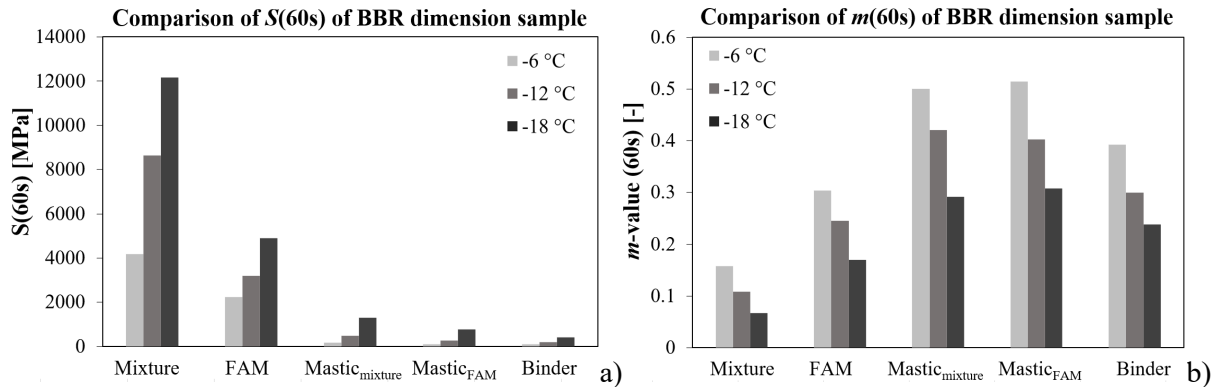


Figure 4. Comparison of multiphase BBR dimension samples: a)  $S(60s)$ , and b)  $m$ -value (60s)

Next, the stiffness over time,  $S(t)$ , was calculated based on the Huet model under three different temperatures, the comparison among all materials was plotted in Figure 5. Two clusters were found, particularly for the evolution of the creep stiffness modulus over time. FAM's modulus is closer to those obtained in the mixture (black dotted ellipse), while two mastic materials and the binder indicate similar performance (red dotted ellipse). In addition, the differences between the two clusters got smaller when the temperature became lower, which further supports the idea that FAM could be used to represent the related mixes response at low temperatures.

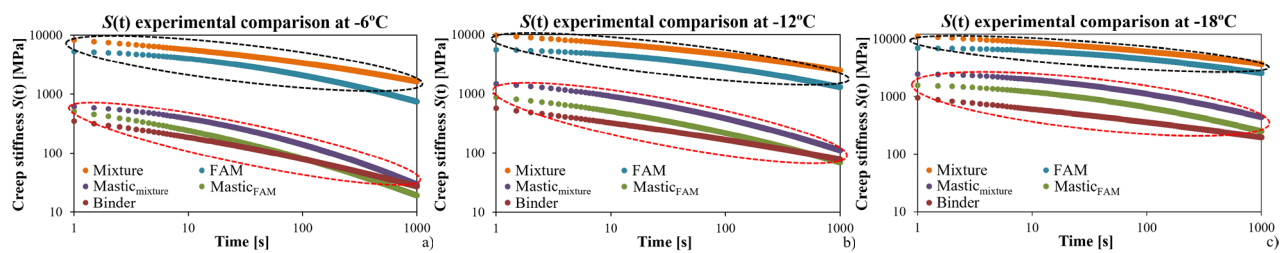


Figure 5. Comparison of  $S(t)$  for multiphase BBR dimension samples: a) -6 °C, b) -12 °C, c) -18 °C.

The creep stiffnesses over time were plotted for all scale-up samples under three different temperatures in Figure 6. It shows that most tests (except  $2\times$  BBR FAM) stopped at 1000 s at -12°C and -18°C; however, all tests at -6 °C finished earlier than 1000s. This is because 1000s or 1% deflection criteria were used for the testing duration. Hence, softer materials that reached 1% before 1000s at higher temperatures were not unexpected. For all the conditions, at the beginning of the loading process, a peak deflection/creep stiffness was realized due to the contact load, then a smooth creep stiffness curve can be recorded. It can be concluded that the effect of contact load indicated greater influences on higher temperatures and simpler phases; overall, decreasing deflection rates were realized when reducing the temperature. In addition, fewer deflection steps were also found at low temperatures; this effect may be attributed to the high load-bear capability in stiffer materials. In future research, larger FAM samples will be fabricated and evaluated to better understand the influence of size effect.

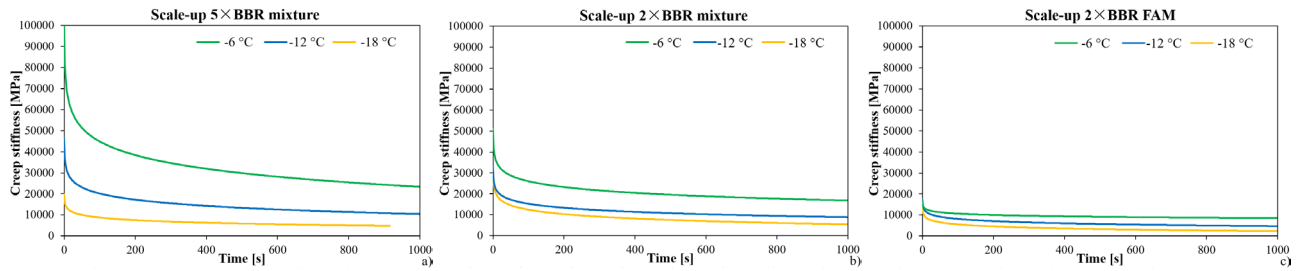


Figure 6. Comparison of creep stiffness results for scale-up BBR dimension samples: a) 5 times mixture; b) 2 times mixture; c) 2 times FAM.

## Conclusions

This study used a modified Bending Beam Rheometer (BBR) test to investigate the low temperature strength properties of five different phases of bituminous materials, including mixture, Fine Aggregate Matrix (FAM), mixture-based mastic, FAM-based mastic, and asphalt binder. Furthermore, the impact of the size effect phenomena was assessed and discussed on the scaled-up BBR dimension samples. The resulting conclusions are as follows:

- FAM can be designed by using the designing and calculation method of Underwood and Kim [9]. Different reference composites (mixture/mixes) will result in considerably different mastic materials based on the method's underlying assumptions.
- The roller sector compactor is a reliable and efficient device for preparing FAM specimens with precise air voids.
- When defining the mastic for the particular bituminous composite, careful consideration is required because the binder content in asphalt mastics greatly influences their low temperature behaviors (i.e., mixture, FAM, mortar).
- In the BBR dimension scale, FAM materials could produce outcomes equal to or comparable to mixes. Hence, when a solid analytical or model correlation can be established, FAM can potentially replace mixture testing by serving as a representative phase of the asphalt mixture at low temperatures.
- The responses of the 2 times BBR dimension FAM and mixed samples were comparable, particularly at lower temperatures, whereas the deflections of the 5 times BBR dimension mixture were significantly lower.

## References

Poulikakos LD, Papadaskalopoulou C, Hofko B et al (2017) Harvesting the unexplored potential of European waste materials for road construction. *Resour Conserv Recycl* 116:32-44.

Cannone Falchetto A, Moon KH, Wang D et al (2018) Investigation on the cooling medium effect in the characterization of asphalt binder with the bending beam rheometer (BBR). *Can J Civ Eng* 45(7):594-604.

Kim SS. Development of an Asphalt Binder Cracking Device," Final Report for NCHRP Highway IDEA Project 99, Transportation Research Board. 2007

Cannone Falchetto A, Moon KH, Wang D et al (2018) Comparison of low-temperature fracture and strength properties of asphalt mixture obtained from IDT and SCB under different testing configurations. *Road Mater Pavement Des* 19(3):591-604.

Office JE, Chen J, Dan H, Ding Y et al (2021) New innovations in pavement materials and engineering: A review on pavement engineering research 2021. *J Traffic Transp Eng* 8(6):815-999.

Kim YS, Sigwarth T, Büchner J et al (2021) Accelerated dynamic shear rheometer fatigue test for investigating asphalt mastic. *Road Mater Pavement Des* 22(sup1):S383-S396.

Cannone Falchetto A, Le JL, Turos MI et al (2014) Indirect determination of size effect on strength of asphalt mixtures at low temperatures. *Mater Struct* 47:157-169.

Lackner R, Spiegl M, Blab R (2005) Is the low-temperature creep of asphalt mastic independent of filler shape and mineralogy Arguments from multiscale analysis. *J Mater Civ Eng* 17 (5):485–491.

Underwood BS, Kim YR (2013) Effect of volumetric factors on the mechanical behavior of asphalt fine aggregate matrix and the relationship to asphalt mixture properties. *Constr Build Mater* 49:672-681.

Wistuba M (2016) The German segmented steel roller compaction method–state-of-the-art report. *Int J Pavement Eng* 17(1):81-86.

Velasquez RA (2009) On the representative volume element of asphalt concrete with applications to low temperature. Ph.D. Thesis. University of Minnesota, Twin Cities, Minneapolis, USA

# A simple method for estimation of the soil pore structure in frozen soils using the nuclear magnetic resonance method

Hao Wang<sup>a</sup>, Sai K. Vanapalli<sup>b</sup>, Xu Li<sup>c</sup>

<sup>a</sup>Department of Civil Engineering, University of Ottawa, Canada, Ottawa, ON, K1N 6N5, Canada, (Email: hwang423@uottawa.ca)

<sup>b</sup>Department of Civil Engineering, University of Ottawa, Canada, Ottawa, ON, K1N 6N5, Canada (Email: Sai.Vanapalli@uottawa.ca)

<sup>c</sup>Key Laboratory of Urban Underground Engineering of Ministry of Education, Beijing Jiaotong University, Beijing 100044, China, (Email: xuli@bjtu.edu.cn)

## Abstract

The nuclear magnetic resonance method (NMR) is widely used as a tool in the pore size characterization of rocks such as sandstones, carbonates, and coals. This technique also has been widely used to estimate the unfrozen water content in frozen soils; however, there are limited studies that focus on the frozen soils pore structure characterization. In the NMR tests, based on the results from the literature, a linear relationship is assumed between the pore size ( $R$ ) and transverse relaxation time ( $T_2$ ), of the transverse magnetization decay. This relationship is mathematically represented as  $\frac{1}{T_2} = \frac{2\rho_2}{R}$ , where  $\rho_2$  is constant representing the surface relaxivity. Traditionally,  $\rho_2$  is determined by  $T_2$  cutoff values, which is a relaxation time threshold that divides the  $T_2$  spectrum into two zones: namely, the bound water and free water in frozen soils. Conventionally, centrifuge experiments are used for determining the cutoff value in the field of petroleum engineering. The key parameter  $\rho_2$  is also approximately estimated or assumed based on the information from the published literature for different types of soils. In other words,  $T_2$  cutoff value is based on approximations that have limitations or based on centrifuge tests that need elaborate testing which is expensive.

In this paper, a new method is proposed to calculate  $T_2$  cutoff value from the NMR test results on a saturated frozen silt clay. The two key advantages of this method include avoiding approximations and the use of expensive centrifuge tests for the estimation of the cutoff value,  $T_2$ . The proposed method in this paper is useful for better understanding the behavior of frozen soils with the aid of simple and inexpensive methods.

# Probabilistic assessment of embankments in seasonally frozen ground in the face of changing climate

Lei Wang<sup>1</sup>, Liang Zhang<sup>2</sup>, Sohail Akhtar<sup>3</sup>, Biao Li<sup>4</sup>

<sup>1</sup> Assistant Professor, University of Cincinnati. Email: wang4li@ucmail.uc.edu

<sup>2</sup> Research Assistant, University of Cincinnati. Email: zhang4lg@mail.uc.edu

<sup>3</sup> Research Assistant, Concordia University. Email: sohail.akhtar@concordia.ca

<sup>4</sup> Assistant Professor, Concordia University. Email: biao.li@concordia.ca

## Abstract

Embankments are critical geotechnical infrastructure and recent records show that the ongoing climate trend has changed the thermal condition of seasonally frozen ground, causing widespread ground surface settlement and damages to embankments. The reliability assessment of these embankments under climate change is important to ensure the safety of humans and properties and minimize the damage to the community. The paper aims to present a probabilistic scheme to evaluate the reliability of embankments using the random finite element method considering the effect of climate change. The effect of spatial variability of soil parameters on the embankment performance will be incorporated based on a discretization of the finite element model proposed in this paper. The finite element model is developed to evaluate how climate change affects the thermal-mechanical performance of embankments based on climate data from 1975 till 2100. A case study will be utilized to demonstrate the effectiveness of the proposed framework for probabilistic assessment of embankments under climate change considering the soil spatial variability effects. The results from this paper can provide useful insights for practitioners to evaluate the risk and reliability of embankments in seasonally frozen areas and make an informed decision in the face of climate change.



# Thermal-stress response analysis and applicability study of energy shaft in winter

Zhou J., Author, Prof.,<sup>1,2,3</sup> Wang X., Author, Ph.D.,<sup>3</sup>

<sup>1</sup>*Department of Geotechnical Engineering, College of Civil Engineering, Tongji University, 1239 Siping Road, Shanghai 200092, China.*

<sup>2</sup>*Key Laboratory of Geotechnical and Underground Engineering (Tongji University), Ministry of Education, 1239 Siping Road, Shanghai 200092, China; email: [zhoujie1001@tongji.edu.cn](mailto:zhoujie1001@tongji.edu.cn)*

<sup>3</sup>*Department of Geotechnical Engineering, College of Civil Engineering, Tongji University, 1239 Siping Road, Shanghai 200092, China; email: [2310504@tongji.edu.cn](mailto:2310504@tongji.edu.cn)*

## Abstract

Energy shafts and energy tunnels are a kind of energy conservation and environmental protection underground structures. They can be used as shallow geothermal energy harvesting systems in cold regions. The theoretical research and practical application of energy shafts are still in the initial stage, and there are relatively few related experiments. This paper takes the Shanghai Taihe energy shaft test section in winter as the research background. It numerically analyzes the thermal-force response test of the energy shaft using COMSOL software. And compared with the Beijing Qinghuayuan energy tunnel for applicability evaluation and analysis. The results show that the heat exchange capacity of the Shanghai energy shaft is better than that of the Beijing energy tunnel due to the difference in the geological environment. Meanwhile, the temperature stress generated during heat exchange in Shanghai energy shafts is less than that in Beijing energy tunnels. Therefore, the energy underground structure is more applicable to the Shanghai strata in winter. Based on the thermal results and economic considerations, it is suggested that the inlet fluid velocity of the energy shaft is around 0.6 m/s in winter. The heat transfer tube spacing between 0.2 m and 0.3 m can ensure a high heat transfer capacity.

# Experimental Investigation of Thermal and Hydraulic Properties of Ice-rich Saline Permafrost in Northern Alaska

Ziyi Wang<sup>1</sup>, Ming Xiao<sup>2</sup>, Matthew Bray<sup>3</sup>, Margaret Darrow<sup>4</sup>

<sup>1</sup>*Department of Civil and Environmental Engineering, The Pennsylvania State University, University Park, PA 16802, United States of America. Email: ziyiawang@psu.edu.*

<sup>2</sup>*Department of Civil and Environmental Engineering, The Pennsylvania State University, University Park, PA 16802, United States of America. Email: mzx102@psu.edu.*

<sup>3</sup>*Institute of Northern Engineering, University of Alaska Fairbanks, Fairbanks, AK 99775-5900, United States of America. Email: mtbray@alaska.edu.*

<sup>4</sup>*Department of Civil, Geological, and Environmental Engineering, University of Alaska Fairbanks, Fairbanks, AK 99775-5900, United States of America. Email: mmdarrow@alaska.edu.*

## Abstract

Unfrozen water content and thermal properties are factors in understanding permafrost degradation processes, yet there is a general lack of information on the hydro-thermal properties of relatively undisturbed ice-rich permafrost in Arctic coastal regions. In this research, we measured the unfrozen water content as a function of temperature in samples from near-surface undisturbed ice-rich permafrost using a pulsed nuclear magnetic resonance (P-NMR) testing system, in a temperature-controlled environment. We measured frozen and unfrozen thermal conductivity and heat capacity of the permafrost samples. The average frozen and unfrozen thermal conductivities are 2.23 and 1.30 W/m·K, respectively, and the average frozen and unfrozen heat capacities are 1.91 and 3.00 MJ/m<sup>3</sup>/K, respectively. To investigate the effect of salinity on unfrozen water content of permafrost, we measured the samples' salinity levels. The salinity levels of the permafrost samples varied, ranging from 0.5 to 15.2 parts per thousand. Based on these data, we established an empirical relationship between salinity and unfrozen water content for ice-rich organic silty permafrost that can be used for engineering purposes.

# **Cryostructure and Uniaxial Compressive Strength of Ice-rich Permafrost in Northern Alaska**

Ziyi Wang<sup>1</sup>, Ming Xiao<sup>2</sup>, Matthew Bray<sup>3</sup>

<sup>1</sup>*Department of Civil and Environmental Engineering, The Pennsylvania State University, University Park, PA 16802, United States of America. Email: ziyiawang@psu.edu.*

<sup>2</sup>*Department of Civil and Environmental Engineering, The Pennsylvania State University, University Park, PA 16802, United States of America. Email: mzx102@psu.edu.*

<sup>3</sup>*Institute of Northern Engineering, University of Alaska Fairbanks, Fairbanks, AK 99775-5900, United States of America. Email: mtbray@alaska.edu.*

## **Abstract**

Knowledge of ground ice type and volume in the upper permafrost are vital for engineering design in cold regions. Cryostructure, which describes the pattern of ice inclusions, is an indicator of the formation characteristics and geology of permafrost soil and affects the geomechanical behavior of permafrost. In this paper, we present field sampling of relatively undisturbed permafrost on the Arctic Coastal Plain near Utqiagvik, Alaska. We characterize the cryostructure of the permafrost samples that were retrieved from five boreholes, which primarily consisted of organic silty sand with suspended ice inclusions. We conducted a series of unconfined compression tests under constant strain rate at temperatures of -2 °C and -10 °C to investigate the geomechanical behavior of selected permafrost cores. Here, we present the effects of temperature, dry density, water content, and cryostructure on the geomechanical behavior of ice-rich permafrost. Considering the effect of temperature, an empirical equation for short-term peak compressive strength is developed based on the experimental results. A quantitative example is provided to demonstrate how the varying geomechanical properties affect ultimate bearing capacity of shallow foundations in permafrost.

# Freezing Mechanism of Water in Clay Nanopores using Molecular Dynamics

Shijun Wei, S.M.ASCE<sup>1</sup>, Shoumik Saha<sup>2</sup>, Dilip Gersappe, Ph.D.<sup>3</sup>,  
and Sherif L. Abdelaziz, Ph.D., M.ASCE<sup>4</sup>

<sup>1</sup>Virginia Tech, Blacksburg, Virginia, 24061; Email: shijunw20@vt.edu

<sup>2</sup>Stony Brook University, New York, 11794; Email: shoumik.saha@stonybrook.edu

<sup>3</sup>Stony Brook University, New York, 11794; Email: dilip.gersappe@stonybrook.edu

<sup>4</sup>Virginia Tech, Blacksburg, Virginia, 24061; Email: saziz@vt.edu

## Abstract

This study evaluates the freezing mechanism of pure water inside nanopores confined by cohesive soil particles using molecular dynamics (MD). The key contribution of this study is to provide an assessment to better understand the physical and chemical particle interactions among water, ice, and clay surfaces within nanopores under supercooling temperatures. The nanopores were simulated by implementing coarse-grained kaolinite surfaces face-to-face with the mW water model filled in between using LAMMPS (Large-scale Atomic/Molecular Massively Parallel Simulator). The distance between face-to-face kaolinite sheets was controlled to target the desired nanopore size with the implementation of the piston model. The isothermal-isobaric ensemble, NPT, was used as the thermostat with hybrid Lennard-Jones and Stillinger-Weber potentials for the simulations. Simulations proceeded under freezing temperatures from 220 K (about -53 °C) to 190 K (about -83 °C) to capture the whole evolution of water crystallization within clay nanopores. CHILL+ algorithm was implemented to detect ice formation and distinguish different types of ice formed within nanopores. Ovito was used as a visualization tool to monitor the progress of crystallization and a descriptive method to observe the interactions within nanopores. The results showed that both hexagonal and cubic ice were formulated almost instantaneously within the clay nanopore at the temperature of 208 K (about -65 °C) with 20% more cubic ice than hexagonal ice. Some water remained liquid even as the temperature dropped to 190 K (about -83 °C).

# Retrofitting a Passively Cooled At-Grade Foundation at Nunam Iqua, AK, USA

Austen Whitney, EIT,<sup>1</sup> and Edward Yarmak, Jr., PE<sup>1</sup>

<sup>1</sup>*Arctic Foundations, Inc., 5621 Arctic Boulevard, Anchorage, Alaska 99518-1667; emails: awhitney@arcticfoundations.com and eyarmak@arcticfoundations.com*

**Keywords:** Thermosyphon, subgrade cooling, at-grade foundation

Passively cooled at-grade foundations on permafrost rely on cold winter air to remove heat to maintain permafrost and structural stability. As the climate warms in northern latitudes, this natural heat sink is truncated, thus reducing the heat removal capacity of passive systems and jeopardizing the stability of the structures being protected. In the Kuskokwim Delta area of western Alaska, the at-grade water treatment plant in Nunam Iqua was built in 1999 using 19 sloping evaporator thermosyphons with 70 SF condensers for passive subgrade cooling. The thermosyphons have always been fully operational. However, the foundation system for this facility was not designed for the warmer climate the region has been experiencing. The structure experienced differential movement due to warming from areas beyond the perimeter of the foundation. The water treatment plant is a critical piece of infrastructure that cannot be readily replaced. The facility is in an area not connected to the road system where the construction costs are high, and the construction season is limited due to the climate. This scenario presented a unique opportunity to investigate the feasibility of extending the life of the structure by retrofitting the existing foundation system before the foundation failed to the extent where the structure would become unserviceable and require replacement.

In the summer of 2021, the Alaska Native Tribal Health Consortium funded a project to upgrade the existing foundation system at the water treatment plant to maintain structural stability and usability into the future. The project plans specified a design life of 20 years and for the 2040 – 2049 period projected a freezing and thawing index of 2200 °F•Days and 3050 °F•Days, respectively. For reference, the historic freezing and thawing index for the 1961 – 1990 period according to the project plans was 3640 °F•Days and 2500 °F•Days, respectively. To achieve this design criteria the existing thermosyphon system was upgraded by adding a new 302 ft long hybrid flat-loop evaporator thermosyphon (FLET) around the west and south sides of the building, increasing the condenser size of the existing thermosyphons with 70 SF condensers to 140 SF, and hybridizing nine existing sloping evaporator thermosyphons on the west side of the building (Figures 1 and 2). The hybrid thermosyphons were cooled with two air-cooled active refrigeration condensing units; one for the FLET and one for the sloping evaporator thermosyphons. Nine temperature sensors were attached to the FLET, and nine temperature sensors were attached to the hybridized sloping evaporator thermosyphons to monitor ground temperatures and the refrigeration performance. Additionally, the perimeter subgrade insulation skirt was extended on the perimeter of the structure to the edge of the pad on the west and south side of the building ranging from a minimum of 10 ft to a maximum of 16 ft. To offset the cost of electricity to run the active refrigeration, solar panels were installed on the roof of the structure.



Figure 1. Hybridized sloping evaporator thermosyphon actively cooling the subgrade soils underneath the structure on the west side of the building in May of 2022.



Figure 2. Attaching the ground temperature instrumentation to the flat-loop evaporator thermosyphon on the southern side of the structure in the summer of 2021.

After the retrofit work was completed in late summer of 2021, the mechanical refrigeration capability of the hybrid thermosyphons was initiated to refreeze and stabilize the soils underneath the structure and around the perimeter of the structure. Since the summer of 2021 the mechanical refrigeration units overall have



operated continuously with intermittent outages. Near the end of the thaw season in October 2023, the average temperatures of the FLET sensors around the perimeter of the structure were  $-10.1\text{ }^{\circ}\text{F}$ , and the average temperatures of the sloping evaporator sensors were  $-1.3\text{ }^{\circ}\text{F}$ .

The short-term results show that retrofitting at-grade foundations utilizing passive subgrade cooling can be accomplished in a short time frame and successfully reduce the ground temperatures around the perimeter of the structure where heat is coming in from a warming climate. The significance of this work provides a potential solution for similar at-grade structures utilizing thermosyphons for passive cooling that have or will have similar issues due to climate warming.

# Reasonable Height of Cellular Concrete Aggregate Interlayer for Air Convection Embankment in Alaskan Permafrost Regions

Hanli Wu<sup>1</sup>, Xiong Zhang<sup>2</sup>, and Jenny Liu<sup>3</sup>

<sup>1</sup>Missouri University of Science and Technology, Rolla MO, USA. Email: hwyfn@mst.edu

<sup>2</sup>Missouri University of Science and Technology, Rolla MO, USA. Email: zhangxi@mst.edu

<sup>3</sup>Corresponding Author, Missouri University of Science and Technology, Rolla MO, USA.  
Email: jennyliu@mst.edu

## Abstract

Air convection embankment (ACE) is an excellent technique that uses open-graded material to create a “semi-conductive system” to provide excellent thermal insulation in summer and enhance the cooling performance in winter to prevent permafrost foundation from thawing. Previous thermal and performance studies indicate that the overall performance of cellular concrete ACE was superior to the conventional crushed-rock ACE. Cellular concrete is promising to be an alternative to crushed rocks for ACE to mitigate thaw settlement of permafrost foundation. However, the reasonable height of cellular concrete ACE needs to be further determined to maximize cost-effectiveness and performance and facilitate future field construction. Hence, a height investigation of the cellular concrete aggregate ACE was conducted by comparing the thermal performance of cellular concrete aggregate ACEs with various interlayer heights. The critical embankment principle was adopted to determine the reasonable height of cellular concrete aggregate interlayer to reduce cost and achieve desired performance.

**Keywords:** air convection embankment, permafrost, cellular concrete, cooling, thermal performance.

# Experimental Investigation on Pile Bearing Capacity Installed in Frozen Sandy Soil

Mohammad A. Abweny<sup>1</sup>, S.M. ASCE, Suguang Xiao<sup>2</sup>, P.E., M. ASCE

<sup>1</sup>Ph.D. student, Department of Civil and Environmental Engineering, Clarkson University, Potsdam, NY 13699; Email: abweny@clarkson.edu

<sup>2</sup>Department of Civil and Environmental Engineering, Clarkson University, Potsdam, NY 13699; Email: sxiao@clarkson.edu

## Abstract

The bearing capacity of piles in frozen soils is a critical consideration in foundation design of cold regions. This paper presents a comprehensive study on the bearing capacity of pile foundations installed in frozen sandy soil. The research was conducted at Clarkson University, where axial loading tests were performed on model piles within a specially designed frozen soil-pile interaction lab. A soil box with dimensions of 1.38 meters length, 0.9 meters width, and 1.22 meters height was constructed in a cold room, allowing precise temperature control ranging from -50 to 75 °C. Two steel model piles (pile 1, pile 2), each with a diameter of 6.35 cm and a length of 81 cm, were installed in the soil box. To monitor strains, strain gauges were strategically placed along the surface of the piles. Notably, one of the piles was equipped with a steel angle to protect the sensors. The ultimate bearing capacity of the pile was conducted by using the ASTM D5780 quick loading test method. Throughout the tests, the temperature of the frozen soil was maintained at -4.62 and -4.35 °C for piles 1 and 2, respectively. The results obtained from the quick loading test showed that the addition of the steel angles has increased the ultimate capacity of the pile by 26%. The load transfer analysis revealed load reduction with increasing depth into the soil.

## **Small Scale Hydropower in Alaska - From Construction to Operations; Challenges in Harsh Conditions**

Ed Zapel, P.E., Thom Fischer, P.E., George Hornberger

### **Abstract**

Stable, low cost energy projects in rural Alaska continues to be a major focus of long term economic stability. Hydropower has played a key role in Alaska, with early development of mining, lumbering, and fishing industries reliant on hydropower beginning in the late 1800's, and continuing development today of hydropower to power communities and their resource extraction industries. In this paper we examine some of the unique challenges facing the design, construction, and operation of small, isolated hydropower facilities in Alaska. These challenges include harsh climate and compressed construction season, difficult design and construction in areas with extreme cold temperatures and wind, material type selection to minimize catastrophic structural failures, and ensuring operation in spite of heavy snowfall and extreme icing. In particular, we examine the various approaches to project design to accommodate severe climate conditions with respect to penstock configuration, intake protection against ice of all types, seasonal hydrology and ice effects on surface water flows, foundation design to prevent issues with deep frost levels and permafrost, and machinery exposure to cold temperatures. We present some innovative solutions that have been applied to some of these challenges through thoughtful project design, including underground facilities to protect operations against cold temperatures, penstock thermal insulation, and power transmission line exposure to shifting soils, high winds, and extreme cold temperatures. At the end of the day, remote communities in subarctic and arctic regions struggle with economic survival that is very closely tied to the high cost of electric power. Throughout the world, wealthy communities arise and are sustained largely because of access to low and stable cost of electric power to ensure long term economic development. Without it, these communities suffer debilitating and sometimes terminal decline as the population seeks a better life where such benefits are plentiful.

## **Identification Method of Permafrost Table Based on Ground-Penetrating Radar**

Feng Zhang<sup>a\*</sup>, Tianci Liu<sup>a</sup>, Chuang Lin<sup>a</sup>, Zhan Wang<sup>a</sup>, Guanfu Wang<sup>a</sup>, Decheng Feng<sup>a</sup>

<sup>a</sup> School of Transportation Science and Engineering, Harbin Institute of Technology, 73 Huanghe Road, Harbin, China 150090. \*Corresponding author. Email: [zhangf@hit.edu.cn](mailto:zhangf@hit.edu.cn)

## Abstract

Ground-penetration radar (GPR) technology has received in-depth analysis and rapid development in the field of permafrost detection. The identification of permafrost table through GPR data analysis is one of the basic and challenging problems in this field. This study employed the finite-difference time-domain (FDTD) method to model ground-penetrating radar scenarios for permafrost detection, with a specific focus on exploring the time-domain signals emanating from the permafrost table, and proposed a permafrost table identification method based on the instantaneous frequency of the first order intrinsic mode function (IMF) after the Hilbert Huang transform (HHT) of the GPR data. Diverse models were formulated, encompassing variable thicknesses, upper limit depths, and dielectric constants of clay at distinct elevated temperatures. Through simulation, raw data of electromagnetic waves and two-dimensional GPR imagery were acquired. The electric field intensity of the electromagnetic waves data at the permafrost interface diminishes as the thickness of the permafrost and the upper limit depth expand, while it amplifies with an increase in the dielectric constant of the medium. Then using HHT to analyze radar signals, the instantaneous frequency of the first-order IMF was utilized to the identification of permafrost interfaces. The instantaneous frequency at the interfaces of radar signals with varying antenna frequencies exhibits distinct patterns of variation in response to changes in the upper limit depth of the permafrost, its thickness, and the dielectric constant of the medium. Through the application of two-dimensional imagery and practical engineering scenarios, it has been discovered that the one-dimensional curve of instantaneous frequency proves to be more effective in the identification of interfaces.

**Keywords:** Permafrost table, Ground-penetration radar (GPR), Hilbert-Huang Transform (HHT), Instantaneous frequency, Finite-difference time-domain (FDTD)

# Seasonal Frost Impact on Liquefaction-induced Lateral Spreading

Yue Zhao, Ph.D. Candidate <sup>1</sup>, Zhaohui (Joey) Yang, Ph.D. <sup>2</sup>

<sup>1</sup> *University of Alaska Fairbanks, Fairbanks, AK. Email: [yzhao8@alaska.edu](mailto:yzhao8@alaska.edu)*

<sup>2</sup> *University of Alaska Anchorage, Anchorage, AK. Email: [zyang2@alaska.edu](mailto:zyang2@alaska.edu)*

## Abstract

Liquefaction-induced lateral spreading can cause significant deformations and damage in structures, such as bridges, highways, and pipelines, including the broad cold regions. This paper assesses how a seasonally occurring ground crust would affect liquefaction-induced lateral spreading. One-dimensional, plane-strain analyses with shear beam boundary conditions were performed with OpenSeesPL, using the soil profile at the Slana River site and a pressure-dependent multiple yield surface constitutive model for liquefaction simulation. Four cases, including the base case (no seasonal frost) and cases with seasonal frost of 0.3 m, 1 m, or 2 m thick, were considered. The East-West motion recorded at Pump Station #10 of the Trans Alaska Pipeline System during the 2002 Denali earthquake was used as the base input. The results, including the time histories of acceleration, excess pore water pressure ratio, shear strain, and ground lateral spreading for selected depths, are presented. The results show that seasonal frost has a minor impact on the lateral spread displacement induced by liquefaction for the study site with a silty gravelly fill of relatively low permeability. Moreover, a parametric study was carried out to analyze the impact of the permeability of the fill on the triggering of liquefaction and ground surface lateral displacement. The medium sand layer almost entirely liquefies when the permeability of the fill is equal to or less than  $10^{-5}$  m/s, resulting in larger lateral spreading displacements.



# Pile Pinning Effects in Ground Lateral Spreading: A Case Study of the Slana River Bridge, AK

Yue Zhao <sup>a</sup>, Zhaohui (Joey) Yang, Ph.D. <sup>b</sup>

<sup>a</sup> *Ph.D. Candidate, University of Alaska Fairbanks, Fairbanks, AK. Email: yzhao8@alaska.edu*

<sup>b</sup> *Professor, University of Alaska Anchorage, Anchorage, AK. Email: zyang2@alaska.edu*

## Abstract

Ground laterally spreads in even mildly sloped ground when liquefaction is triggered by earthquakes. The amount of lateral spreading at a bridge abutment underlain by liquefiable soil may be reduced by the restraining forces from the pile foundation. This effect is also known as pile pinning and can be beneficial for bridge foundation design. This paper aims to demonstrate such an effect and how it can be quantified by conducting a case study using solid-fluid coupled three-dimensional modeling. The highway bridge, i.e., the new Slana River bridge, located in Tok Cutoff, Alaska, was constructed in 2015 to replace the old one that was damaged during the 2002 Denali earthquake. The Open System for Earthquake Engineering Simulation (OpenSees) and the graphic user interface OpenseesPL were used to perform the analysis. Concrete-filled steel pipe piles widely used for constructing highway bridge foundations in Alaska were used to analyze. Factors considered include pile size and thickness of seasonal frost. The diameter was varied to 0.3 m, 0.45 m, and 0.6 m to assess the pile size impact. The cases with piles of 0.45 m in diameter were examined for the effect of seasonal frost of varying thickness, including 0.3 m, 1 m, and 2 m. The results of a 0.45 m pile with no seasonal frost, as an example, present pile and soil responses, including acceleration, frequency, displacement, and excess pore pressure ratio. The end-of-shaking deflection, maximum rotation, maximum bending moment, and maximum shear force of the outmost pile are shown. The FE modeling results of models with piles of different pile sizes and embedded in varying seasonal frost thickness all reveal the obvious pile-pinning effect. The presence of pile foundations of sufficient lateral resistance without rupture can reduce lateral spreading by up to 80%. It would be very useful if one could factor in the pile-pinning effect in assessing lateral ground spreading for design purposes.

**Keywords:** pile pinning effects, seasonal frost, OpenSees, Slana River bridge

# Quantitative analysis of unfrozen water content of muddy clay under extremely low temperatures freezing conditions

Zhou J., Prof.,<sup>1,2</sup> Zhou H.D., Ph.D.,<sup>3</sup>

<sup>1</sup>*Department of Geotechnical Engineering, College of Civil Engineering, Tongji University, 1239 Siping Road, Shanghai 200092, China.*

<sup>2</sup>*Key Laboratory of Geotechnical and Underground Engineering (Tongji University), Ministry of Education, 1239 Siping Road, Shanghai 200092, China; email: [zhoujie1001@tongji.edu.cn](mailto:zhoujie1001@tongji.edu.cn)*

<sup>3</sup>*Department of Geotechnical Engineering, College of Civil Engineering, Tongji University, 1239 Siping Road, Shanghai 200092, China; email: [huadezhou@tongji.edu.cn](mailto:huadezhou@tongji.edu.cn)*

## Abstract

Water sealing of shafts and repair of subway tunnels all use liquid nitrogen for rapid freezing to realize emergency rescue, due to the unfrozen water content in the soil at extremely low temperatures will significantly affect the rescue project safety, therefore, it is necessary to quantitatively study unfrozen water content in soil at extremely low temperature. In this paper, based on LF-NMR, the unfrozen water content of the muddy clay at extremely low-temperatures was measured, and the three cut-off values of the four types of unfrozen water in artificially frozen were quantified. The surface relaxivity value of muddy clay was obtained for the first time by combining with the MIP test. Results show that the three  $T_2$  cutoff values for the classification of strongly bound water, weakly bound water, capillary water, and bulk water are 0.13 ms, 0.56 ms, and 2.58 ms, respectively, and the freezing characteristic curve of clay at extremely low temperatures can be divided into the rapid decline stage and the slow decline stage. The value of surface relaxivity of the muddy clay is 12 nm/ms. This study facilitates the stability analysis of artificially frozen projects by investigating the unfrozen water content of the soil under extremely low-temperature conditions.

# Analysis on pore-fissure extension and evolution mechanism of one-dimensional clay column under unidirectional freezing conditions

Zhou J., Prof. <sup>1,2</sup>, Zhou H.D., Ph.D. <sup>1</sup>, ChenjunLiu Ph.D. <sup>1</sup>

<sup>1</sup> *Department of Geotechnical Engineering, College of Civil Engineering, Tongji University, 1239 Siping Road, Shanghai 200092, China; email: zhoujie1001@tongji.edu.cn*

<sup>2</sup> *Key Laboratory of Geotechnical and Underground Engineering (Tongji University), Ministry of Education, 1239 Siping Road, Shanghai 200092, China*

## Abstract

The artificial ground freezing (AGF) method can produce pores-fissures in soft clay that increase their permeability and create engineering problems such as leakage and uneven settlement. In this paper, One-dimensional soil column experiments under unidirectional freezing were carried out to investigate the effects of freezing temperatures (-5°C, -10°C, -20°C, -30°C) and initial water content of the soil (30%, 40%, 50%) on the pore-fissure evolution. The distribution of pore-fissure extension direction and the characteristic evolution of pore-fissure parameters (fissure continuity rate and maximum fissure width) due to unidirectional freezing under the action of multiple factors were analyzed from qualitative and quantitative perspectives, respectively. The results show that the distribution direction of pores-fissures is generally perpendicular to the expansion direction of the freezing front (i.e., transverse fissures), and the average ratio of transverse fissures to total fissures within 8 cm of the freezing height was 64%. The distribution of fissures parallel to the freezing front (vertical fissures) within the frozen inner fringe is more than that of the frozen outer fringe. Elevated freezing temperature or reduced initial water content significantly increases the fissure continuity at the frozen outer fringe (the fissure continuity rate was 100% at -5°C and 71.96% at 30%) and facilitates the inter-fracture connectivity. Moreover, the increase of freezing temperature or the decrease of initial water content significantly increased the maximum width of frozen outer fringe fissures (the maximum fissure width was 1.79 mm at -5°C and 1.2 mm at 30%), promoting the generation of larger fissures. The experimental results further revealed the expansion mechanism of pores-fissures in artificially frozen clay, which can provide scientific basis for Intelligent and refined settlement prevention in the later stages of artificially frozen projects.

**Keywords:** Pores-fissures; extension mechanism; fissure continuity rate and maximum fissure width; artificial ground freezing;

## Introduction

The artificial ground freezing (AGF) method has been widely used in urban underground engineering construction, which can improve the soil strength and build a water curtain, and play the role of reinforcement and water insulation. However, more and more engineering cases and scientific research have confirmed that the use of this method in the distribution of soft clay is prone to causing post-construction settlement and leakage of subway tube sheets [1,2], which is because freezing and thawing change the pore structure of soft clay and increase the permeability of the soil layer [3,4]. In fact, the pores and fissures in frozen clay are important channels for water migration before and after freeze-thawing, and their expansion mechanisms can essentially reflect the distribution of permeability coefficients after freeze-thawing and the parts that need the most attention in the region, which will provide theoretical guidance for the subsequent artificial grouting to achieve accurate grouting and precise control of subsidence.

## Methodology

In this study, the unidirectional freezing test of the one-dimensional soil column was carried out by a self-developed device. The soil sample used in the experiment was the fourth layer of Shanghai soft clay (the actual frozen soil layer). The influencing factors considered in this study included the freezing temperatures ( $-5^{\circ}\text{C}$ ,  $-10^{\circ}\text{C}$ ,  $-20^{\circ}\text{C}$ ,  $-30^{\circ}\text{C}$ ) and the initial water content of soil (30%, 40%, 50%). To analyze the pores-fissures extension mechanism of artificially frozen saturated soft clay, the pores-fissures extension direction of frozen clay was qualitatively described from the pores-fissures distribution direction. Moreover, two indexes, the fissure continuity rate, and maximum fissure width were chosen to quantitatively describe the pores-fissures expansion law of frozen clay under the action of freezing temperature and initial water content. Here, the fissure continuity rate refers to the ratio of fissure length of more than one-third length in the horizontal direction to the total length to reflect the connectivity degree of the transverse fissure. The unidirectional freezing test process of the one-dimensional soil column is shown in Figs. 1-2.



Fig.1. Test flow chart.

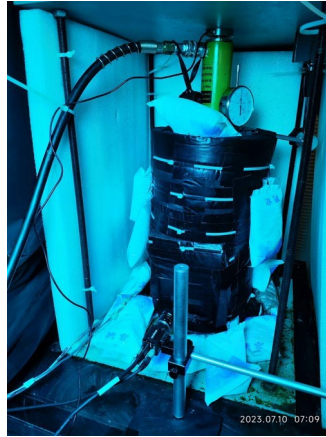


Fig.2. Self-made test device diagram.

## Findings or Results

### *Pore-fissure direction distribution*

To investigate the directionality of pores-fissures in frozen soft clay, the total length of freezing pores-fissures in a certain directional interval in the region was counted against the total length of pores-fissures in the region using a nodal rose diagram simulating the direction of pores-fissures in the rock, deriving a histogram of pores-fissures distribution, which in turn led to the main direction of pores-fissures development. The result is shown in Fig. 3 (the freezing temperature is  $-30^{\circ}\text{C}$ , the initial water content of the soil is 50%).

Fig.3. Pores-fissures direction distribution diagram

As shown in Fig. 3, the results show that the distribution direction of pores-fissures is generally perpendicular to the expansion direction of the freezing front (i.e., transverse fissures), and the average ratio of transverse fissures to total fissures within 8 cm of the freezing height was 64%. The distribution of fissures parallel to the freezing front (vertical fissures) within the frozen inner fringe is more than that of the frozen outer fringe.

*Effect of temperature and initial water content on pores-fissures parameters*

Freezing temperature and initial water content of soil are important factors affecting the change of fissures. The changes of key fissure parameters (fissure continuity rate and maximum fissure width) of frozen clay were calculated with the change of freezing temperature or initial water content. The result is shown in Fig. 4.

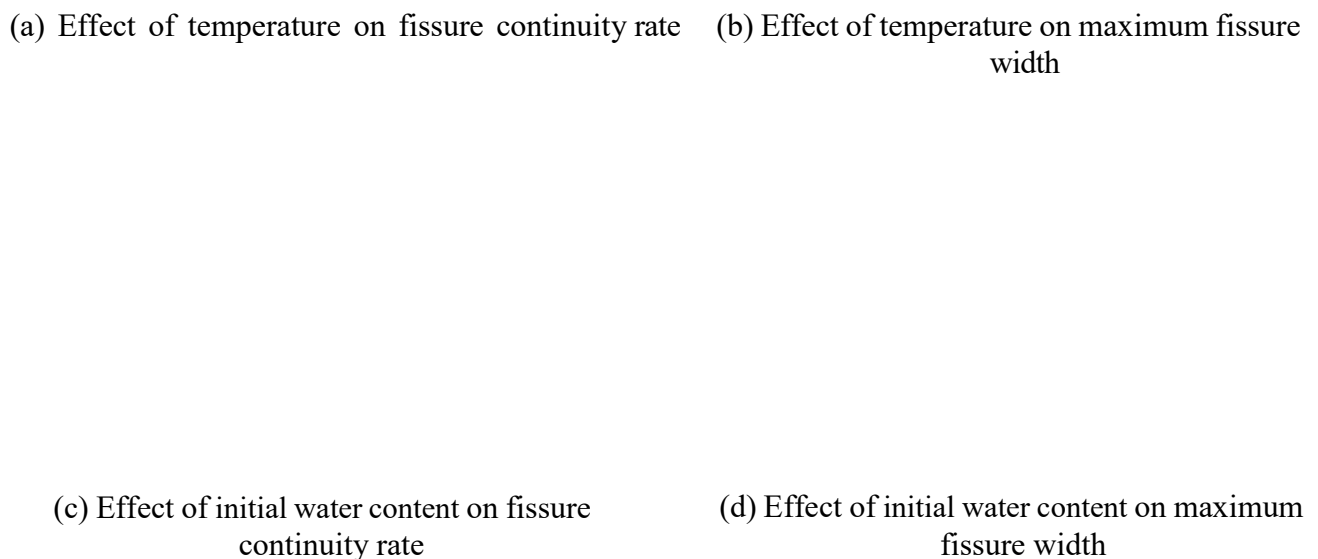


Fig.4. Schematic diagram of the effect of temperature and initial water content on pore-fracture parameters

As shown in Fig. 4(a), with the increase of freezing temperature, the fissure continuity rate of the frozen outer fringe increases gradually, and when the freezing temperature is  $-5^{\circ}\text{C}$ , the fissure continuity rate of the frozen outer fringe is 100%. As shown in Fig. 4(b), with the increase of freezing temperature, the maximum fissure width of the frozen outer fringe increases gradually, and the maximum fissure width of the frozen outer fringe is 1.79 mm when the freezing temperature is  $-5^{\circ}\text{C}$ . The increase of the fissure continuity rate of the frozen outer fringe leads to the enhancement of the inter-fracture connectivity. As shown in Fig. 4(c), the fissure continuity rate of the frozen outer fringe increased gradually with the decrease of initial water content, and the fissure continuity rate of the frozen outer fringe was 71.96% when the initial water content was 30%. As shown in Fig. 4(d), as the initial water content decreases, the fissure continuity rate of the freezing outer edge gradually increases, and when the initial water content is



30%, the maximum fissure width of the freezing outer edge is 1.2 mm. The increase in freezing temperature or the decrease in initial water content promoted the generation of larger fissures.

## Conclusions

1. The distribution direction of pores-fissures is generally perpendicular to the expansion direction of the freezing front (i.e., transverse fissures), and the average ratio of transverse fissures to total fissures within 8 cm of the freezing height was 64%.
2. The distribution of fissures parallel to the freezing front (vertical fissures) within the frozen inner fringe is more than that of the frozen outer fringe.
3. Elevated freezing temperature or reduced initial water content significantly increases the fissure continuity at the frozen outer fringe (the fissure continuity rate was 100% at  $-5^{\circ}\text{C}$  and 71.96% at 30%) and increases the inter-fracture connectivity.
4. The increase of freezing temperature or the decrease of initial water content significantly increased the maximum width of frozen outer fringe fissures (the maximum fissure width was 1.79 mm at  $-5^{\circ}\text{C}$  and 1.2 mm at 30%), promoting the generation of larger fissures.

## Acknowledgments

The research work herein was supported by the Program for Young Changjiang Scholars of the Ministry of Education of China (No. Q2022101), the National Natural Science Foundation of China (No. 41702299) and the Foundation of State Key Laboratory of Frozen Soil Engineering of China (No. SKLFSE201916).

## References

- Brownstein, K.R., Tarr, C.E. (1979). "Importance of classical diffusion in NMR studies of water in biological cells". *Phys. Rev. A* 19 (6), 2446-2453.
- Xi, J. M., Xiong, Y.L., Ma, X. M, Xie, J. T. (2020). "Research status of freezing method for subway communication channel construction". *Science Technology and Engineering*, 20(17):6720-6728. (in Chinese)
- Zhao, Q., Ding, S. L. (2020). "Analysis and treatment of water leakage in the late stage of subway connection passage construction by freezing method". *Urban Rail Transit Research*, 23(05): 128-130. (in Chinese)
- Tang, Y., Yan, J. (2015). "Effect of freeze-thaw on hydraulic conductivity and microstructure of soft soil in Shanghai area". *Environmental Earth Sciences*, 73(11): 7679-7690.
- Zhou, J., Tang, Y. Q. (2018). "Experimental inference on dual-porosity aggravation of soft clay after freeze-thaw by fractal and probability analysis". *Cold Regions Science and Technology*, 153: 181-196.

**ASCE** AMERICAN SOCIETY  
OF CIVIL ENGINEERS



**UAA** College of Engineering  
UNIVERSITY *of* ALASKA ANCHORAGE

